

THE UNIVERSITY OF CALGARY

Motion of Rigid Bodies:

the Euler Top and the Rattleback

by

Emil Simeonov Savev

A THESIS

SUBMITTED TO THE FACULTY OF GRADUATE STUDIES
IN PARTIAL FULFILLMENT OF THE REQUIREMENTS FOR THE
DEGREE OF MASTER OF SCIENCE

DEPARTMENT OF MATHEMATICS AND STATISTICS

CALGARY, ALBERTA

March, 2002

© Emil Simeonov Savev 2002

THE UNIVERSITY OF CALGARY
FACULTY OF GRADUATE STUDIES

The undersigned certify that they have read, and recommend to the Faculty of Graduate Studies for acceptance, a thesis entitled “Motion of Rigid Bodies: the Euler Top and the Rattleback” submitted by Emil Simeonov Savev in partial fulfillment of the requirements for the degree of Master of Science.



Supervisor, Dr. L. Bates
Department of Mathematics and Statistics



Dr. R. Westbrook
Department of Mathematics and Statistics



Dr. M. Epstein
Department of Mechanical and Manufacturing Engineering

2002.03.10

Date

Abstract

The Euler top is a rigid body fixed at its centre of mass and free to rotate without external torques. Its angular momentum in the space frame is constant. In this thesis, there are several herpolhode graphs that compare and contrast various configurations of the Euler top. In addition, an important identity is found that relates the angle of rotation of the body around the angular momentum vector and the angle swept by the herpolhode. An explanation for the phenomenon is provided that uses the fact that the motion takes place on a torus embedded in the $SO(3)$ group of rotations. This explanation is then confirmed by numerical simulations.

The rattleback is a spinning top that reverses the direction of motion on its own. Depending on its moments of inertia and shape, it can reverse one or more times or it can spin at an axis other than the vertical. The equations of motion are linearized and parameter ranges are found such that the rattleback exhibits qualitatively different behaviours. These parameters are then used in numerical simulations that confirm the predictions of the linearized equations of motion. The numerical simulations also indicate that a spin reversal occurs precisely when the wobbling angle is at its maximum - something that has been observed in real rattlebacks.

Table of Contents

Approval Page	ii
Abstract	iii
Table of Contents	iv
List of Figures	vi
List of Symbols	viii
1 Euler Top	1
1.1 Introduction	1
1.2 Definitions	2
1.3 Initial Conditions	4
1.4 Euler-Arnol'd Equations	6
1.5 Herpolhode	10
1.5.1 Mathematical Analysis	10
1.5.2 Computing the Herpolhode Coordinates	12
1.5.3 The Herpolhode: Numerical Examples	13
1.5.4 Discussion of the Numerical Examples	27
1.6 Solid Ball Model	28
1.6.1 Mathematical Analysis	28
1.6.2 Explanation of the Herpolhode Results	29
1.6.3 The Torus: Numerical Examples	32
2 Equations for a Rigid Body Rolling on the Plane	45
2.1 General Equations	45
2.2 Examples of Rolling Rigid Bodies	48
2.2.1 Sphere	48
2.2.2 Disk	49
2.2.3 Rattleback	49
3 Rattleback	52
3.1 Historical Perspective	52
3.1.1 Definitions	52
3.1.2 Popular Articles	52
3.1.3 Scientific Articles	53
3.2 Linearization about the Walker equilibrium	56

3.2.1	Low Energy Analysis ($\omega_3 = 0$)	60
3.2.2	High Energy Analysis ($\omega_3 \neq 0$)	61
3.2.3	Bifurcations	62
3.3	Numerical Simulations	63
3.3.1	Type 0 Rattleback	65
3.3.2	Type 1 Rattleback	69
3.3.3	Type 2 Rattleback	83
3.4	Calculation of the Rotation Matrix $A(t)$ and Translation Vector $v(t)$ for the Rattleback	99
4	Conclusion	101
4.1	New Results for the Euler Top	101
4.2	New Results for the Rattleback	101
	Bibliography	103
A	Computer Program for the Euler Top	106
B	Computer Program for the Rattleback	120
C	Tables of Elliptic Functions	131
C.1	Complete Elliptic Integral $K(k)$	131
C.2	$f(t)=\text{sn}(t m = k^2)$	132
C.3	$f(t)=\text{cn}(t m = k^2)$	134
C.4	$f(t)=\text{dn}(t m = k^2)$	136

List of Figures

1.1	Rotational Motion of a Rigid Body	4
1.2	Euler angles	5
1.3	Geometrical Representation of ϑ	7
1.4	Invariable Plane and Herpolhode	10
1.5	Herpolhode	15
1.6	Jacobi Elliptic Functions vs. Time	16
1.7	Herpolhode Angle ξ and Projection Angle ϑ as Functions of Time . .	17
1.8	Herpolhode	18
1.9	Jacobi Elliptic Functions vs. Time	19
1.10	Herpolhode Angle ξ and Projection Angle ϑ as Functions of Time . .	20
1.11	Herpolhode	21
1.12	Jacobi Elliptic Functions vs. Time	22
1.13	Herpolhode Angle ξ and Projection Angle ϑ as Functions of Time . .	23
1.14	Herpolhode	24
1.15	Jacobi Elliptic Functions vs. Time	25
1.16	Herpolhode Angle ξ and Projection Angle ϑ as Functions of Time . .	26
1.17	Longitudinal circle along the torus	30
1.18	Lattitudinal circle along the torus	30
1.19	Longitudinal motion along the torus	31
1.20	Lattitudinal motion along the torus	31
1.21	Solid Ball Model for the Euler Top	33
1.22	Solid Ball Model for the Euler Top	34
1.23	Solid Ball Model for the Euler Top	35
1.24	Solid Ball Model for the Euler Top	36
1.25	Solid Ball Model for the Euler Top	37
1.26	Solid Ball Model for the Euler Top	38
1.27	Solid Ball Model for the Euler Top	39
1.28	Solid Ball Model for the Euler Top	40
1.29	Solid Ball Model for the Euler Top	41
1.30	Solid Ball Model for the Euler Top	42
1.31	Solid Ball Model for the Euler Top	43
1.32	Solid Ball Model for the Euler Top	44
2.1	Rattleback Spinning on the Plane	50
2.2	The Shape of the Rattleback	51
3.1	Type 0 Rattleback: Bondi Diagram	66
3.2	Type 0 Rattleback: Spin Angle vs. Time	67

3.3	Type 0 Rattleback: Wobble Angle vs. Time	68
3.4	Type 1 Rattleback: Bondi Diagram	69
3.5	Type 1 Rattleback: Routh-Hurwitz Stability Criteria	71
3.6	Type 1 Rattleback: Eigenvalues Crossing the Imaginary Axis	72
3.7	Type 1 Rattleback, $\omega_3 = -0.5$	74
3.8	Type 1 Rattleback, $\omega_3 = -0.5$	75
3.9	Type 1 Rattleback	76
3.10	Type 1 Rattleback, $\omega_3 = 0.5$	77
3.11	Type 1 Rattleback, $\omega_3 = 0.5$	78
3.12	Type 1 Rattleback, $\omega_3 = -1.2$	79
3.13	Type 1 Rattleback, $\omega_3 = -1.2$	80
3.14	Type 1 Rattleback, $\omega_3 = 1.2$	81
3.15	Type 1 Rattleback, $\omega_3 = 1.2$	82
3.16	Type 2A Rattleback: Bondi Diagram	83
3.17	Type 2A Rattleback, $\omega_3 = -0.5$	85
3.18	Type 2A Rattleback, $\omega_3 = -0.5$	86
3.19	Type 2A Rattleback, $\omega_3 = 0.5$	87
3.20	Type 2A Rattleback, $\omega_3 = 0.5$	88
3.21	Type 2 Rattleback: Routh-Hurwitz Stability Criteria	90
3.22	Type 2 Rattleback: Eigenvalues for 3 different ω_3	91
3.23	Type 2A Rattleback, $\omega_3 = -1.5$	92
3.24	Type 2A Rattleback, $\omega_3 = -1.5$	93
3.25	Type 2A Rattleback, $\omega_3 = 1.5$	94
3.26	Type 2A Rattleback, $\omega_3 = 1.5$	95
3.27	Type 2B Rattleback	97
3.28	Type 2B Rattleback	98

List of Symbols

- A Rotation matrix, 3
- C_1 A circle that forms the basis of a torus, 30
- C_2 A circle that forms the basis of a torus, 30
- C_{max} Outer circle of herpolhode graph, 11
- C_{min} Inner circle of herpolhode graph, 11
- E Total energy of the rigid body, 9
- E_H Energy when Hopf bifurcation occurs, 70
- E_{P_1} Energy when first pitchfork bifurcation occurs, 89
- E_{P_2} Energy when second pitchfork bifurcation occurs, 96
- I_1 Principal moment of inertia about the x' -axis, 3
- I_2 Principal moment of inertia about the y' -axis, 3
- I_3 Principal moment of inertia about the z' -axis, 3
- K Complete elliptic integral, 8
- L Magnitude of angular momentum in space frame, 6
- M Mass of the rigid body, 45
- $P(w)$ A parabola that is a function of $w = \omega^2$, 63
- $Q(w)$ A line that is a function of $w = \omega^2$, 63
- $R(t)$ Radius squared of herpolhode at time t , 12
- S A 3-dimensional vector related to the general equations of a rolling body, 47
- T A 3 by 3 matrix related to the general equations of a rolling body, 46
- V Volume of rigid body, 2
- Δ Parameter related to linearized rattleback equations, 60
- Γ Spin angle of the rattleback, 64
- Ω_2 Amplitude of $\omega_2(t)$, 8
- Φ Parameter related to the shape of the rattleback, 64
- Ψ Parameter related to the shape of the rattleback, 64
- Θ Parameter related to the shape of the rattleback, 64
- α Parameter related to the moments of inertia, 64
- α_4 Parameter related to linearized rattleback equations, 61
- β Parameter related to the moments of inertia, 64
- β_2 Parameter related to linearized rattleback equations, 61
- β_4 Parameter related to linearized rattleback equations, 61
- χ Euler characteristic of a surface, 30
- δ Parameter related to the shape of the rattleback, 58
- ϵ Time shift coefficient, 8
- η Wobble angle of the rattleback, 64
- γ Parameter related to the moments of inertia, 64

- γ_2 Parameter related to linearized rattleback equations, 60
- γ_4 Parameter related to linearized rattleback equations, 60
- κ Parameter whose sign determines the type of the rattleback, 64
- λ Variable in the characteristic polynomial, 59
- μ Parameter whose sign determines the type of the rattleback, 64
- ω_1 Angular velocity about the x' -axis, 3
- ω_2 Angular velocity about the y' -axis, 3
- ω_3 Angular velocity about the z' -axis, 3
- ϕ Euler angle of precession, 4
- ψ Euler angle of spin, 4
- σ_{11} Parameter related to the shape of the rattleback, 49
- σ_{12} Parameter related to the shape of the rattleback, 49
- σ_{22} Parameter related to the shape of the rattleback, 49
- τ Period of Jacobian elliptic functions, 8
- θ Euler angle of nutation, 4
- ϑ Angle of rotation about the angular momentum (projection angle), 6
- ξ Angle swept by the herpolhode since the beginning of motion, 12
- ζ An angle between 0 and π that indicates amount of rotation, 29
- a_1 A_{11} element of rotation matrix, 3
- a_2 A_{21} element of rotation matrix, 3
- a_3 A_{31} element of rotation matrix, 3
- b_1 A_{12} element of rotation matrix, 3
- b_2 A_{22} element of rotation matrix, 3
- b_3 A_{32} element of rotation matrix, 3
- c_1 A_{13} element of rotation matrix, 3
- c_2 A_{23} element of rotation matrix, 3
- c_3 A_{33} element of rotation matrix, 3
- g Acceleration due to gravity, 45
- h Distance from the centre of mass to the lowest point of the rattleback, 49
- k Modulus of Jacobian elliptic functions, 8
- m $m = k^2$ Parameter of Jacobian elliptic functions, 11
- n Time scale coefficient, 8
- p_1 First component of a point on the rattleback after translation, 100
- p_2 Second component of a point on the rattleback after translation, 100
- p_3 Third component of a point on the rattleback after translation, 100
- q_1 First component of a point on the rattleback before translation, 100
- q_2 Second component of a point on the rattleback before translation, 100
- q_3 Third component of a point on the rattleback before translation, 100
- $r(t)$ Radius of herpolhode at time t , 12
- r_1 x -component of a vector that specifies axis of rotation, 29

r_2 y -component of a vector that specifies axis of rotation, 29
 r_3 z -component of a vector that specifies axis of rotation, 29
 r_{max} Radius of outer circle of herpolhode graph, 11
 r_{min} Radius of inner circle of herpolhode graph, 11
 t Time elapsed since the beginning of motion, 3
 t_1 Time for the herpolhode to reach its first maximum, 27
 t_3 Time for the herpolhode to reach its third maximum, 27
 u_1 First component of a unit vector that determines the point of contact, 45
 u_2 Second component of a unit vector that determines the point of contact, 45
 u_3 Third component of a unit vector that determines the point of contact, 45
 v_1 First component of translation vector, 100
 v_2 Second component of translation vector, 100
 v_3 Third component of translation vector, 100
 w ω_3^2 , 63
 x' First coordinate axis in the body frame, 2
 x_h x -coordinate of the herpolhode in space frame, 10
 x_r x -component of a vector that describes the rotation, 29
 y' Second coordinate axis in the body frame, 2
 y_h y -coordinate of the herpolhode in space frame, 10
 y_r y -component of a vector that describes the rotation, 29
 z' Third coordinate axis in the body frame, 2
 z_h z -coordinate of the herpolhode in space frame, 10
 z_r z -component of a vector that describes the rotation, 29
 \mathbf{l} Angular momentum in the body frame, 7
 \mathbf{I} Moment of inertia diagonal matrix, 45
 \mathbf{L} Angular momentum in space frame, 6
 $\mathbf{s}(\mathbf{u})$ Inverse of the Gauss map, 45

Chapter 1

Euler Top

1.1 Introduction

The Euler top is a rigid body that is fixed at its centre of mass and is free to move without external torques. The equations of motion were first derived by Euler in 1758 [9]. In 1834, Poinsot [23] showed how the motion of the Euler top can be represented as an ellipsoid fixed at its centre of mass and rolling on a plane. The curve traced by the point of contact on the ellipsoid is called the *polhode*. The curve traced by the point of contact on the plane is called the *herpolhode*. In his paper, Poinsot drew a graph of a herpolhode with inflection points - which happens when the Euler top is not physically realizable. For a physically realizable Euler top, the herpolhode is always locally convex and has no inflection points. One of the earliest pictures of a realistic herpolhode was shown by Routh [24] in 1884. In 1886, Darboux [8] was probably the first to prove that a realistic herpolhode has no inflection points, and another article on the matter was published by Lecornu [16] in 1906. In 1966 Arnold [1] published an article that treated the Euler top problem using Lie groups. In 1991, Montgomery [21] published a paper that found a relationship between the projection angle ϑ and the herpolhode angle ξ . In 1993 Levi [17] published an article related to the Euler top. In his book Cushman [7] corrected a slight error in Arnold's and Montgomery's calculations and claimed that the change in angle ϑ over a period τ equals the angle ξ swept by the herpolhode after every *other* maximum of its radius

- a conclusion that was very close to the actual truth. The author of this thesis, in collaboration with L. Bates and R. Cushman, has further clarified previous results, notably by finding the relationship between the angle ϑ and the herpolhode angle ξ for all possible cases. It turns out that for certain conditions, Cushman's identity found in [7] is valid while for other conditions, there is a difference of 2π between the two sides of Cushman's identity.

1.2 Definitions

A *rigid body* is a system of point masses such that the distance between every two points is constant. The *mass* of the rigid body measures the quantity of matter present in it, while the *volume* measures the space that the rigid body occupies. Define $x'-y'-z'$ coordinate system fixed in the body. The *moment of inertia* $I_{x'y'}$ about the $x'-y'$ plane and the moment of inertia about the x' -axis are defined as:

$$\begin{aligned} I_{x'y'} &= \int_V (x'^2 + y'^2) dm \\ I_{x'} &= \int_V x'^2 dm \end{aligned} \tag{1.1}$$

where dm is an infinitesimal mass element and V is the volume of the rigid body.

The *moment of inertia tensor* is the 3×3 matrix:

$$\mathbf{I} = \begin{bmatrix} I_{x'} & -I_{x'y'} & -I_{x'z'} \\ -I_{x'y'} & I_{y'} & -I_{y'z'} \\ -I_{x'z'} & -I_{y'z'} & I_{z'} \end{bmatrix} \tag{1.2}$$

Since this matrix is symmetric, it is diagonalizable by an orthogonal transformation. Therefore every rigid body has three mutually orthogonal *principal axes* along which the inertia matrix is diagonal. These axes meet at the *centre of mass* of the body.

From now on, we will assume that x' - y' - z' coordinate system coincides with the three principal axes of the body. An *Euler top* is a rigid body that is fixed at its centre of mass and is free to rotate without external torques acting on it. For example, the rotational motion of the Earth has some similarities with the motion of an ideal Euler top. To describe the motion of the body mathematically, choose two coordinate frames: one that is fixed in space (the *space frame*) and one that is fixed in the body (the *body frame*). Choose the three coordinate axes of the body frame to coincide with the three principal axes. Let I_1 , I_2 and I_3 be the three *principal moments of inertia* (about the x' -, y' - and z' -axes in the body frame, respectively). In every instant, there is an *angular velocity* vector $[\omega_1, \omega_2, \omega_3]$ in the body frame that changes with time. ω_1, ω_2 and ω_3 are the instantaneous angular velocities about x' -, y' - and z' -axes respectively in the body frame. Each rotation can be represented by a 3×3 orthogonal matrix with determinant 1. The matrix must be *orthogonal* since the body is rigid and does not deform. The determinant of the matrix must equal +1 since the motion is continuous. Let A be such a matrix.

$$A = \begin{bmatrix} a_1 & b_1 & c_1 \\ a_2 & b_2 & c_2 \\ a_3 & b_3 & c_3 \end{bmatrix}$$

All such matrices form the $SO(3)$ group of rotations. Let t be the time elapsed since the beginning of motion. The map $t \rightarrow A(t)$ describes the motion of the body.

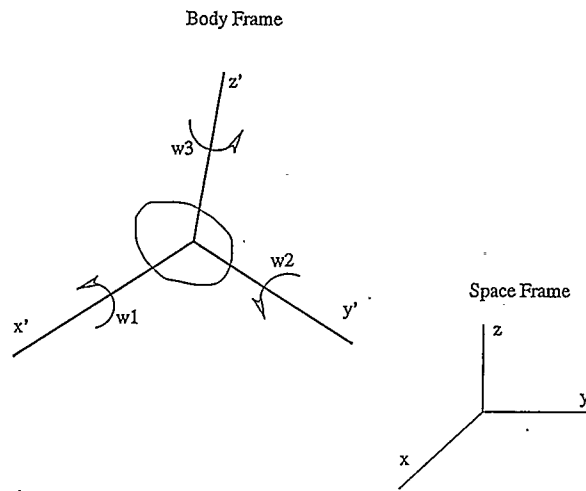


Figure 1.1: Rotational Motion of a Rigid Body

The *space frame* x - y - z is fixed in space. The *body frame* x' - y' - z' is fixed in the body and rotates with the body. x' , y' and z' are the three principal axes. The moment of inertia around x' is I_1 , around y' is I_2 and around z' is I_3 . The instantaneous angular velocity around x' is ω_1 , around y' is ω_2 and around z' is ω_3 .

1.3 Initial Conditions

One way to parametrize the matrix $A(t)$ is in terms of the Euler angles θ (angle of nutation), ϕ (angle of precession) and ψ (angle of spin). Graumann [11] has shown all different possibilities that can arise but for the purposes of this thesis the reader can refer to the following Figure 1.2. If the initial orientation of the rigid body is given in terms of its Euler angles (ϕ, ψ, θ) then the initial matrix $A(0)$ can be found

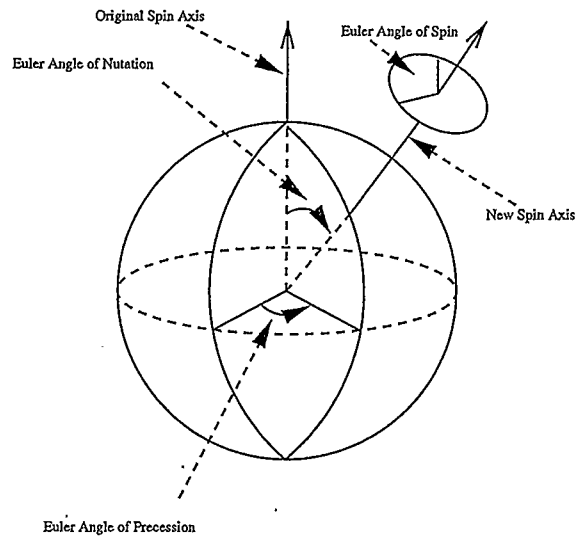


Figure 1.2: Euler angles

by using the following identities (see [11]):

$$\begin{aligned}
 a_1 &= \cos \theta \cos \phi \cos \psi - \sin \phi \sin \psi, \\
 a_2 &= \cos \theta \sin \phi \cos \psi + \cos \phi \sin \psi, \\
 a_3 &= -\sin \theta \cos \psi, \\
 b_1 &= -\cos \theta \cos \phi \sin \psi - \sin \phi \cos \psi, \\
 b_2 &= -\cos \theta \sin \phi \sin \psi + \cos \phi \cos \psi, \\
 b_3 &= \sin \theta \sin \psi, \\
 c_1 &= \sin \theta \cos \phi, \\
 c_2 &= \sin \theta \sin \phi, \\
 c_3 &= \cos \theta.
 \end{aligned} \tag{1.3}$$

Once we know the initial orientation of the body, we must apply Newton's second law to see how the motion changes with time. This will be accomplished in the next section, but for now it is important to know that the angular momentum in the space

frame remains constant (due to the lack of external torques). Choose the z axis of the space frame to coincide with the constant angular momentum. If, in addition to the three Euler angles, the magnitude L of the constant angular momentum vector \mathbf{L} in the space frame is also known, then the initial ω_i and ϑ are determined from the formulas:

$$\begin{aligned}\omega_{1i} &= \frac{a_3 L}{I_1}, \\ \omega_{2i} &= \frac{b_3 L}{I_2}, \\ \omega_{3i} &= \frac{c_3 L}{I_3}, \\ \vartheta_i &= \arctan \frac{a_2}{a_1}.\end{aligned}\tag{1.4}$$

The angle ϑ is the angle between the projection of $[a_1, a_2, a_3]$ onto the x - y plane and the x -axis in the space frame. Call this angle the *projection angle*. It measures the amount of rotation of the body around the angular momentum vector \mathbf{L} in space frame. Many authors have shown (see, for example, [7]) that the four variables $\omega_1, \omega_2, \omega_3$ and ϑ are necessary and sufficient to parametrize the rotation matrix $A(t)$. Therefore, knowing $[\omega_1, \omega_2, \omega_3]$ and ϑ as functions of time is sufficient to reconstruct the motion of the Euler top. Thus, four initial conditions are always needed for describing the motion of the Euler top: either $(\omega_1, \omega_2, \omega_3, \vartheta)$ or (ϕ, ψ, θ, L) .

1.4 Euler-Arnol'd Equations

Let \mathbf{L} equal the *angular momentum* vector of the body in the space frame:

$$\mathbf{L} = A(t) * [I_1 \omega_1, I_2 \omega_2, I_3 \omega_3]^T\tag{1.5}$$

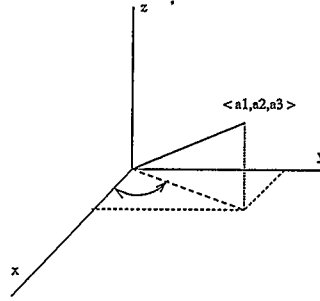


Figure 1.3: Geometrical Representation of ϑ

The angle ϑ : The angle between the projection of $[a_1, a_2, a_3]$ onto the x - y plane and the x -axis in the space frame

The absence of external torques means that the angular momentum \mathbf{L} of the body in the space frame remains constant:

$$\frac{d\mathbf{L}}{dt} = 0 \quad (1.6)$$

The z -axis in the space frame has been chosen so that its positive direction coincides with the positive direction of vector \mathbf{L} . Let \mathbf{l} equal the angular momentum of the body in the body frame:

$$\mathbf{l} = [I_1\omega_1, I_2\omega_2, I_3\omega_3] \quad (1.7)$$

Converting from space frame to body frame coordinates and using the Coriolis Theorem, equation (1.6) then becomes:

$$\frac{d\mathbf{l}}{dt} = \mathbf{l} \times [\omega_1, \omega_2, \omega_3] \quad (1.8)$$

Expanding this vector equation, we get the differential equations that govern the motion of the Euler Top (the *Euler equations*):

$$\begin{aligned} I_1 \dot{\omega}_1 &= (I_2 - I_3) \omega_2 \omega_3, \\ I_2 \dot{\omega}_2 &= (I_3 - I_1) \omega_1 \omega_3, \\ I_3 \dot{\omega}_3 &= (I_1 - I_2) \omega_1 \omega_2. \end{aligned} \tag{1.9}$$

These three equations can be solved explicitly by using *Jacobian elliptic functions* sn, cn and dn (see, for example, [27],[7]). Let I_2 be the second largest moment of inertia. Then the solution for ω_2 can be expressed using the formula:

$$\omega_2 = \Omega_2 sn(n(t - \epsilon)|k) \tag{1.10}$$

where

Ω_2 = Amplitude of $\omega_2(t)$

n = Time scale coefficient

ϵ = Time shift coefficient

k = Modulus of Jacobian elliptic functions.

Each of the Jacobian elliptic functions is periodic. When the Euler equations are solved, two of the three elliptic functions (sn and cn) have the same period which we will call τ , while the period of the third one (dn) is $\frac{1}{2}\tau$. The period τ of sn and cn can be found with the formula:

$$\tau = \frac{4}{n} K(k) \tag{1.11}$$

where $K(k)$ is the *complete elliptic integral* $K(k) = \int_0^{\frac{\pi}{2}} \frac{dt}{\sqrt{1-k^2 \sin^2 t}}$.

By themselves, the three Euler equations (1.9) are not sufficient to parametrize the rotation matrix $A(t)$. When a fourth equation for ϑ is added to the three Euler

equations, the new system of four equations is called the *Euler-Arnol'd equations*. This system then is necessary and sufficient to parametrize $A(t)$. Shown below is the fourth equation of the Euler-Arnol'd equations (see [7] for derivation):

$$\dot{\vartheta} = \frac{L(I_2\omega_2^2 + I_3\omega_3^2)}{L^2 - I_1^2\omega_1^2} \quad (1.12)$$

The equation for $\dot{\vartheta}$ is valid as long as I_2 is the second largest moment of inertia. The energy E is an important integral of the Euler equations (1.9):

$$E = \frac{1}{2}(I_1\omega_1^2 + I_2\omega_2^2 + I_3\omega_3^2) \quad (1.13)$$

The rotation matrix is computed from the solutions of the Euler-Arnol'd equations as follows (for derivation, see [7]):

$$A(t) = \begin{bmatrix} a_1 & b_1 & c_1 \\ a_2 & b_2 & c_2 \\ a_3 & b_3 & c_3 \end{bmatrix}$$

$$\begin{aligned} a_3 &= \frac{I_1\omega_1}{L}, \\ b_3 &= \frac{I_2\omega_2}{L}, \\ c_3 &= \frac{I_3\omega_3}{L}, \\ a_1 &= \sqrt{1 - a_3^2} \cos \vartheta, \\ a_2 &= \sqrt{1 - a_3^2} \sin \vartheta, \\ b_1 &= -\frac{a_3 b_3 \cos \vartheta + c_3 \sin \vartheta}{\sqrt{1 - a_3^2}}, \\ b_2 &= \frac{c_3 \cos \vartheta - a_3 b_3 \sin \vartheta}{\sqrt{1 - a_3^2}}, \\ c_1 &= -\frac{a_3 c_3 \cos \vartheta - b_3 \sin \vartheta}{\sqrt{1 - a_3^2}}, \\ c_2 &= -\frac{b_3 \cos \vartheta + a_3 c_3 \sin \vartheta}{\sqrt{1 - a_3^2}}. \end{aligned} \quad (1.14)$$

These equations are valid as long as $a_3 \neq 0$ (or equivalently, $\omega_1 \neq 0$). The case when $\omega_1 = 0$ is trivial.

1.5 Herpolhode

1.5.1 Mathematical Analysis

Poinsot [23] showed that the motion of the Euler top can be represented as an ellipsoid fixed at the centre of mass of the Euler top and rolling on a plane perpendicular to the constant angular momentum vector L . This plane is called the *invariable plane* Π . The curve traced by the point of contact of the rolling ellipsoid on the invariable plane is called the *herpolhode*. Its parametric representation can be obtained when the solution $[\omega_1, \omega_2, \omega_3]$ of the Euler equations is transformed to space frame coordinates. Call this vector $[x_h, y_h, z_h]$. This is the angular velocity of the body in the space frame. Here is how the $x_h(t)$ and $y_h(t)$ coordinates of the herpolhode are

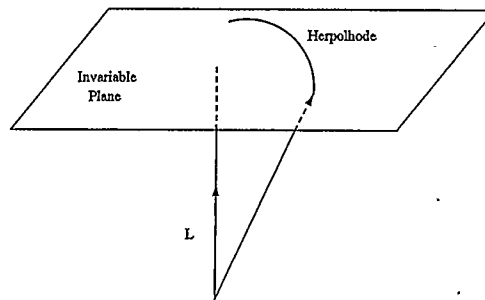


Figure 1.4: Invariable Plane and Herpolhode

computed (see [7] for derivation):

$$\begin{aligned}
x_h &= -\frac{(\omega_1 - \frac{2Ea_3}{L}) \cos \vartheta - (c_3\omega_2 - b_3\omega_3) \sin \vartheta}{\sqrt{1-a_3^2}}, \\
y_h &= -\frac{(c_3\omega_2 - b_3\omega_3) \cos \vartheta + (\omega_1 - \frac{2Ea_3}{L}) \sin \vartheta}{\sqrt{1-a_3^2}}.
\end{aligned} \tag{1.15}$$

Here E is the total energy of the Euler Top (1.13). The remaining variables can be computed from (1.9), (1.12) and (1.14).

If the rotation matrix $A(t)$ is known, then the coordinates of the herpolhode can be computed using the following formulas:

$$\begin{aligned}
x_h &= a_1\omega_1 + b_1\omega_2 + c_1\omega_3 \\
y_h &= a_2\omega_1 + b_2\omega_2 + c_2\omega_3
\end{aligned} \tag{1.16}$$

The path of the herpolhode always remains in an annular region between two circles C_{min} and C_{max} . As the time t increases, the herpolhode follows a locally convex curve (when the 3 principal moments of inertia have physically realizable values) that alternately touches C_{min} and C_{max} . Let r_{min} be the radius of C_{min} and r_{max} be the radius of C_{max} . Cushman and Bates [7] have shown how to calculate r_{min} and r_{max} . If $I_1 > I_2 > I_3$ then r_{max} is calculated to be:

$$r_{max} = \frac{2}{L} \sqrt{\left(\frac{L^2}{2I_3} - E\right)\left(E - \frac{L^2}{2I_1}\right)}. \tag{1.17}$$

If $I_1 < I_2 < I_3$ then r_{max} is calculated to be:

$$r_{max} = \frac{2}{L} \sqrt{\left(\frac{L^2}{2I_1} - E\right)\left(E - \frac{L^2}{2I_3}\right)}. \tag{1.18}$$

When $L^2 - 2I_2E = 0$, the modulus k (and the parameter $m = k^2$) of the Jacobian elliptic functions equals one. r_{min} depends on the sign of $L^2 - 2I_2E$ and on whether $I_1 > I_2 > I_3$ or $I_1 < I_2 < I_3$.

Let $I_1 > I_2 > I_3$. If $L^2 - 2I_2E > 0$, the formula for r_{min} is (see [7] for derivation):

$$r_{min} = \frac{2}{L} \sqrt{\left(\frac{L^2}{2I_2} - E\right)\left(E - \frac{L^2}{2I_1}\right)}. \tag{1.19}$$

If $L^2 - 2I_2E < 0$, then r_{min} is given by:

$$r_{min} = \frac{2}{L} \sqrt{\left(\frac{L^2}{2I_3} - E\right)\left(E - \frac{L^2}{2I_2}\right)} \quad (1.20)$$

Now let $I_1 < I_2 < I_3$. If $L^2 - 2I_2E > 0$, the formula for r_{min} is (see [7] for derivation):

$$r_{min} = \frac{2}{L} \sqrt{\left(\frac{L^2}{2I_1} - E\right)\left(E - \frac{L^2}{2I_2}\right)} \quad (1.21)$$

If $L^2 - 2I_2E < 0$, then r_{min} is given by:

$$r_{min} = \frac{2}{L} \sqrt{\left(\frac{L^2}{2I_2} - E\right)\left(E - \frac{L^2}{2I_3}\right)} \quad (1.22)$$

Cushman and Bates [7] further prove that the time it takes for the herpolhode to reach C_{max} twice equals the period τ of two of the three Jacobi elliptic functions that are the solutions to the Euler equations (1.9). In addition, numerical experiments suggest that the time between two successive maximums of the herpolhode radius is $\frac{\tau}{2}$.

1.5.2 Computing the Herpolhode Coordinates

Let ξ be the angle swept by the herpolhode after time t , and $\xi(0) = 0$. Numerically, this angle can be computed as follows. Let $R(t) = r(t)^2 = x_h(t)^2 + y_h(t)^2$. Since the computer program computes discrete points, it is not always possible to determine whether $r(t) = r_{max}$. Moreover, the very time when this happens can be missed due to the step size. Thus, another approach is taken. Note that all the relative maximums of $R(t)$ coincide with its absolute maximum (that is, when the herpolhode moves toward C_{max} it never starts going back to C_{min} before reaching C_{max} first).

(Likewise, the relative minimums of $R(t)$ coincide with its absolute minimum but this is not important from computational viewpoint). The computer program tracks 3 consecutive herpolhode points at a time. Let $R(t)$ at each of these points be equal to $R_1 = R(t), R_2 = R(t - dt)$ and $R_3 = R(t - 2dt)$ where dt is an infinitesimal change in time t . Therefore R_1 "leads" while R_3 "trails". When $R_1 > R_2 > R_3$ the herpolhode is moving toward the outer circle. At the time when R reaches its maximum, $R_2 > R_1$ and $R_2 > R_3$. It is at this time that the herpolhode is tangent to the outer circle and the coordinates are recorded. Afterwards, several logical true/false switches determine whether the herpolhode touches the outer circle again (in which case nothing is recorded) and then once again (in which case the time and coordinates are recorded). The angle swept by the herpolhode is recorded from the very beginning and at each time step this angle increases by the appropriate amount $d\xi$ as determined by the two leading points (x_{h1}, y_{h1}) and (x_{h2}, y_{h2}) : $d\xi = \arccos \frac{x_{h1}x_{h2} + y_{h1}y_{h2}}{\sqrt{(x_{h1}^2 + y_{h1}^2)(x_{h2}^2 + y_{h2}^2)}}$

1.5.3 The Herpolhode: Numerical Examples

Shown below are several graphs that can help us understand the motion of the Euler top. There are four cases to be considered:

1. $I_1 > I_2 > I_3$ and $L^2 - 2I_2E < 0$

2. $I_1 > I_2 > I_3$ and $L^2 - 2I_2E > 0$

3. $I_1 < I_2 < I_3$ and $L^2 - 2I_2E < 0$

4. $I_1 < I_2 < I_3$ and $L^2 - 2I_2E > 0$

For each of these cases, there are three graphs:

1. Herpolhode. Note that the motion in all herpolhode graphs is *counterclockwise*.

The time that it takes the herpolhode to reach the outer circle twice is found.

2. $[\omega_1, \omega_2, \omega_3]$ as functions of time. Obviously, the solutions are the Jacobian elliptic functions sn, cn and dn. The period τ of two of them equals the time it takes the herpolhode to reach the outer circle twice.

3. Herpolhode angle ξ and projection angle ϑ as functions of time. In two cases, the two graphs almost overlap and the difference $(\xi(t_3) - \xi(t_1)) - (\vartheta(\tau) - \vartheta(0))$ is zero. In the other two cases the two graphs show different trends and this difference is $\pm 2\pi$.

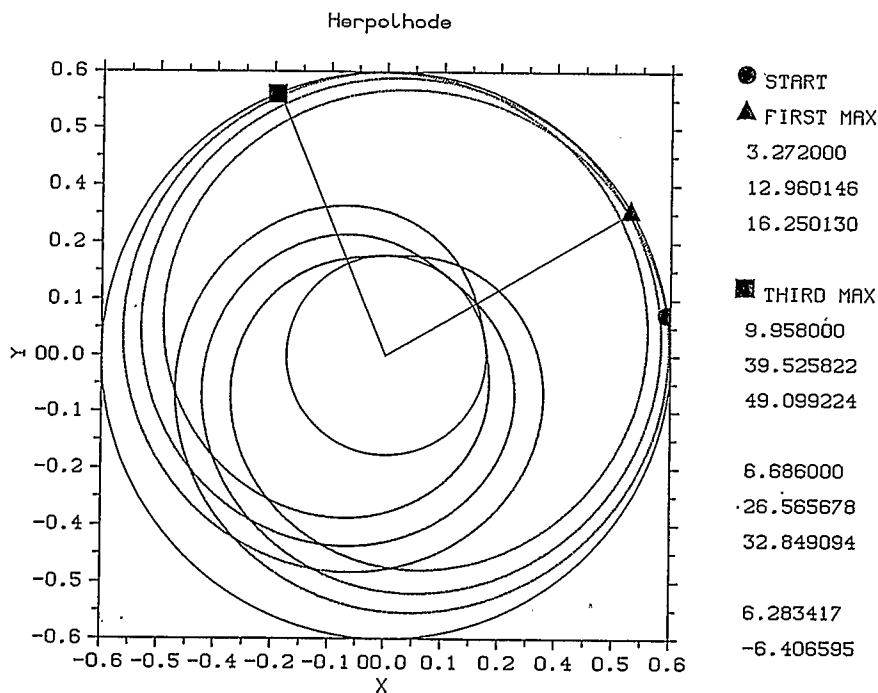


Figure 1.5: Herpolhode

Parameters:

Principal moments of inertia: $I_1 = 4, I_2 = 2.2, I_3 = 2$ Angular momentum in the space frame: $L = 10$ Initial Euler frame: $\theta = 15, \phi = 0, \psi = 10$

Output:

First time when herpolhode radius reaches its maximum: $t_1 = 3.272$ Angle swept by herpolhode from $t = 0$ to $t = t_1$: $\xi(t_1) = 12.960146$ radiansAngle ϑ when $t = t_1$: $\vartheta(t_1) = 16.250130$ radiansThird time when herpolhode radius reaches its maximum: $t_3 = 9.958$ Angle swept by herpolhode from $t = 0$ to $t = t_3$: $\xi(t_3) = 39.525822$ radiansAngle ϑ when $t = t_3$: $\vartheta(t_3) = 49.099224$ radiansPeriod of Jacobian elliptic functions = $t_3 - t_1 = 6.686$ Change in herpolhode angle from t_1 to t_3 : $\xi(t_3) - \xi(t_1) = 26.565678$ radiansChange in ϑ from t_1 to t_3 : $\vartheta(t_3) - \vartheta(t_1) = 32.849094$ radiansDifference between change in ϑ and change in herpolhode angle = $6.283417 = 2\pi$ Value of $L^2 - 2I_2E = -6.406595$

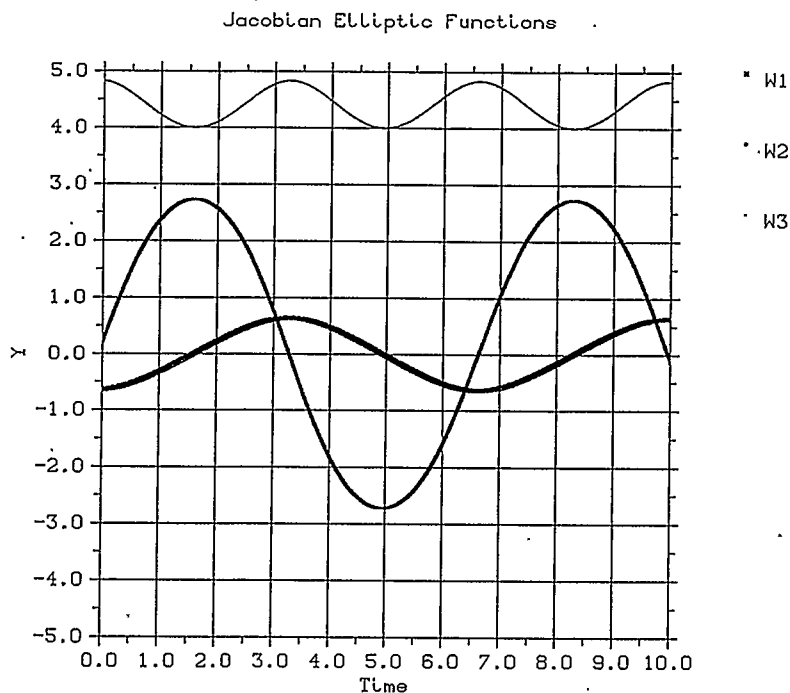


Figure 1.6: Jacobi Elliptic Functions vs. Time

Parameters:

Principal moments of inertia: $I_1 = 4, I_2 = 2.2, I_3 = 2$

Angular momentum in the space frame: $L = 10$

Initial Euler frame: $\theta = 15, \phi = 0, \psi = 10$

Calculation of the period τ of sn and cn:

$$\begin{aligned}
 k &= \sqrt{\frac{(I_1 - I_2)(L^2 - 2I_3 E)}{(I_2 - I_3)(2I_1 E - L^2)}} = 0.561 \\
 n &= \sqrt{\frac{(I_2 - I_3)(2I_1 E - L^2)}{I_1 I_2 I_3}} = 1.031 \\
 \tau &= \frac{4}{n} K(k) = 6.685
 \end{aligned} \tag{1.23}$$

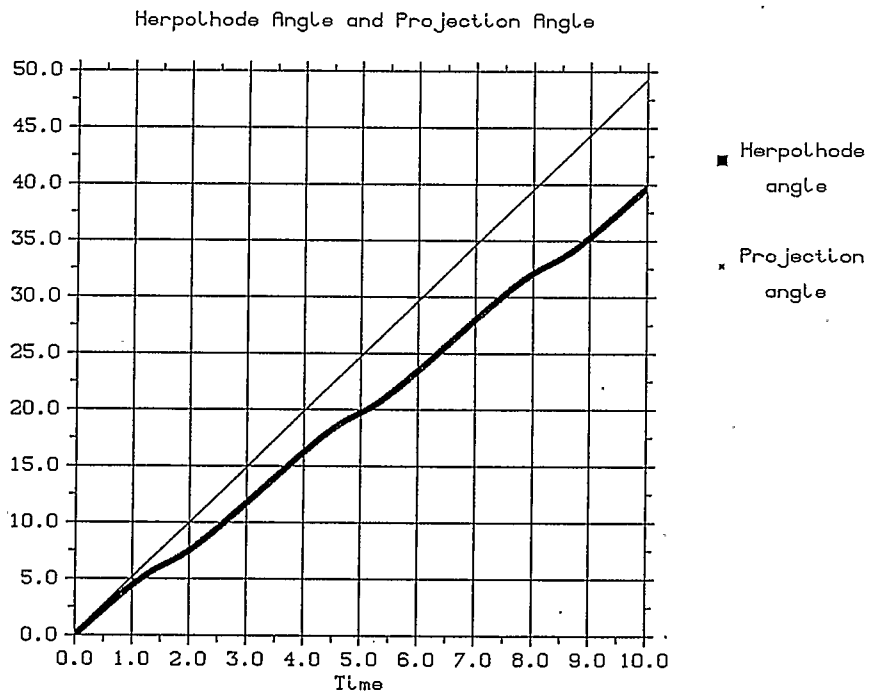


Figure 1.7: Herpolhode Angle ξ and Projection Angle ϑ as Functions of Time

Parameters:

Principal moments of inertia: $I_1 = 4, I_2 = 2.2, I_3 = 2$

Angular momentum in the space frame: $L = 10$

Initial Euler frame: $\theta = 15, \phi = 0, \psi = 10$

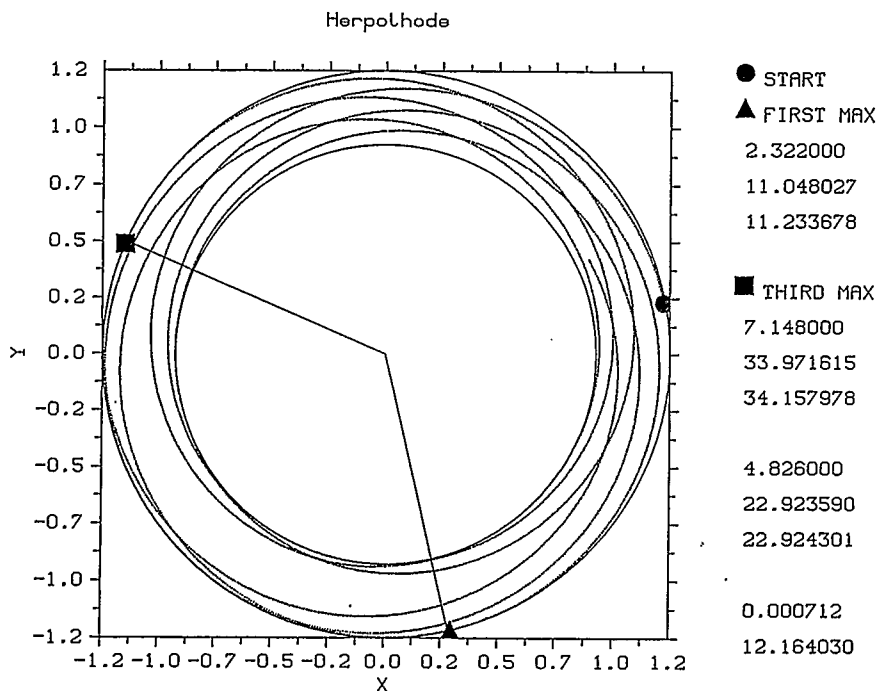


Figure 1.8: Herpolhode

Parameters:

Principal moments of inertia: $I_1 = 4, I_2 = 2.2, I_3 = 2$ Angular momentum in the space frame: $L = 10$ Initial Euler frame: $\theta = 40, \phi = 0, \psi = 10$

Output:

First time when herpolhode radius reaches its maximum: $t_1 = 2.322$ Angle swept by herpolhode from $t = 0$ to $t = t_1$: $\xi(t_1) = 11.048027$ radiansAngle ϑ when $t = t_1$: $\vartheta(t_1) = 11.233678$ radiansThird time when herpolhode radius reaches its maximum: $t_3 = 7.148$ Angle swept by herpolhode from $t = 0$ to $t = t_3$: $\xi(t_3) = 33.971615$ radiansAngle ϑ when $t = t_3$: $\vartheta(t_3) = 34.157978$ radiansPeriod of Jacobian elliptic functions = $t_3 - t_1 = 4.826$ Change in herpolhode angle from t_1 to t_3 = $\xi(t_3) - \xi(t_1) = 22.923590$ radiansChange in ϑ from t_1 to t_3 = $\vartheta(t_3) - \vartheta(t_1) = 22.924301$ radiansDifference between change in ϑ and change in herpolhode angle = 0.000712Value of $L^2 - 2I_2E = 12.164030$

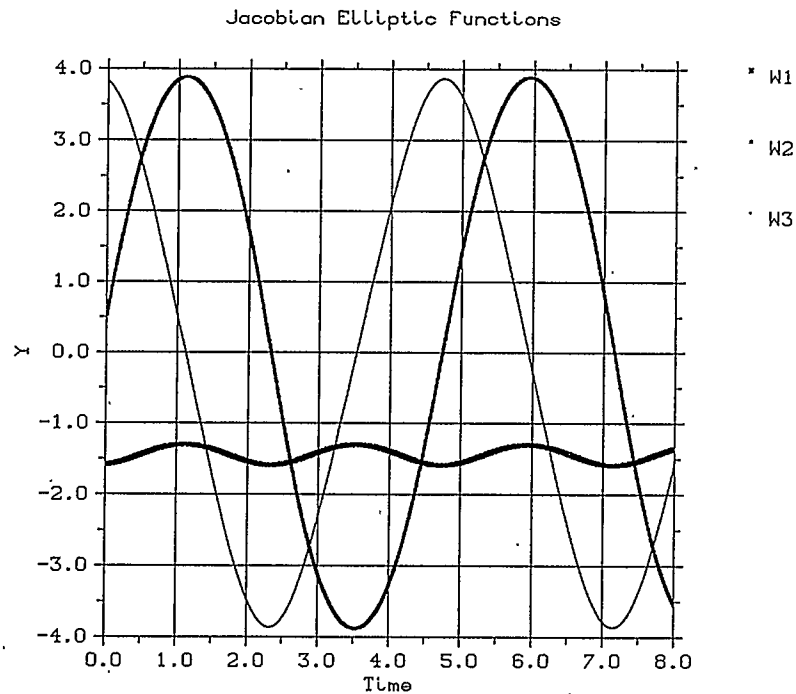


Figure 1.9: Jacobi Elliptic Functions vs. Time
Parameters:

Principal moments of inertia: $I_1 = 4, I_2 = 2.2, I_3 = 2$

Angular momentum in the space frame: $L = 10$

Initial Euler frame: $\theta = 40, \phi = 0, \psi = 10$

Calculation of the period τ of sn and cn:

$$\begin{aligned}
 k &= \sqrt{\frac{(I_2 - I_3)(2I_1 E - L^2)}{(I_1 - I_2)(L^2 - 2I_3 E)}} = 0.574 \\
 n &= \sqrt{\frac{(I_1 - I_2)(L^2 - 2I_3 E)}{I_1 I_2 I_3}} = 1.436 \\
 \tau &= \frac{4}{n} K(k) = 4.824
 \end{aligned} \tag{1.24}$$

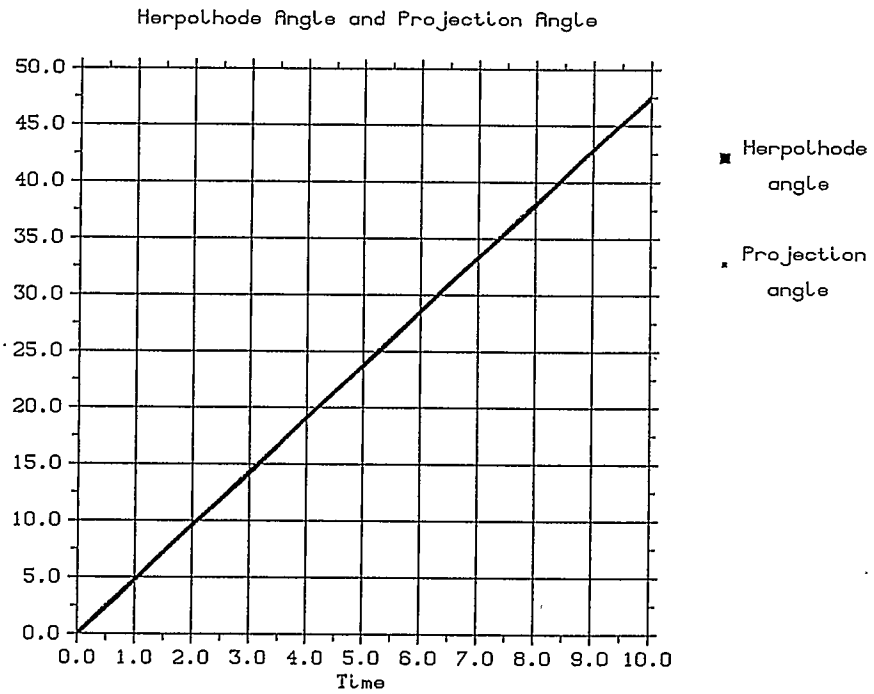


Figure 1.10: Herpolhode Angle ξ and Projection Angle ϑ as Functions of Time

Parameters:

Principal moments of inertia: $I_1 = 4, I_2 = 2.2, I_3 = 2$

Angular momentum in the space frame: $L = 10$

Initial Euler frame: $\theta = 40, \phi = 0, \psi = 10$

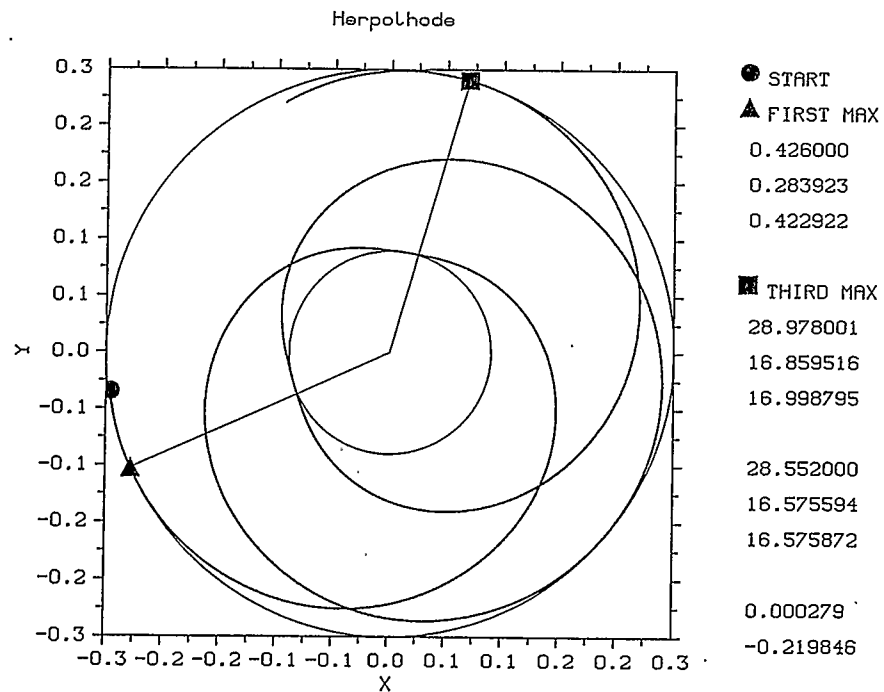


Figure 1.11: Herpolhode

Parameters:

Principal moments of inertia: $I_1 = 2, I_2 = 3, I_3 = 4.8$ Angular momentum in the space frame: $L = 2$ Initial Euler frame: $\theta = 45, \phi = 0, \psi = 10$

Output:

First time when herpolhode radius reaches its maximum: $t_1 = 0.426$ Angle swept by herpolhode from $t = 0$ to $t = t_1$: $\xi(t_1) = 0.283923$ radiansAngle ϑ when $t = t_1$: $\vartheta(t_1) = 0.422922$ radiansThird time when herpolhode radius reaches its maximum: $t_3 = 28.978001$ Angle swept by herpolhode from $t = 0$ to $t = t_3$: $\xi(t_3) = 16.859516$ radiansAngle ϑ when $t = t_3$: $\vartheta(t_3) = 16.998795$ radiansPeriod of Jacobian elliptic functions = $t_3 - t_1 = 28.552$ Change in herpolhode angle from t_1 to $t_3 = \xi(t_3) - \xi(t_1) = 16.575594$ radiansChange in ϑ from t_1 to $t_3 = \vartheta(t_3) - \vartheta(t_1) = 16.575872$ radiansDifference between change in ϑ and change in herpolhode angle = 0.000279Value of $L^2 - 2I_2E = -0.219846$

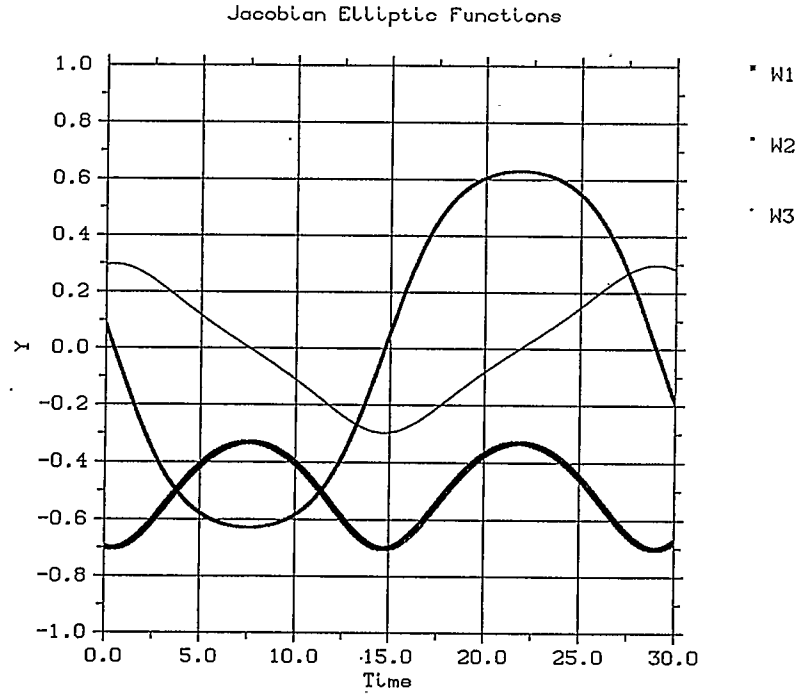


Figure 1.12: Jacobi Elliptic Functions vs. Time

Parameters:

Principal moments of inertia: $I_1 = 2, I_2 = 3, I_3 = 4.8$

Angular momentum in the space frame: $L = 2$

Initial Euler frame: $\theta = 45, \phi = 0, \psi = 10$

Calculation of the period τ of sn and cn:

$$\begin{aligned}
 k &= \sqrt{\frac{(I_3 - I_2)(L^2 - 2I_1 E)}{(I_2 - I_1)(2I_3 E - L^2)}} = 0.881 \\
 n &= \sqrt{\frac{(I_2 - I_1)(2I_3 E - L^2)}{I_1 I_2 I_3}} = 0.309 \\
 \tau &= \frac{4}{n} K(k) = 28.553
 \end{aligned}
 \tag{1.25}$$

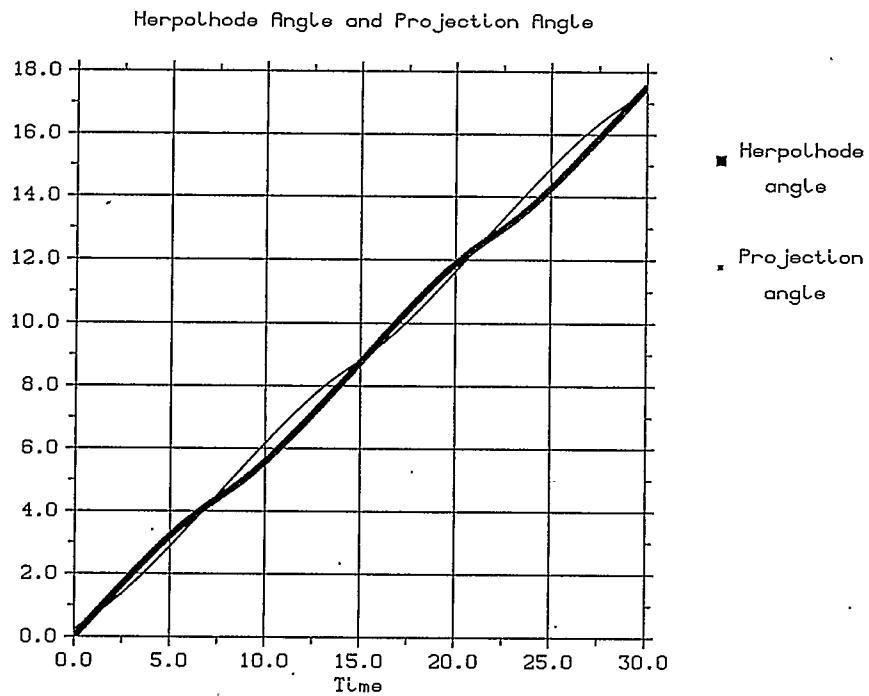


Figure 1.13: Herpolhode Angle ξ and Projection Angle ϑ as Functions of Time
 Parameters:

Principal moments of inertia: $I_1 = 2, I_2 = 3, I_3 = 4.8$

Angular momentum in the space frame: $L = 10$

Initial Euler frame: $\theta = 45, \phi = 0, \psi = 10$

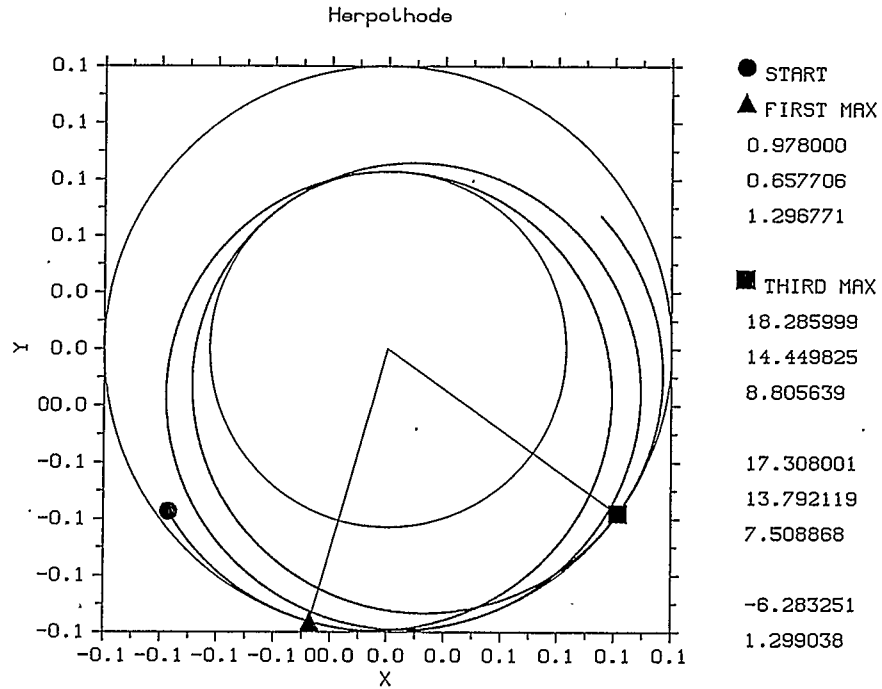


Figure 1.14: Herpolhode

Parameters:

Principal moments of inertia: $I_1 = 2, I_2 = 3, I_3 = 4.8$ Angular momentum in the space frame: $L = 2$ Initial Euler frame: $\theta = 15, \phi = 20, \psi = 30$

Output:

First time when herpolhode radius reaches its maximum: $t_1 = 0.978$ Angle swept by herpolhode from $t = 0$ to $t = t_1$: $\xi(t_1) = 0.657706$ radiansAngle ϑ when $t = t_1$: $\vartheta(t_1) = 1.296771$ radiansThird time when herpolhode radius reaches its maximum: $t_3 = 18.285999$ Angle swept by herpolhode from $t = 0$ to $t = t_3$: $\xi(t_3) = 14.449825$ radiansAngle ϑ when $t = t_3$: $\vartheta(t_3) = 8.805639$ radiansPeriod of Jacobian elliptic functions = $t_3 - t_1 = 17.308001$ Change in herpolhode angle from t_1 to t_3 = $\xi(t_3) - \xi(t_1) = 13.792119$ radiansChange in ϑ from t_1 to t_3 = $\vartheta(t_3) - \vartheta(t_1) = 7.508868$ radiansDifference between change in ϑ and change in herpolhode angle = $-6.283251 = -2\pi$ Value of $L^2 - 2I_2E = 1.299038$

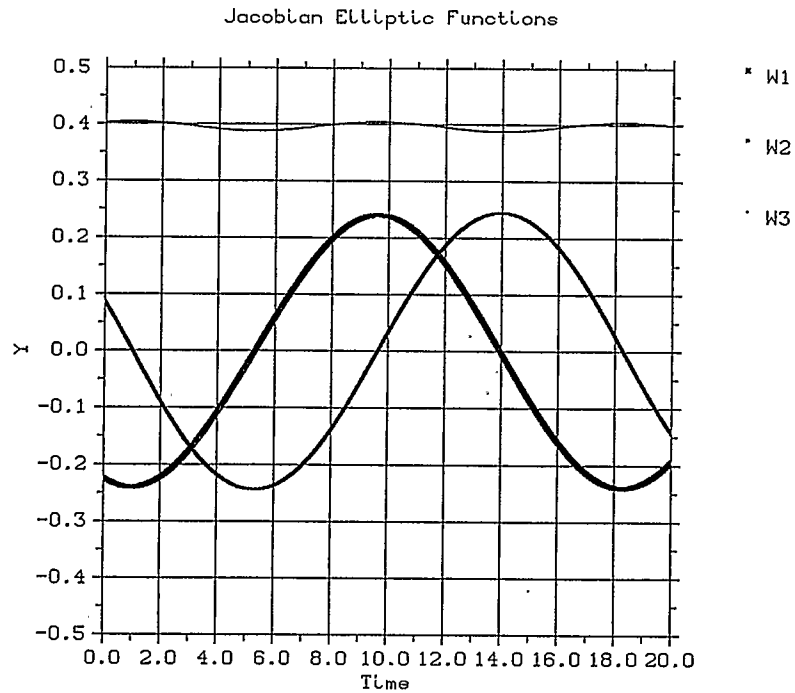


Figure 1.15: Jacobi Elliptic Functions vs. Time
Parameters:

Principal moments of inertia: $I_1 = 2, I_2 = 3, I_3 = 4.8$

Angular momentum in the space frame: $L = 2$

Initial Euler frame: $\theta = 15, \phi = 20, \psi = 30$

Calculation of the period τ of sn and cn:

$$\begin{aligned}
 k &= \sqrt{\frac{(I_2 - I_1)(2I_3 E - L^2)}{(I_3 - I_2)(L^2 - 2I_1 E)}} = 0.285 \\
 n &= \sqrt{\frac{(I_3 - I_2)(L^2 - 2I_1 E)}{I_1 I_2 I_3}} = 0.371 \\
 \tau &= \frac{4}{n} K(k) = 17.308
 \end{aligned}
 \tag{1.26}$$

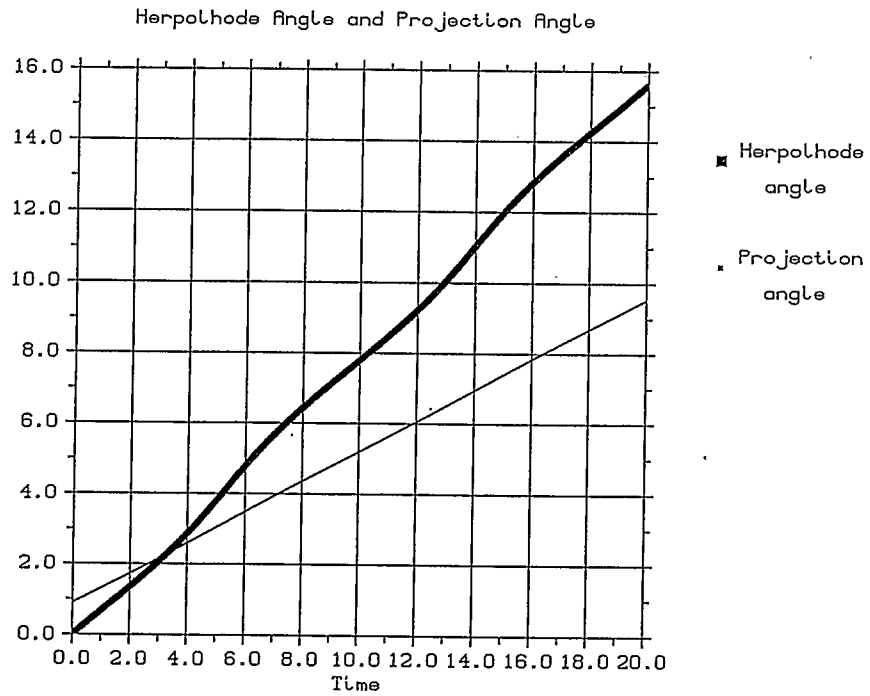


Figure 1.16: Herpolhode Angle ξ and Projection Angle ϑ as Functions of Time
Parameters:

Principal moments of inertia: $I_1 = 2, I_2 = 3, I_3 = 4.8$

Angular momentum in the space frame: $L = 10$

Initial Euler frame: $\theta = 15, \phi = 20, \psi = 30$

1.5.4 Discussion of the Numerical Examples

According to Montgomery [21], the difference $\vartheta(\tau) - \vartheta(0)$ equals the angle swept by the herpolhode between two successive maximums of its radius. However, according to Cushman [7], it is the angle swept by the herpolhode between every *other* maximum $\xi(t_3) - \xi(t_1)$ that equals $\vartheta(\tau) - \vartheta(0)$ (where t_1 is the time of first maximum, t_3 is the time of third maximum and ξ is the herpolhode angle swept since the beginning of motion). The numerical experiments in the previous section suggest that this is not always the case depending on the moments of inertia and the initial conditions:

1. $I_1 > I_2 > I_3$ and $L^2 - 2I_2E < 0$ (see Figures 1.5,1.6,1.7)

In this case, $\xi(t_3) - \xi(t_1) = \vartheta(\tau) - \vartheta(0) - 2\pi$

2. $I_1 > I_2 > I_3$ and $L^2 - 2I_2E > 0$ (see Figures 1.8,1.9,1.10)

In this case, $\xi(t_3) - \xi(t_1) = \vartheta(\tau) - \vartheta(0)$

3. $I_1 < I_2 < I_3$ and $L^2 - 2I_2E < 0$ (see Figures 1.11,1.12,1.13)

In this case, $\xi(t_3) - \xi(t_1) = \vartheta(\tau) - \vartheta(0)$

4. $I_1 < I_2 < I_3$ and $L^2 - 2I_2E > 0$ (see Figures 1.14,1.15,1.16)

In this case, $\xi(t_3) - \xi(t_1) = \vartheta(\tau) - \vartheta(0) + 2\pi$

L. Bates and R. Cushman, in several conversations with the author, have suggested an explanation for the observed phenomena which will be discussed in the next section.

1.6 Solid Ball Model

1.6.1 Mathematical Analysis

To better visualize how the rotations change in time, the solid ball model is used. To describe a rotation $A(t)$, one needs an axis of rotation and an angle of rotation, noting that a rotation of π radians is identical to a rotation of $-\pi$ radians. The axis of rotation can be represented by a 3-dimensional unit vector $[r_1, r_2, r_3]$. When this unit vector is multiplied by the angle of rotation ζ , a new vector is obtained that has a magnitude between 0 and π . Hence each element of $SO(3)$ can be represented as a 3-dimensional point in a "solid ball" of radius π . Topologically, every two opposite points of the boundary of the solid ball are identified. Suppose that at a given time t , we have computed the rotation matrix $A(t)$. Then the 3-dimensional point of the

solid ball model is computed as follows (for derivation, see [7]):

$$\begin{aligned}
 \text{trace}(A) &= a_1 + b_2 + c_3, \\
 \zeta &= \arccos \frac{\text{trace}(A)-1}{2}, \\
 r_1 &= \frac{b_3 - c_2}{2 \sin \zeta}, \\
 r_2 &= \frac{c_1 - a_3}{2 \sin \zeta}, \\
 r_3 &= \frac{a_2 - b_1}{2 \sin \zeta}, \\
 x_r &= r_1 \zeta, \\
 y_r &= r_2 \zeta, \\
 z_r &= r_3 \zeta.
 \end{aligned} \tag{1.27}$$

Here $[r_1, r_2, r_3]$ is a vector of norm 1 which specifies the direction of the axis of rotation, while ζ indicates the amount of rotation about that axis which can be between 0 and π . Thus, the point $[x_r, y_r, z_r]$ completely describes the instantaneous rotation at a time t .

1.6.2 Explanation of the Herpolhode Results

While the Solid Ball model describes the motion of the Euler top, this does not mean that the motion would pass through *every* point of $SO(3)$. The *configuration space* is the tangent bundle $TSO(3)$ which is a 6-dimensional manifold diffeomorphic to $R^3 \times SO(3)$. $L = \text{constant}$ is an *invariant submanifold* in $TSO(3)$ (meaning that if the motion started along this submanifold, it would stay there). This submanifold is 3-dimensional and has the topology of $SO(3)$. The energy E is also constant. Therefore the level set $\{E = \text{constant} \cap L = \text{constant}\}$ is a 2-dimensional submanifold imbedded in $SO(3)$. It is along this invariant submanifold that the motion of the Euler top takes place. This 2-dimensional manifold is compact and orientable,

therefore it can be represented as a sphere with $\frac{2-\chi}{2}$ handles where χ is the Euler characteristic of the surface. Since $E > 0$, the vector field along this manifold is nonvanishing. Hence the Euler characteristic χ of the surface must be zero and so the surface must be a *torus* imbedded in $SO(3)$. If the torus is defined abstractly as the points of a square with opposite sides identified, one cannot distinguish between the two circles C_1 and C_2 that form the basis of the torus. So the information that the torus is imbedded in $SO(3)$ is important because it allows one to distinguish between *latitude* and *longitude*, as the next two figures illustrate.

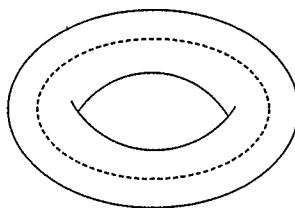


Figure 1.17: Longitudinal circle along the torus

This circle is not the boundary of a disk in a solid torus imbedded in $SO(3)$ and cannot be continuously deformed to a point

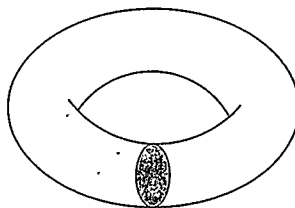


Figure 1.18: Latitudinal circle along the torus

This circle is the boundary of a disk in a solid torus imbedded in $SO(3)$ and can be continuously deformed to a point

Depending on the sign of the value of $L^2 - 2I_2E$ and depending on whether

$I_1 > I_2 > I_3$ or $I_1 < I_2 < I_3$, the motion along the torus can be longitudinal or latitudinal.

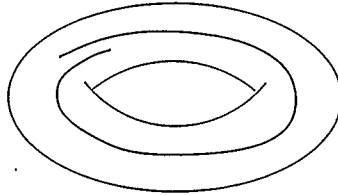


Figure 1.19: Longitudinal motion along the torus

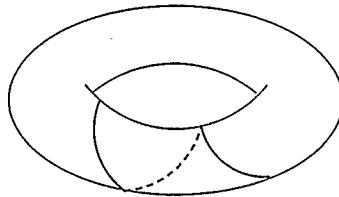


Figure 1.20: Latitudinal motion along the torus

Recall that $\xi(t)$ equals the angle that the herpolhode has swept after time t .

Case 1: $I_1 > I_2 > I_3$

1.1: $L^2 - 2I_2E < 0$ (see Figures 1.21,1.22,1.23,1.5,1.6,1.7)

In this case, the motion along the torus is longitudinal and the angle $\xi(t)$ lags behind $\vartheta(t)$ so that $\xi(t_3) - \xi(t_1) = \vartheta(\tau) - \vartheta(0) - 2\pi$.

1.2: $L^2 - 2I_2E > 0$ (see Figures 1.24,1.25,1.26,1.8,1.9,1.10)

In this case, the motion along the torus is latitudinal and $\xi(t_3) - \xi(t_1) = \vartheta(\tau) - \vartheta(0)$.

Case 2: $I_1 < I_2 < I_3$

2.1: $L^2 - 2I_2E < 0$ (see Figures 1.27,1.28,1.29,1.11,1.12,1.13)

In this case, the motion along the torus is latitudinal and $\xi(t_3) - \xi(t_1) = \vartheta(\tau) - \vartheta(0)$.

2.2: $L^2 - 2I_2E > 0$ (see Figures 1.30,1.31,1.32,1.14,1.15,1.16)

In this case, the motion along the torus is longitudinal and the angle $\xi(t)$ moves ahead of $\vartheta(t)$ so that $\xi(t_3) - \xi(t_1) = \vartheta(\tau) - \vartheta(0) + 2\pi$.

1.6.3 The Torus: Numerical Examples

Shown below are several plots of the projections of the torus on the coordinate planes after some time has elapsed for different parameters. In these numerical simulations, the torus actually looks like a cylinder. Since it is imbedded in the solid ball $SO(3)$ of radius π , a point on the cylinder that is π units away from the origin is identical to the diametrically opposite point - hence what looks like a cylinder is actually a torus. Note the difference between longitudinal and latitudinal motions.

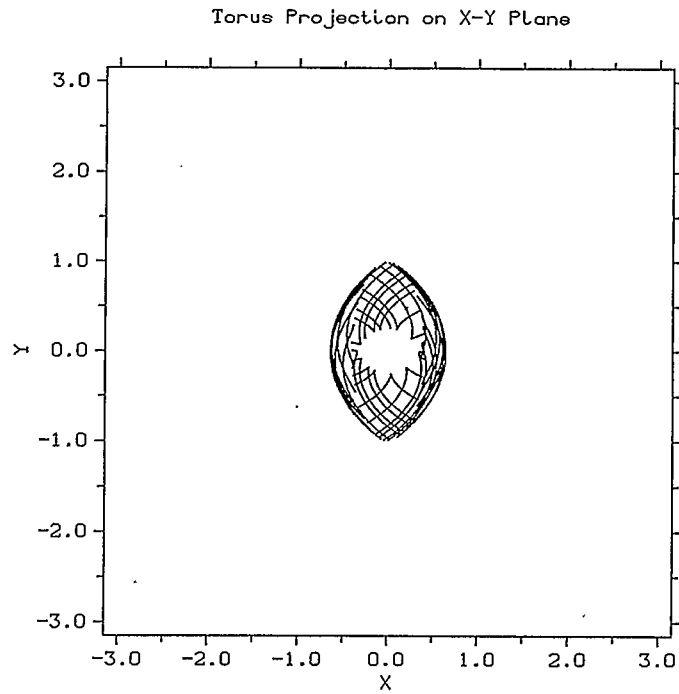


Figure 1.21: Solid Ball Model for the Euler Top
Parameters:

Principal moments of inertia: $I_1 = 4, I_2 = 2.2, I_3 = 2$

Angular momentum in the space frame: $L = 10$

Initial Euler frame: $\theta = 15, \phi = 0, \psi = 10$

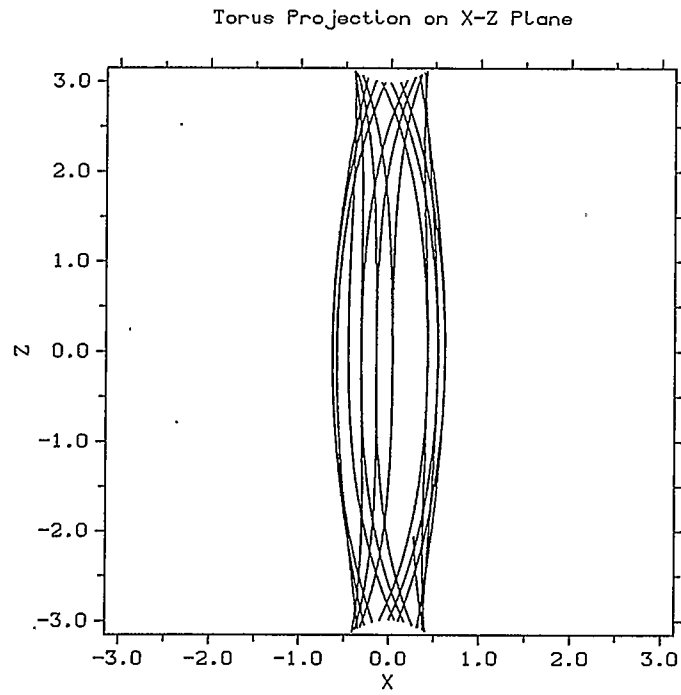


Figure 1.22: Solid Ball Model for the Euler Top
Parameters:

Principal moments of inertia: $I_1 = 4, I_2 = 2.2, I_3 = 2$

Angular momentum in the space frame: $L = 10$

Initial Euler frame: $\theta = 15, \phi = 0, \psi = 10$

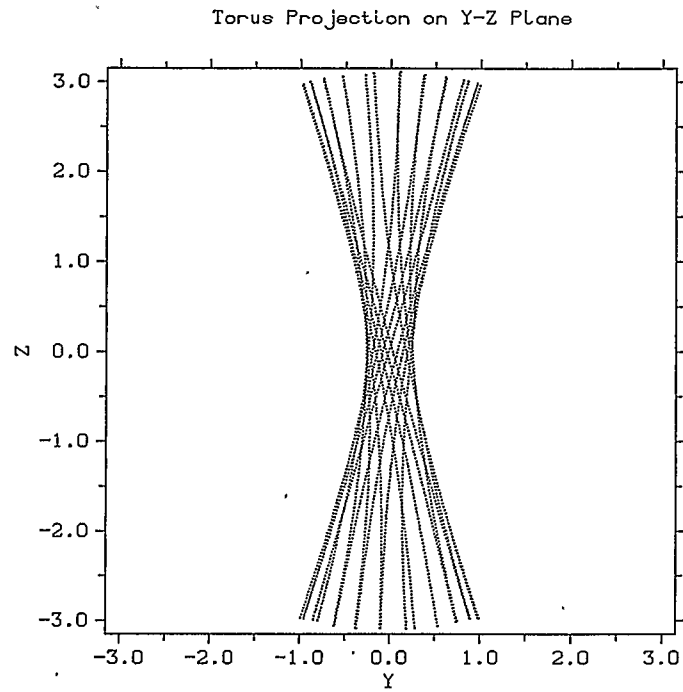


Figure 1.23: Solid Ball Model for the Euler Top
Parameters:

Principal moments of inertia: $I_1 = 4, I_2 = 2.2, I_3 = 2$

Angular momentum in the space frame: $L = 10$

Initial Euler frame: $\theta = 15, \phi = 0, \psi = 10$

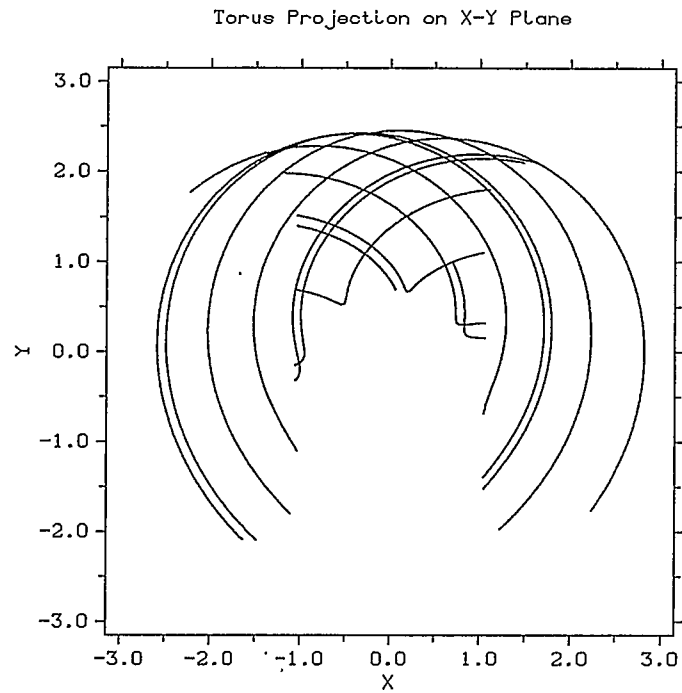


Figure 1.24: Solid Ball Model for the Euler Top
Parameters:

Principal moments of inertia: $I_1 = 4, I_2 = 2.2, I_3 = 2$

Angular momentum in the space frame: $L = 10$

Initial Euler frame: $\theta = 40, \phi = 0, \psi = 10$

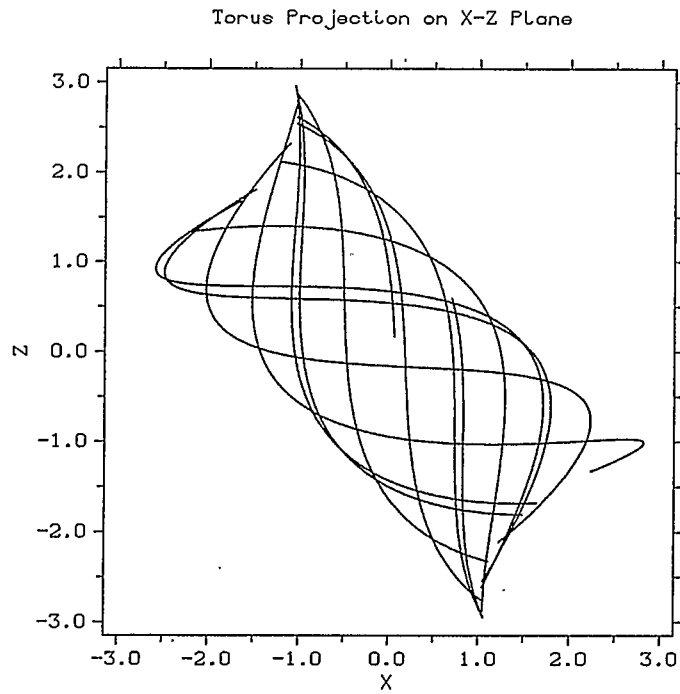


Figure 1.25: Solid Ball Model for the Euler Top

Parameters:

Principal moments of inertia: $I_1 = 4, I_2 = 2.2, I_3 = 2$

Angular momentum in the space frame: $L = 10$

Initial Euler frame: $\theta = 40, \phi = 0, \psi = 10$

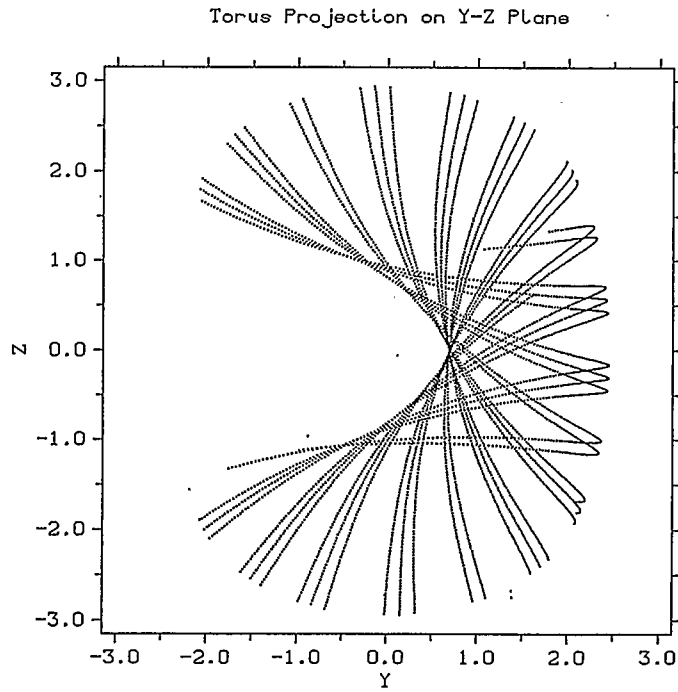


Figure 1.26: Solid Ball Model for the Euler Top
Parameters:

Principal moments of inertia: $I_1 = 4, I_2 = 2.2, I_3 = 2$

Angular momentum in the space frame: $L = 10$

Initial Euler frame: $\theta = 40, \phi = 0, \psi = 10$

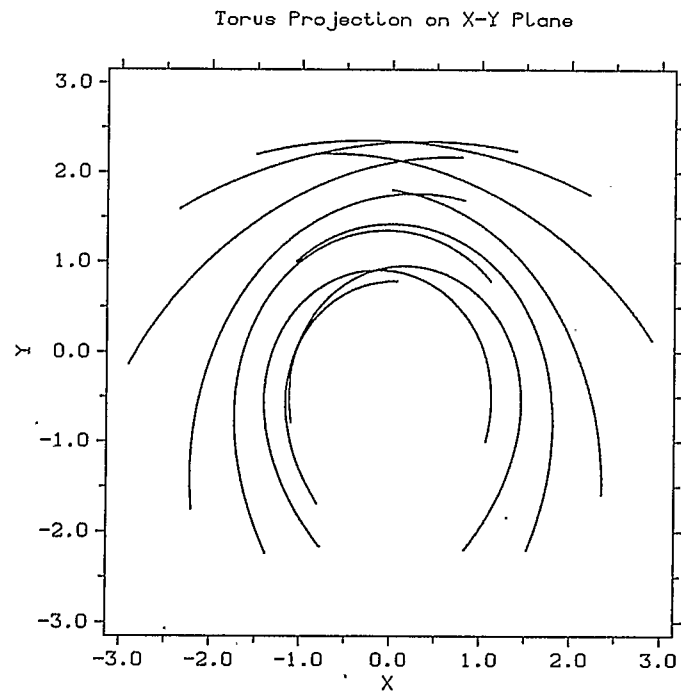


Figure 1.27: Solid Ball Model for the Euler Top
Parameters:

Principal moments of inertia: $I_1 = 2, I_2 = 3, I_3 = 4.8$

Angular momentum in the space frame: $L = 2$

Initial Euler frame: $\theta = 45, \phi = 0, \psi = 10$

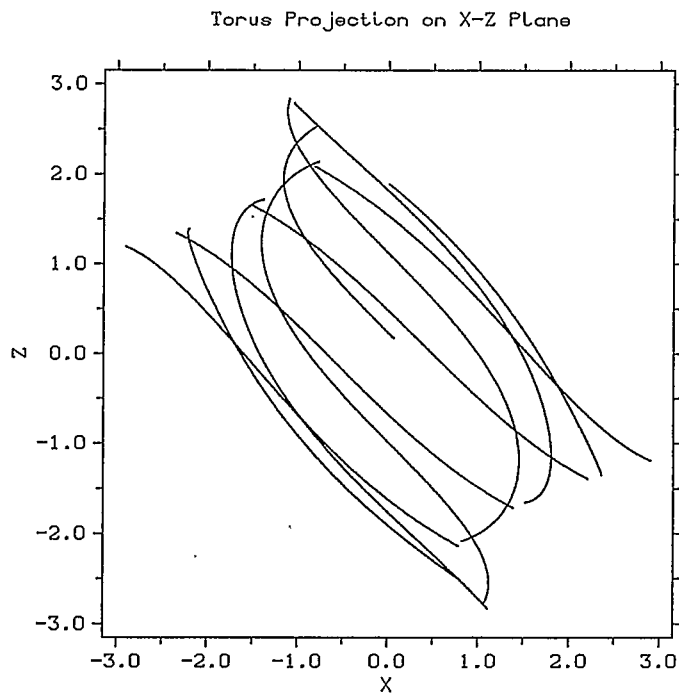


Figure 1.28: Solid Ball Model for the Euler Top

Parameters:

Principal moments of inertia: $I_1 = 2, I_2 = 3, I_3 = 4.8$

Angular momentum in the space frame: $L = 2$

Initial Euler frame: $\theta = 45, \phi = 0, \psi = 10$

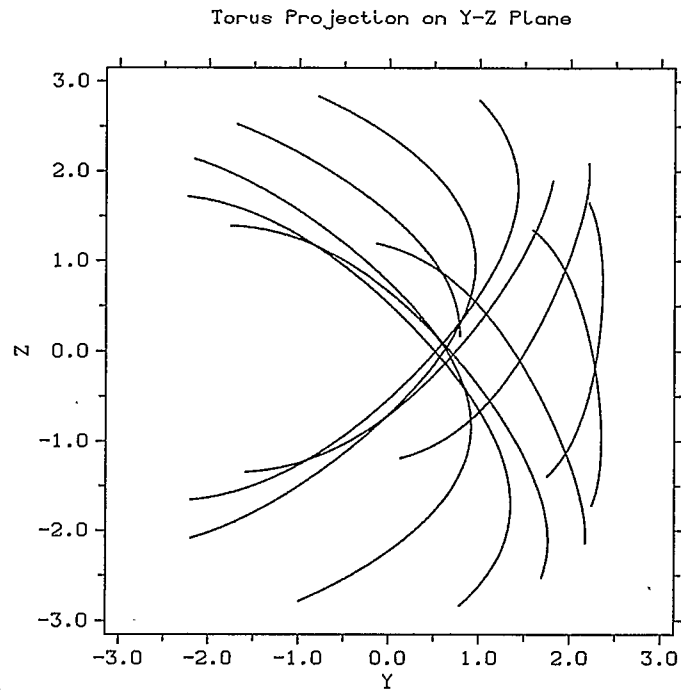


Figure 1.29: Solid Ball Model for the Euler Top
Parameters:

Principal moments of inertia: $I_1 = 2, I_2 = 3, I_3 = 4.8$

Angular momentum in the space frame: $L = 2$

Initial Euler frame: $\theta = 45, \phi = 0, \psi = 10$

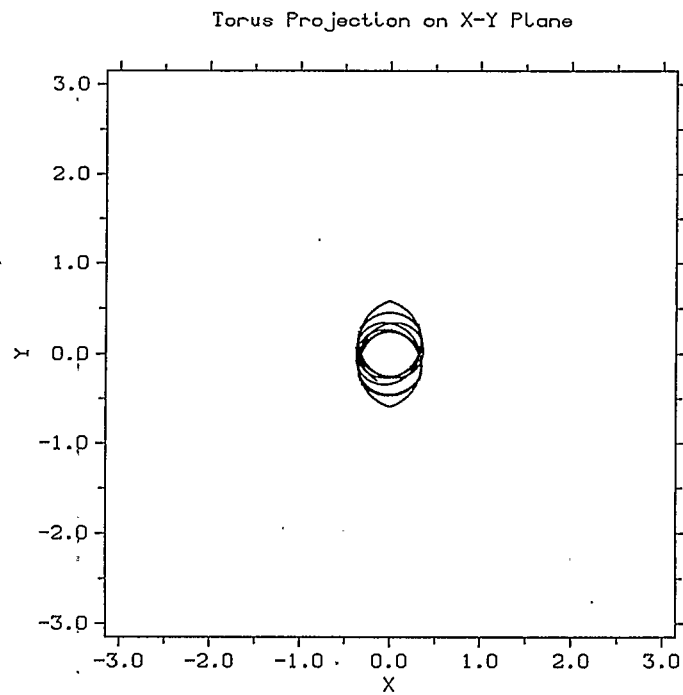


Figure 1.30: Solid Ball Model for the Euler Top
Parameters:

Principal moments of inertia: $I_1 = 2, I_2 = 3, I_3 = 4.8$

Angular momentum in the space frame: $L = 2$

Initial Euler frame: $\theta = 15, \phi = 20, \psi = 30$

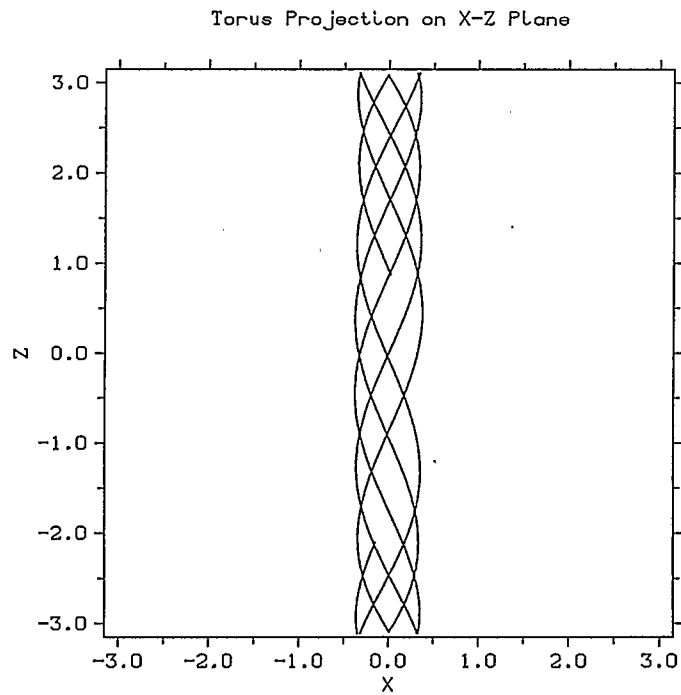


Figure 1.31: Solid Ball Model for the Euler Top

Parameters:

Principal moments of inertia: $I_1 = 2, I_2 = 3, I_3 = 4.8$

Angular momentum in the space frame: $L = 2$

Initial Euler frame: $\theta = 15, \phi = 20, \psi = 30$

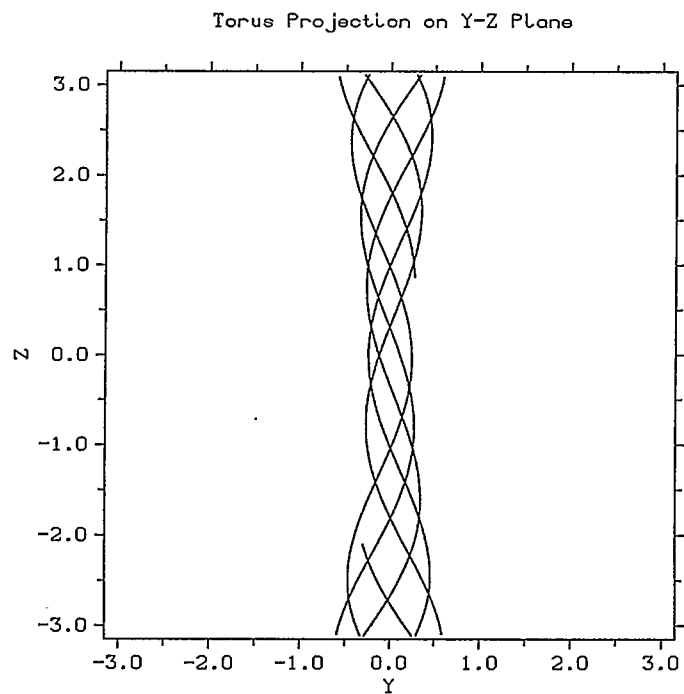


Figure 1.32: Solid Ball Model for the Euler Top
Parameters:

Principal moments of inertia: $I_1 = 2, I_2 = 3, I_3 = 4.8$

Angular momentum in the space frame: $L = 2$

Initial Euler frame: $\theta = 15, \phi = 20, \psi = 30$

Chapter 2

Equations for a Rigid Body Rolling on the Plane

2.1 General Equations

The variables necessary to describe the motion of a rolling rigid body on the plane are $[u_1, u_2, u_3, \omega_1, \omega_2, \omega_3]$. Here ω_1, ω_2 and ω_3 are the magnitudes of the angular velocities about the three principal axes x', y' and z' respectively. u_1, u_2 and u_3 are the components of a unit vector that determines the point of contact between the rigid body and the plane. When energy dissipation and slipping are ignored and using Newton's second law, the equations of motion of a rolling rigid body on the plane are derived to be (see for example ([6], [13]) for derivation):

$$\begin{aligned} \dot{\mathbf{u}} &= \mathbf{u} \times \boldsymbol{\omega} \\ \mathbf{I}\dot{\boldsymbol{\omega}} + M\mathbf{s} \times (\dot{\boldsymbol{\omega}} \times \mathbf{s}) &= M\mathbf{s} \times (\dot{\mathbf{s}} \times \boldsymbol{\omega}) + M\mathbf{s} \times (\boldsymbol{\omega} \times \mathbf{s}) \times \boldsymbol{\omega} + M\mathbf{g}\mathbf{s} \times \mathbf{u} + (\mathbf{I}\boldsymbol{\omega}) \times \boldsymbol{\omega} \end{aligned} \quad (2.1)$$

where

\mathbf{I} = Moment of inertia diagonal matrix

M = Mass of rigid body

g = Downward Acceleration due to Gravity

\mathbf{s} = Inverse of the Gauss map (3-dimensional vector $[x, y, z]$ that is a function of $[u_1, u_2, u_3]$ and depends on the shape of the rigid body.)

The differential equations for \mathbf{u} are:

$$\begin{aligned} \dot{u}_1 &= u_2\omega_3 - u_3\omega_2 \\ \dot{u}_2 &= u_3\omega_1 - u_1\omega_3 \\ \dot{u}_3 &= u_1\omega_2 - u_2\omega_1 \end{aligned} \quad (2.2)$$

The equations for the angular velocities $[\omega_1, \omega_2, \omega_3]$ are more complicated and it is useful to store intermediate values. The vector $\mathbf{s}(\mathbf{u}) = [x, y, z]$ is a function of $[u_1, u_2, u_3]$. The physical meaning of the vector $[x, y, z]$ is that it is the "path" followed by the point of contact along the surface of the rigid body when no rotations or translations are accounted for. The left hand side $\mathbf{I}\dot{\omega} + M\mathbf{s} \times (\dot{\omega} \times \mathbf{s})$ of (2.1) is $T\dot{\omega}$ where T is the matrix:

$$T = \begin{bmatrix} I_1 + My^2 + Mz^2 & -Mxy & -Mxz \\ -Mxy & I_2 + Mx^2 + Mz^2 & -Myz \\ -Mxz & -Myz & I_3 + Mx^2 + My^2 \end{bmatrix} \quad (2.3)$$

The inverse of matrix T is:

$$\frac{1}{D} \begin{bmatrix} I_2I_3 + I_2R_{xy} + I_3R_{xz} + Mx^2R & Mxy(I_3 + R) & Mxz(I_2 + R) \\ Mxy(I_3 + R) & I_1I_3 + I_1R_{xy} + I_3R_{yz} + My^2R & Myz(I_1 + R) \\ Mxz(I_2 + R) & Myz(I_1 + R) & I_1I_2 + I_1R_{xz} + I_2R_{yz} + Mz^2R \end{bmatrix} \quad (2.4)$$

where

$$\begin{aligned} D &= I_1I_2I_3 + M((I_1I_2(x^2 + y^2) + I_1I_3(x^2 + z^2) + I_2I_3(y^2 + z^2)) + M(I_1x^2 + I_2y^2 + I_3z^2)R) \\ R &= M(x^2 + y^2 + z^2) \\ R_{xy} &= M(x^2 + y^2) \\ R_{xz} &= M(x^2 + z^2) \\ R_{yz} &= M(y^2 + z^2) \end{aligned} \quad (2.5)$$

Now we'll compute the terms of the right hand side of equation (2.1). The term $\mathbf{I}\omega \times \omega$ is:

$$[(I_2 - I_3)\omega_2\omega_3, (I_3 - I_1)\omega_1\omega_3, (I_1 - I_2)\omega_1\omega_2] \quad (2.6)$$

The term $Mg\mathbf{s} \times \mathbf{u}$ equals:

$$[Mgyu_3 - Mgz u_2, Mgz u_1 - Mgx u_3, Mgx u_2 - Mgy u_1] \quad (2.7)$$

The term $M\mathbf{s} \times (\boldsymbol{\omega} \times \mathbf{s}) \times \boldsymbol{\omega}$ equals:

$$\begin{bmatrix} M(y\omega_2^2 z - \omega_2\omega_3 y^2 - y\omega_1\omega_3 x + z\omega_1\omega_2 x + \omega_3\omega_2 z^2 - z\omega_3^2 y) \\ M(z\omega_3^2 x - \omega_3\omega_1 z^2 - z\omega_2\omega_1 y + x\omega_2\omega_3 y + \omega_1\omega_3 x^2 - x\omega_1^2 z) \\ M(x\omega_1^2 y - \omega_1\omega_2 x^2 - x\omega_3\omega_2 z + y\omega_3\omega_1 z + \omega_2\omega_1 y^2 - y\omega_2^2 x) \end{bmatrix} \quad (2.8)$$

The three terms above can be added $M\mathbf{s} \times (\boldsymbol{\omega} \times \mathbf{s}) \times \boldsymbol{\omega} + M\mathbf{g}\mathbf{s} \times \mathbf{u} + I\boldsymbol{\omega} \times \boldsymbol{\omega}$ and we get:

$$\begin{bmatrix} M(y\omega_2^2 z - \omega_2\omega_3 y^2 - y\omega_1\omega_3 x + z\omega_1\omega_2 x + \omega_3\omega_2 z^2 - z\omega_3^2 y + gyu_3 - gzu_2) + (I_2 - I_3)\omega_2\omega_3 \\ M(z\omega_3^2 x - \omega_3\omega_1 z^2 - z\omega_2\omega_1 y + x\omega_2\omega_3 y + \omega_1\omega_3 x^2 - x\omega_1^2 z + gzu_1 - gxu_3) + (I_3 - I_1)\omega_1\omega_3 \\ M(x\omega_1^2 y - \omega_1\omega_2 x^2 - x\omega_3\omega_2 z + y\omega_3\omega_1 z + \omega_2\omega_1 y^2 - y\omega_2^2 x + gxu_2 - gyu_1) + (I_1 - I_2)\omega_1\omega_2 \end{bmatrix} \quad (2.9)$$

Finally, we must compute the term $M\mathbf{s} \times (\dot{\mathbf{s}} \times \boldsymbol{\omega})$ of the right hand side of equation (2.1).

The term $M\mathbf{s} \times (\dot{\mathbf{s}} \times \boldsymbol{\omega})$ then equals:

$$\begin{bmatrix} M(y(\dot{x}\omega_2 - \dot{y}\omega_1) - z(\dot{z}\omega_1 - \dot{x}\omega_3)) \\ M(z(\dot{y}\omega_3 - \dot{z}\omega_2) - x(\dot{x}\omega_2 - \dot{y}\omega_1)) \\ M(x(\dot{z}\omega_1 - \dot{x}\omega_3) - y(\dot{y}\omega_3 - \dot{z}\omega_2)) \end{bmatrix} \quad (2.10)$$

Equation (2.1) can be written in matrix form as $T\dot{\boldsymbol{\omega}} = S$ where the 3-dimensional vector S is:

$$\begin{bmatrix} M(y\omega_2^2 z - \omega_2\omega_3 y^2 - y\omega_1\omega_3 x + z\omega_1\omega_2 x + \omega_3\omega_2 z^2 - z\omega_3^2 y + gyu_3 - gzu_2) + (I_2 - I_3)\omega_2\omega_3 + M(y(\dot{x}\omega_2 - \dot{y}\omega_1) - z(\dot{z}\omega_1 - \dot{x}\omega_3)) \\ M(z\omega_3^2 x - \omega_3\omega_1 z^2 - z\omega_2\omega_1 y + x\omega_2\omega_3 y + \omega_1\omega_3 x^2 - x\omega_1^2 z + gzu_1 - gxu_3) + (I_3 - I_1)\omega_1\omega_3 + M(z(\dot{y}\omega_3 - \dot{z}\omega_2) - x(\dot{x}\omega_2 - \dot{y}\omega_1)) \\ M(x\omega_1^2 y - \omega_1\omega_2 x^2 - x\omega_3\omega_2 z + y\omega_3\omega_1 z + \omega_2\omega_1 y^2 - y\omega_2^2 x + gxu_2 - gyu_1) + (I_1 - I_2)\omega_1\omega_2 + M(x(\dot{z}\omega_1 - \dot{x}\omega_3) - y(\dot{y}\omega_3 - \dot{z}\omega_2)) \end{bmatrix} \quad (2.11)$$

Finally equation (2.1) can be written as $\dot{\boldsymbol{\omega}} = T^{-1}S$ where T^{-1} is (2.4) and S is (2.11). Note that this equation is valid for any rigid body rolling on the plane. The vectors $[x, y, z]$ and $[\dot{x}, \dot{y}, \dot{z}]$ depend on $[u_1, u_2, u_3]$ and are determined by the shape of the body.

2.2 Examples of Rolling Rigid Bodies

2.2.1 Sphere

Assume the centre of mass of the sphere coincides with its geometric centre. In this case, the inverse Gauss map is the identity map:

$$\begin{aligned}
 x &= u_1 & \dot{x} &= \dot{u}_1 \\
 y &= u_2 & \dot{y} &= \dot{u}_2 \\
 z &= u_3 & \dot{z} &= \dot{u}_3
 \end{aligned}
 \tag{2.12}$$

If the sphere is homogeneous (uniform mass distribution) or symmetric (spherically symmetric mass distribution) the three principal moments of inertia are equal. In this case, Graumann [11] has developed the following equations in terms of Euler angles.

$$\begin{aligned}
 \dot{x} &= R(v_\theta \cos \phi + v_\psi \sin \theta \sin \phi) \\
 \dot{y} &= R(v_\theta \sin \phi - v_\psi \sin \theta \cos \phi) \\
 \dot{\theta} &= v_\theta \\
 \dot{\phi} &= v_\phi \\
 \dot{\psi} &= v_\psi \\
 \dot{v}_\theta &= -v_\theta v_\phi \sin \theta \\
 \dot{v}_\phi &= \frac{v_\theta(v_\psi - v_\phi \cos \theta)}{\sin \theta} \\
 \dot{v}_\psi &= \frac{v_\theta(v_\phi - v_\psi \cos \theta)}{\sin \theta}
 \end{aligned}
 \tag{2.13}$$

Another example is the Chaplygin sphere which has its centre of mass at its geometric centre, but the three principal moments of inertia are not equal. In this case, too, Graumann [11] has found the differential equations in terms of Euler angles parametrization. Unfortunately, these equations are several pages long and

seem unsuitable for stability analysis or numerical computer program.

2.2.2 Disk

For reference, these are the equations for a rolling disk in terms of Euler angles derived by Graumann [11]¹:

$$\begin{aligned}
 \dot{x} &= R(\cos \phi \sin \theta v_\theta - \cos \theta \sin \phi v_\phi + \sin \phi v_\psi) \\
 \dot{y} &= R(\sin \phi \sin \theta v_\theta - \cos \theta \cos \phi v_\phi - \cos \phi v_\psi) \\
 \dot{\theta} &= v_\theta \\
 \dot{\phi} &= v_\phi \\
 \dot{\psi} &= v_\psi \\
 \dot{v}_\theta &= \frac{Av_\phi^2 \cos \theta \sin \theta - MgR \cos \theta - (C + MR^2)(v_\psi + v_\phi \cos \theta)v_\phi \sin \theta}{A + MR^2} \\
 \dot{v}_\phi &= \frac{v_\theta(C(v_\psi + v_\phi \cos \theta) - 2Av_\phi \cos \theta)}{A \sin \theta} \\
 \dot{v}_\psi &= \frac{(C + MR^2)v_\theta v_\phi \sin \theta}{C + MR^2} - \frac{v_\theta \cos \theta(C(v_\psi + v_\phi \cos \theta) - 2Av_\phi \cos \theta)}{A \sin \theta}
 \end{aligned} \tag{2.14}$$

2.2.3 Rattleback

Let the body fixed reference frame be centred at the centre of mass of the rattleback, with the three axes coinciding with the three principal moments of inertia. This configuration has been used by almost all authors (for example, [26],[6],[13]). Let the positive z -axis be vertically upward. Assume that the surface of the rattleback is parabolic with equation:

$$z = \frac{1}{2}\sigma_{11}x^2 + \sigma_{12}xy + \frac{1}{2}\sigma_{22}y^2 - h \tag{2.15}$$

¹There is a typographical error on page 135 of [11]. The denominator of the equation for \dot{v}_ϕ should be $A \sin \theta$ as it is here, instead of $A + MR^2$

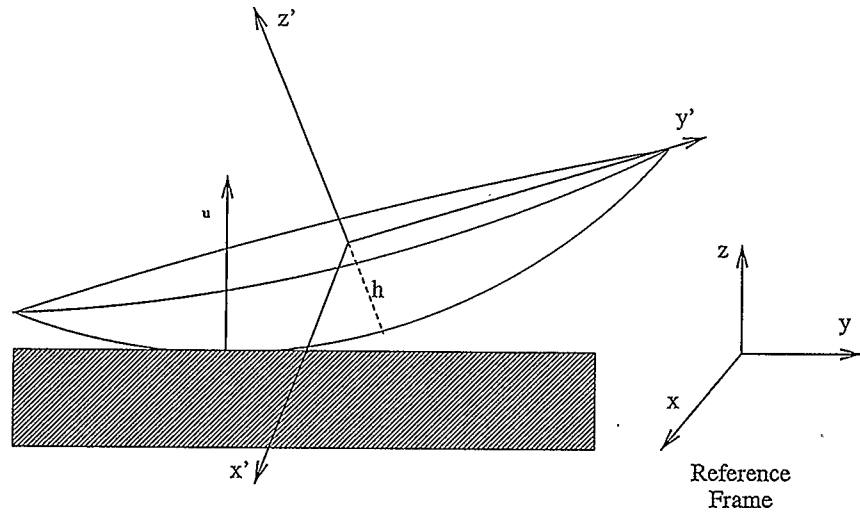


Figure 2.1: Rattleback Spinning on the Plane

Here $\sigma_{11}\sigma_{22} - \sigma_{12}^2 > 0$, $\sigma_{11} > 0$, $\sigma_{22} > 0$ since the surface is convex. In addition, $h > 0$. For example if $\sigma_{11} = 0.24$, $\sigma_{12} = 0.12$, $\sigma_{22} = 0.56$, $h = 1.0$ then the surface of the rattleback in three dimensions looks as displayed in Figure 2.2. The upward unit normal $[u_1, u_2, u_3]$ at any point (x, y, z) on the surface is given by the formula:

$$\mathbf{u} = \frac{[-\sigma_{11}x - \sigma_{12}y, -\sigma_{12}x - \sigma_{22}y, 1]}{\sqrt{1 + (\sigma_{11}x + \sigma_{12}y)^2 + (\sigma_{12}x + \sigma_{22}y)^2}} \quad (2.16)$$

Therefore

$$\begin{aligned} u_1 &= -(\sigma_{11}x + \sigma_{12}y)u_3 \\ u_2 &= -(\sigma_{12}x + \sigma_{22}y)u_3 \end{aligned} \quad (2.17)$$

Solving these equations for x and y , we get $s(\mathbf{u})$ which is the inverse of the Gauss map:

$$\begin{aligned} x &= \frac{-\sigma_{22}u_1 + \sigma_{12}u_2}{(\sigma_{11}\sigma_{22} - \sigma_{12}^2)u_3} \\ y &= \frac{\sigma_{12}u_1 - \sigma_{11}u_2}{(\sigma_{11}\sigma_{22} - \sigma_{12}^2)u_3} \\ z &= \frac{\sigma_{22}u_1^2 - 2\sigma_{12}u_1u_2 + \sigma_{11}u_2^2}{2(\sigma_{11}\sigma_{22} - \sigma_{12}^2)u_3^2} \end{aligned} \quad (2.18)$$

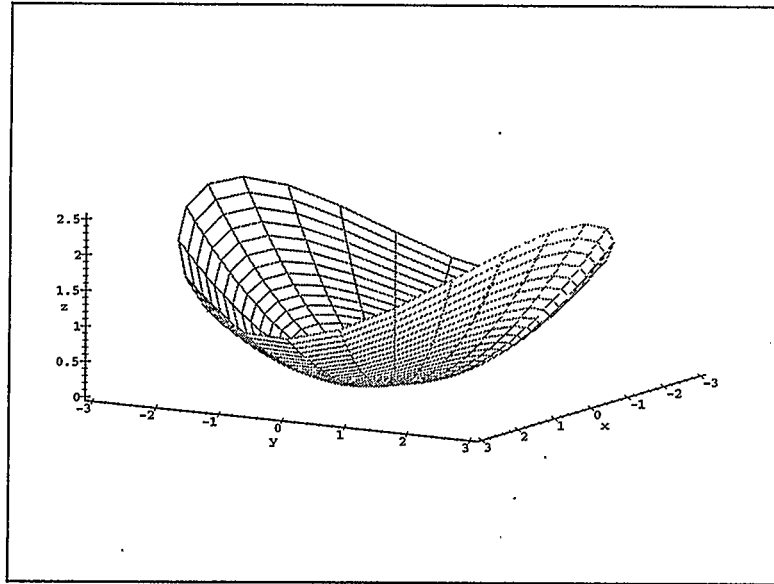


Figure 2.2: The Shape of the Rattleback

Now we can also find $[\dot{x}, \dot{y}, \dot{z}]$: The vector \dot{s} can be computed in the following way:

$$\begin{aligned}
 \dot{x} &= -\frac{\sigma_{22}(u_2\omega_3 - u_3\omega_2)}{(\sigma_{11}\sigma_{22} - \sigma_{12}^2)u_3} + \frac{\sigma_{12}(u_3\omega_1 - u_1\omega_3)}{(\sigma_{11}\sigma_{22} - \sigma_{12}^2)u_3} + \frac{(\sigma_{22}u_1 - \sigma_{12}u_2)(u_1\omega_2 - u_2\omega_1)}{\sigma_{11}\sigma_{22} - \sigma_{12}^2}u_3^2 \\
 \dot{y} &= \frac{\sigma_{12}(u_2\omega_3 - u_3\omega_2)}{(\sigma_{11}\sigma_{22} - \sigma_{12}^2)u_3} - \frac{\sigma_{11}(u_3\omega_1 - u_1\omega_3)}{(\sigma_{11}\sigma_{22} - \sigma_{12}^2)u_3} + \frac{(\sigma_{11}u_2 - \sigma_{12}u_1)(u_1\omega_2 - u_2\omega_1)}{\sigma_{11}\sigma_{22} - \sigma_{12}^2}u_3^2 \\
 \dot{z} &= -\frac{u_1}{u_3}\dot{x} - \frac{u_2}{u_3}\dot{y}
 \end{aligned} \tag{2.19}$$

Chapter 3

Rattleback

3.1 Historical Perspective

3.1.1 Definitions

A *rattleback* is a spinning top that has the unusual property of reversing the direction of spin on its own. As it spins, it begins to rattle then miraculously starts spinning in the opposite direction - hence the name *rattleback*. Some rattlebacks reverse their spin direction several times. Other rattlebacks, if spun in the unstable direction, reverse the direction of motion once, then continue spinning in the stable direction. If spun in the stable direction, however, they do not reverse their spin. Such rattlebacks are said to exhibit a *spin bias* in one direction. The first known rattlebacks were found by archaeologists when digging in ancient Celtic ruins ([25],[11]). That is why a rattleback is sometimes called a *Celtic stone*. Another name for a rattleback that is mentioned in the literature occasionally is a *wobblestone*.

3.1.2 Popular Articles

In 1979, Walker [25] published a popular article about the rattleback. This article had very little mathematics but tried to explain why the rattleback reverses its spin. In 1985, Boardman [5] wrote an article that describes in detail how to make a rattleback. The article begins with a poem dedicated to the rattleback:

*Behold the mysterious celt,
With a property that amuses.
One way it will spin,
The other way it refuses.*

3.1.3 Scientific Articles

The first rigorous mathematical model of the rattleback was developed by G.T. Walker in 1896 [26]. The model ignored the effects of slipping and friction. In his article, Walker proved that stable motion in one direction is possible without energy dissipation by using a method similar to modern-day linearization and eigenvalue analysis. The two equilibrium points that he found have been named the Walker equilibria. Subsequent authors ([15], [6], [13]) also linearized the equations of the rattleback about the Walker equilibria and analyzed the stability of the dynamical system. A portion of this thesis also takes this approach and examines the signs of the real parts of the eigenvalues. In addition, Walker's prediction of stable motion in one direction for some parameters is confirmed by numerical experiments done in this thesis. Chronologically, the next paper on the rattleback was written by Herglotz in 1941, and is mentioned by Magnus [18] and Astapov [4] but there is no other information where this article can be found. In 1974, Magnus [20] wrote a short article where he had a diagram with stable and unstable regions in the ω_3 - h parameter space. In 1980, Astapov [4] developed a model of the rattleback with the following assumptions: no energy dissipation, elliptic paraboloid shape. In his article, the body fixed frame was along the 3 axes of symmetry of the paraboloid while the moment of inertia matrix was not diagonal. Only one other article ([14]) assumes

this configuration. In all other articles (as well as in this thesis) the body fixed frame is along the three principle moments of inertia while the paraboloid is rotated. Astapov [4] then linearized the equations, used Routh-Hurwitz criteria and derived a stability diagram in the $\omega_3 - h$ space similar to the one in the article of Magnus [20]. Chronologically, the next paper on the rattleback was written by Kane and Levinson [14] in 1982. The rattleback shape was assumed to be ellipsoid and friction was taken into account. The paper describes how to write a computer program for the rattleback and gives several numerical examples. Kane and Levinson demonstrated numerically that without energy dissipation, infinitely many reversals occur while with energy dissipation there is only one reversal. However, as this thesis and many articles ([26], [6], [15], [13]) have demonstrated, for some parameters there can be only one reversal even when energy is conserved. In 1985, Karapetyan [15] proved that for certain rattlebacks, as the energy increases a Hopf bifurcation occurs and one of the two Walker equilibria becomes stable. In this thesis, numerical experiments will confirm the occurrence of Hopf bifurcation for some parameters as predicted by Karapetyan [15]. In 1986, Bondi [6] wrote a comprehensive article on the rattleback. He did not assume energy dissipation to be present and the rattleback shape was assumed to be an elliptic paraboloid. He linearized the equations of motion and drew an important stability diagram where he classified the rattlebacks into Type 1 and Type 2 rattlebacks (later authors have named the third region of the Bondi diagram a "Type 0" rattleback). Bondi [6] proved the following:

A Type 0 rattleback exhibits multiple reversals and the wobbling motion is always unstable. The eigenvalues corresponding to both Walker equilibria have positive real parts regardless of the energy. The author of this thesis gives a numerical example of

a Type 0 rattleback. Such a rattleback has been observed. A Type 1 rattleback can exhibit two distinct types of behaviour, depending on its initial spin (energy). For lower energies, it reverses direction many times and the wobbling motion is always unstable (Zone 0 behaviour). For higher energies, it reverses direction once and the wobbling motion decays to zero. In this thesis, several numerical experiments show all the possibilities that can arise for a Type 1 rattleback (see also similar graphs in [10]). Bondi [6] did not elaborate much on the Type 2 case, but future authors ([10],[13]) have studied this type in more detail. According to them, there are several possibilities depending on the energy. If the energy is low, the wobbling motion is unstable for both Walker equilibria. If the energy is between two critical values, at most one reversal occurs after which the wobbling motion decays and one of the two Walker equilibria is stable. For high energies, one reversal occurs after which the wobbling motion decays toward an axis *different* than the vertical axis. New equilibria appear and their stability has not yet been studied in full. The author of this thesis gives some numerical examples that can provide a hint about the complexity of the Type 2 rattleback behaviour. In 1988, an article by Garcia and Hubbart [10] appeared where they summarized previous research, ran several numerical simulations and even compared the results with an actual rattleback. It seems that they were the first to plot numerically the motion of a rattleback that spins about an axis other than the vertical (and so there is a new stable equilibrium point while the Walker equilibrium is unstable - indicating the possibility of a pitchfork bifurcation which was later mentioned also by Hermans [13]). In this thesis, the author too has plotted numerically such motion about a tilted axis. According to Garcia and Hubbart [10], previous researchers have tried to explain the rattleback phenomena

in two ways. G.T. Walker [26], Bondi [6] and others have argued that spin reversal can be explained solely by the intrinsic inertial and geometric properties of the rattleback while ignoring the effects of slipping or dissipation - a view shared by the author of this thesis as well. On the other hand, Kane and Levinson [14] have argued that energy dissipation must be taken into account in order to fully explain the behaviour of the rattleback. In 1994, Graumann [11] wrote a Masters thesis about the rattleback. He demonstrated theoretically how the rattleback equations can be written in terms of Euler angles. Hermans [13] in his Ph.D. thesis in 1995 linearized the equations of motion about the Walker equilibria (something that has also been done in this thesis) and predicted that not only Hopf but also pitchfork bifurcations are possible. The numerical work in this thesis has indeed shown the presence of pitchfork bifurcations for some parameter values.

3.2 Linearization about the Walker equilibrium

Given a system of differential equations, an *equilibrium point* is a solution for which the vector field vanishes. For the rattleback, an important equilibrium point is the *Walker equilibrium*: $[u_1, u_2, u_3, \omega_1, \omega_2, \omega_3] = [0, 0, 1, 0, 0, \omega_3]$. Physically, it corresponds to the rattleback rotating with constant angular velocity ω_3 about the vertical axis with point of contact $[x, y, z] = [0, 0, -h]$. Strictly speaking, when the rattleback is moving there are actually two Walker equilibria corresponding to angular velocities $\pm\omega_3$.¹ An equilibrium is *asymptotically stable* if a solution close to it approaches it as $t \rightarrow \infty$. Such an equilibrium is also called a *sink*. An equilibrium

¹When the rattleback is at rest there is of course only one Walker equilibrium corresponding to $\omega_3 = 0$.

is *unstable* if a solution close to it does not remain close to it for all time. When a rattleback reverses its direction of spin, this means that the Walker equilibrium is unstable for that direction. In order to determine the local stability properties of the Walker equilibrium, we must linearize the nonlinear equations of motion.

The matrix T^{-1} (2.4) evaluated at the Walker equilibrium is:

$$\begin{bmatrix} (I_1 + Mz^2)^{-1} & 0 & 0 \\ 0 & (I_2 + Mz^2)^{-1} & 0 \\ 0 & 0 & I_3^{-1} \end{bmatrix} \quad (3.1)$$

For linearization $[I, 0|0, T^{-1}]$ (a 6×6 matrix where I is the identity 3×3 matrix) must be multiplied by the gradient of the vector three-dimensional vector S (2.11) with respect to the 6 variables $[u_1, u_2, u_3, \omega_1, \omega_2, \omega_3]$, evaluated at the Walker equilibrium (a 6×6 matrix). The 6×6 matrix for the overall system before multiplication by matrix $[I, 0|0, T^{-1}]$ then is:

$$\begin{bmatrix} 0 & \omega_3 & 0 & 0 & -1 & 0 \\ -\omega_3 & 0 & 0 & 1 & 0 & 0 \\ 0 & 0 & 0 & 0 & 0 & 0 \\ \frac{M\sigma_{12}}{\delta}(2h\omega_3^2 + g) & d_{42} & 0 & -\frac{Mh\sigma_{12}\omega_3}{\delta} & d_{45} & 0 \\ d_{51} & -\frac{M\sigma_{12}}{\delta}(2h\omega_3^2 + g) & 0 & d_{54} & \frac{Mh\sigma_{12}\omega_3}{\delta} & 0 \\ 0 & 0 & 0 & 0 & 0 & 0 \end{bmatrix} \quad (3.2)$$

where

$$\begin{aligned}
\delta &= \sigma_{11}\sigma_{22} - \sigma_{12}^2 \\
d_{42} &= \frac{M}{\delta}(h\omega_3^2(\sigma_{22} - \sigma_{11}) - g\sigma_{11} + gh\delta) \\
d_{45} &= Mh^2\omega_3 + (I_2 - I_3)\omega_3 - \frac{Mh\sigma_{22}\omega_3}{\delta} \\
d_{51} &= \frac{M}{\delta}(h\omega_3^2(\sigma_{22} - \sigma_{11}) + g\sigma_{22} - gh\delta) \\
d_{54} &= -Mh^2\omega_3 + (I_3 - I_1)\omega_3 + \frac{Mh\sigma_{11}\omega_3}{\delta}
\end{aligned} \tag{3.3}$$

The product of $[I, 0|0, T^{-1}]$ (a 6×6 matrix where I is the identity 3×3 matrix) with the matrix (3.2) (a 6×6 matrix) then equals a 6×6 matrix:

$$\begin{bmatrix}
0 & \omega_3 & 0 & 0 & -1 & 0 \\
-\omega_3 & 0 & 0 & 1 & 0 & 0 \\
0 & 0 & 0 & 0 & 0 & 0 \\
\frac{M\sigma_{12}(2h\omega_3^2+g)}{\delta(I_1+Mh^2)} & d_{42} & 0 & -\frac{Mh\sigma_{12}\omega_3}{\delta(I_1+Mh^2)} & d_{45} & 0 \\
d_{51} & -\frac{M\sigma_{12}(2h\omega_3^2+g)}{\delta(I_2+Mh^2)} & 0 & d_{54} & \frac{Mh\sigma_{12}\omega_3}{\delta(I_2+Mh^2)} & 0 \\
0 & 0 & 0 & 0 & 0 & 0
\end{bmatrix} \tag{3.4}$$

where

$$\begin{aligned}
d_{42} &= \frac{M(h\omega_3^2(\sigma_{22}-\sigma_{11})-g\sigma_{11}+gh\delta)}{\delta(I_1+Mh^2)} \\
d_{45} &= \frac{Mh^2\omega_3\delta+(I_2-I_3)\omega_3\delta-Mh\sigma_{22}\omega_3}{\delta(I_1+Mh^2)} \\
d_{51} &= \frac{M(h\omega_3^2(\sigma_{22}-\sigma_{11})+g\sigma_{22}-gh\delta)}{\delta(I_2+Mh^2)} \\
d_{54} &= \frac{-Mh^2\omega_3\delta+(I_3-I_1)\omega_3\delta+Mh\sigma_{11}\omega_3}{\delta(I_2+Mh^2)}
\end{aligned} \tag{3.5}$$

While this appears to be a 6-dimensional vector field, in reality it is restricted to $S^2 \times R^3$ (since due to the rolling constraint $[u_1, u_2, u_3]$ is a unit vector and so an element of the 2-sphere S^2). This is the reason why there are zeros along the sixth

row and the third column. The characteristic polynomial is:

$$\begin{vmatrix} -\lambda & \omega_3 & 0 & 0 & -1 & 0 \\ -\omega_3 & -\lambda & 0 & 1 & 0 & 0 \\ 0 & 0 & -\lambda & 0 & 0 & 0 \\ \frac{M\sigma_{12}(2h\omega_3^2+g)}{\delta(I_1+Mh^2)} & d_{42} & 0 & -\frac{Mh\sigma_{12}\omega_3}{\delta(I_1+Mh^2)} - \lambda & d_{45} & 0 \\ d_{51} & \frac{M\sigma_{12}(2h\omega_3^2+g)}{\delta(I_2+Mh^2)} & 0 & d_{54} & \frac{Mh\sigma_{12}\omega_3}{\delta(I_2+Mh^2)} - \lambda & 0 \\ 0 & 0 & 0 & 0 & 0 & -\lambda \end{vmatrix} \quad (3.6)$$

where

$$\begin{aligned} d_{42} &= \frac{M(h\omega_3^2(\sigma_{22}-\sigma_{11})-g\sigma_{11}+gh\delta)}{\delta(I_1+Mh^2)} \\ d_{45} &= \frac{Mh^2\omega_3\delta+(I_2-I_3)\omega_3\delta-Mh\sigma_{22}\omega_3}{\delta(I_1+Mh^2)} \\ d_{51} &= \frac{M(h\omega_3^2(\sigma_{22}-\sigma_{11})+g\sigma_{22}-gh\delta)}{\delta(I_2+Mh^2)} \\ d_{54} &= \frac{-Mh^2\omega_3\delta+(I_3-I_1)\omega_3\delta+Mh\sigma_{11}\omega_3}{\delta(I_2+Mh^2)} \end{aligned} \quad (3.7)$$

Expansion of the determinant along the third and sixth rows yields:

$$\lambda^2 \begin{vmatrix} -\lambda & \omega_3 & 0 & -1 \\ -\omega_3 & -\lambda & 1 & 0 \\ \frac{M\sigma_{12}(2h\omega_3^2+g)}{\delta(I_1+Mh^2)} & d_{32} & -\frac{Mh\sigma_{12}\omega_3}{\delta(I_1+Mh^2)} - \lambda & d_{34} \\ d_{41} & -\frac{M\sigma_{12}(2h\omega_3^2+g)}{\delta(I_2+Mh^2)} & d_{43} & \frac{Mh\sigma_{12}\omega_3}{\delta(I_2+Mh^2)} - \lambda \end{vmatrix} = 0 \quad (3.8)$$

where

$$\begin{aligned} d_{32} &= \frac{M(h\omega_3^2(\sigma_{22}-\sigma_{11})-g\sigma_{11}+gh\delta)}{\delta(I_1+Mh^2)} \\ d_{34} &= \frac{Mh^2\omega_3\delta+(I_2-I_3)\omega_3\delta-Mh\sigma_{22}\omega_3}{\delta(I_1+Mh^2)} \\ d_{41} &= \frac{M(h\omega_3^2(\sigma_{22}-\sigma_{11})+g\sigma_{22}-gh\delta)}{\delta(I_2+Mh^2)} \\ d_{43} &= \frac{-Mh^2\omega_3\delta+(I_3-I_1)\omega_3\delta+Mh\sigma_{11}\omega_3}{\delta(I_2+Mh^2)} \end{aligned} \quad (3.9)$$

There are two eigenvalues equal to zero. The reason for the first one has been explained - the vector field is restricted to $S^2 \times R^3$. The second eigenvalue zero occurs because there are infinitely many equilibria along the line $[0, 0, 1, 0, 0, \omega_3]$ for all real ω_3 . The other four eigenvalues are the roots of a fourth-order polynomial.

3.2.1 Low Energy Analysis ($\omega_3 = 0$)

For simplicity, let us first consider the case when $\omega_3 = 0$. Physically this means that the rattleback is not moving. The 4 by 4 determinant (3.8) then becomes:

$$\begin{vmatrix} -\lambda & 0 & 0 & -1 \\ 0 & -\lambda & 1 & 0 \\ \frac{M\sigma_{12}g}{\delta(I_1+Mh^2)} & \frac{M(-g\sigma_{11}+gh\delta)}{\delta(I_1+Mh^2)} & -\lambda & 0 \\ \frac{M(g\sigma_{22}-gh\delta)}{\delta(I_2+Mh^2)} & -\frac{M\sigma_{12}g}{\delta(I_2+Mh^2)} & 0 & -\lambda \end{vmatrix} = 0 \quad (3.10)$$

Now let $A = \frac{Mg\sigma_{12}}{\delta(I_2+Mh^2)}$, $B = \frac{Mg(-\sigma_{11}+h\delta)}{\delta(I_1+Mh^2)}$, $C = \frac{Mg(\sigma_{22}-h\delta)}{\delta(I_2+Mh^2)}$ and $D = -\frac{Mg\sigma_{12}}{\delta(I_2+Mh^2)}$. Then the characteristic equation is:

$$\lambda^4 + (C - B)\lambda^2 + AD - CB = 0 \quad (3.11)$$

Using the notation of Hermans [13] page 62, this equation can be written in the following way: ²

$$\lambda^4 + \gamma_2\lambda^2 + \gamma_4 = 0 \quad (3.12)$$

with

$$\begin{aligned} \gamma_2 &= \frac{Mg((I_2+Mh^2)(\frac{\sigma_{11}}{\delta}-h)+(I_1+Mh^2)(\frac{\sigma_{22}}{\delta}-h))}{(I_1+Mh^2)(I_2+Mh^2)} \\ \gamma_4 &= \frac{M^2g^2\Delta}{(I_1+Mh^2)(I_2+Mh^2)} \end{aligned} \quad (3.13)$$

where

$$\Delta = \left(\frac{\sigma_{11}}{\delta} - h\right)\left(\frac{\sigma_{22}}{\delta} - h\right) - \left(\frac{\sigma_{12}}{\delta}\right)^2 \quad (3.14)$$

²There is a typographical error in equation (3.10) of Hermans [13]: the sign in front of γ_2 must be positive.

3.2.2 High Energy Analysis ($\omega_3 \neq 0$)

The determinant (3.8) can be written as follows:

$$\begin{vmatrix} -\lambda & \omega_3 & 0 & -1 \\ -\omega_3 & -\lambda & 1 & 0 \\ A\omega_3^2 + B & C\omega_3^2 + D & E\omega_3 - \lambda & F\omega_3 \\ G\omega_3^2 + H & I\omega_3^2 + J & K\omega_3 & L\omega_3 - \lambda \end{vmatrix}$$

When expanded, the determinant becomes equal to:

$$\begin{aligned} & \lambda^4 + (-E - L)\omega_3\lambda^3 + ((-C + EL + G - FK + 1)\omega_3^2 + (H - D))\lambda^2 + \\ & ((-A + AK + CL - EG - FI - I - E - L)\omega_3^2 + (-B + BK + DL - EH - FJ - J))\omega_3\lambda \\ & + (AI + AL - CG - CK + EI + EL - FG - FK)\omega_3^4 + \\ & (AJ + BI + BL - CH - DG - DK + EJ - FH)\omega_3^2 + (BJ - DH) \end{aligned}$$

Using the notation of Hermans [13] on page 74, this can be written as follows:

$$p(\lambda) = \lambda^4 + a_1\lambda^3 + a_2\lambda^2 + a_3\lambda + a_4 \quad (3.15)$$

$$a_1 = \frac{-Mh\sigma_{12}(I_1 - I_2)}{\delta(I_1 + Mh^2)(I_2 + Mh^2)}\omega_3$$

$$a_2 = \beta_2\omega_3^2 + \gamma_2 \quad (3.16)$$

$$a_3 = \omega_3^2 a_1$$

$$a_4 = \alpha_4\omega_3^4 + \beta_4\omega_3^2 + \gamma_4$$

where

$$\alpha_4 = \frac{(I_3 - I_2)(I_3 - I_1) + (Mh)^2\Delta - Mh((I_2 - I_3)(\frac{\sigma_{22}}{\delta} - h) + (I_1 - I_3)(\frac{\sigma_{11}}{\delta} - h))}{(I_1 + Mh^2)(I_2 + Mh^2)}$$

$$\beta_4 = \frac{Mg((I_3 - I_2)(\frac{\sigma_{22}}{\delta} - h) + (I_3 - I_1)(\frac{\sigma_{11}}{\delta} - h) + 2Mh\Delta)}{(I_1 + Mh^2)(I_2 + Mh^2)}$$

$$\beta_2 = \alpha_4 + 1$$

$$\gamma_2 = \frac{Mg((I_2 + Mh^2)(\frac{\sigma_{11}}{\delta} - h) + (I_1 + Mh^2)(\frac{\sigma_{22}}{\delta} - h))}{(I_1 + Mh^2)(I_2 + Mh^2)}$$

$$\gamma_4 = \frac{M^2g^2\Delta}{(I_1 + Mh^2)(I_2 + Mh^2)}$$

$$\Delta = (\frac{\sigma_{11}}{\delta} - h)(\frac{\sigma_{22}}{\delta} - h) - (\frac{\sigma_{12}}{\delta})^2$$

(3.17)

Besides Hermans [13], Karapetyan [15] has also arrived at this result.

3.2.3 Bifurcations

The characteristic equation (3.15) has four roots and since the coefficients are real, all complex roots must be conjugate pairs. The signs of the real parts of the roots yield information about the local stability properties of the Walker equilibrium. If all roots have negative real parts, then the Walker equilibrium is locally stable. If at least one root has a positive real part, then the Walker equilibrium is locally unstable. Besides the signs of the positive real parts, it is also important to know how the roots move in the complex plane as the parameters change. If a change in parameters causes a pair of complex roots to cross the imaginary axis with nonzero velocity, then a *Hopf bifurcation* occurs. If before the Hopf bifurcation the equilibrium was unstable (some roots were with positive real parts), after the Hopf bifurcation it becomes stable (all roots are with negative real parts). A *pitchfork bifurcation* can occur when all roots have negative real parts, and after a parameter change, a *real* root crosses the imaginary axis at the origin and becomes positive. In this case, the Walker equilibrium becomes unstable and two *new equilibria* appear (they are locally stable at least initially). More information on the theory of bifurcations can be found in [12].

Applying the Routh-Hurwitz criteria to the characteristic equation (3.15), we see that necessary and sufficient conditions for all roots to be in the left complex half-plane (that is, for one Walker equilibrium to be stable) are:

$$a_1 > 0, a_3 > 0, a_4 > 0, a_3(a_1a_2 - a_3) - a_1^2a_4 > 0 \quad (3.18)$$

Or, assuming $I_1 > I_2$:

$$\begin{aligned}\omega_3 &< 0 \\ \alpha_4\omega_3^4 + \beta_4\omega_3^2 + \gamma_4 &> 0 \\ (\gamma_2 - \beta_4)\omega_3^2 - \gamma_4 &> 0\end{aligned}\tag{3.19}$$

The inequalities (3.19) can be combined as:

$$w(\alpha_4w + \gamma_2) > (\gamma_2 - \beta_4)w - \gamma_4 > 0\tag{3.20}$$

where $w = \omega_3^2 > 0$.

Graphically, condition (3.20) can be displayed as a parabola $P(w) = w(\alpha_4w + \gamma_2)$ and a line $Q(w) = (\gamma_2 - \beta_4)w - \gamma_4$ in the w - $f(w)$ plane. Whenever the line is above the w -axis and below the parabola, the Walker equilibrium $[0, 0, 1, 0, 0, -\omega_3]$ is stable; in all other cases it is unstable. If the line $Q(w)$ is never between the w -axis and the parabola $P(w)$, both Walker equilibria are unstable regardless of the energy (*Type 0* rattleback). When the slope of the line $(\gamma_2 - \beta_4)$ is positive, a Hopf bifurcation is possible when the line crosses the w -axis (*Type 1* rattleback). Afterwards, it can cross the parabola once (*Type 2A* rattleback) or twice (*Type 2B* rattleback) depending on the graph of the parabola in which case pitchfork bifurcations leading to new equilibria arise.

3.3 Numerical Simulations

While Bondi [6] classifies rattlebacks according to their shapes, Hermans [13] classifies them according to energy and moments of inertia. An overall review of types of rattlebacks and their behaviours is presented below. Slipping and friction are ignored. All numerical simulations used the following parameters: $M = 1, h = 1, g = 1$. The

time step size was chosen to be 0.001 for most cases. In the numerical simulations that follow, two important angles are graphed as functions of time: the spin angle Γ and the wobble angle η . The spin angle measures how much the rattleback has spun around the body fixed vertical axis. When the spin angle reaches local maximum or minimum, this means that the rattleback reverses its direction of motion. The spin angle is computed using the following formula: $\dot{\Gamma} = \frac{u_1\omega_2 + u_2\omega_1}{u_1^2 + u_2^2}$. This formula was derived from a similar formula in [14]. The wobble angle measures the angle between the absolute vertical axis and the body fixed vertical axis. It is between 0 and 90 degrees. Note that when the wobble angle is maximum, a spin reversal occurs. This is confirmed by the numerical simulations in the subsequent pages. The wobble angle can be computed as follows (see also [14]): $\eta = \arccos u_3$. At the beginning of the discussion of each type of rattleback, there is a diagram based on Bondi's model [6]. Instead of $I_1, I_2, I_3, \sigma_{11}, \sigma_{12}, \sigma_{22}, M, h, g$ Bondi uses new parameters that are derived from the shape of the rattleback and the moments of inertia. These parameters are $\alpha, \beta, \gamma, \Theta, \Phi, \Psi$. Bondi then computed κ and μ , the signs of which determine the type

of the rattleback. Bondi's parameters are computed using the following equations:

$$\begin{aligned}
\alpha &= \frac{I_1 + Mh^2}{Mh^2} \\
\beta &= \frac{I_2 + Mh^2}{Mh^2} \\
\gamma &= \frac{I_3}{Mh^2} \\
\Theta &= \frac{h}{2}(\sigma_{11} + \sigma_{22} + \sqrt{(\sigma_{11} - \sigma_{22})^2 + 4\sigma_{12}^2}) \\
\Phi &= \frac{h}{2}(\sigma_{11} + \sigma_{22} - \sqrt{(\sigma_{11} - \sigma_{22})^2 + 4\sigma_{12}^2}) \\
\Psi &= \frac{\sigma_{11} - \sigma_{22}}{\sqrt{(\sigma_{11} - \sigma_{22})^2 + 4\sigma_{12}^2}} \\
\kappa &= \frac{1 - 0.5(\alpha + \beta - 2\gamma)(\Theta + \Phi) + (\alpha - \gamma)(\beta - \gamma)\Theta\Phi - 0.5(\alpha - \beta)(\Theta - \Phi)\Psi}{\alpha\beta\Theta\Phi} \\
\mu &= \frac{2 - (\Theta + \Phi) - (\alpha + \beta - \gamma)(\Theta + \Phi - 2\Theta\Phi)}{\alpha\beta\Theta\Phi}
\end{aligned} \tag{3.21}$$

We have included these values as well for reference with each diagram and the reader can refer to Bondi's article [6] for more detailed explanation.

3.3.1 Type 0 Rattleback

1. $E = E_{min}$

The rattleback is not moving. There is only one equilibrium point:

$$[0, 0, 1, 0, 0, 0].$$

2. $E > E_{min}$

The rattleback has two equilibrium points: $[0, 0, 1, 0, 0, \pm\omega_3]$ These are the Walker equilibria. They are both unstable. The rattleback reverses direction infinitely many times (unless of course the initial conditions are exactly at the Walker equilibrium in which case the rattleback never reverses its direction). Multiple reversals have been observed in real rattlebacks. A sample set of parameter values that would yield a Type 0 rattleback are: $I_1 = 4, I_2 = 1, I_3 = 3.5, \sigma_{11} = 0.25, \sigma_{12} = 0.05, \sigma_{22} = 0.25$

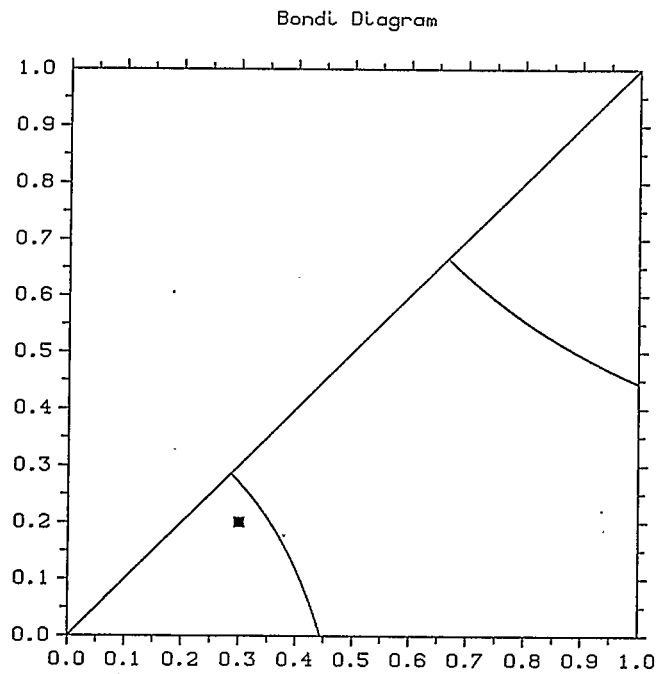


Figure 3.1: Type 0 Rattleback: Bondi Diagram

Parameters:

$$M = 1, h = 1, g = 1, I_1 = 4, I_2 = 1, I_3 = 3.5, \sigma_{11} = 0.25, \sigma_{12} = 0.05, \sigma_{22} = 0.25$$

Bondi Parameters:

$$\Theta = 0.3, \Phi = 0.2, \Psi = 0, \alpha = 5, \beta = 2, \gamma = 3.5, \kappa = 1.442, \mu = 0.283$$

(In this case the slope of the line $Q(w)$ is negative and the equilibria are always unstable). The following graphs show how the spin angle and wobble angle change with time for a Type 0 rattleback with the above parameters:

Spin Angle as a Function of Time

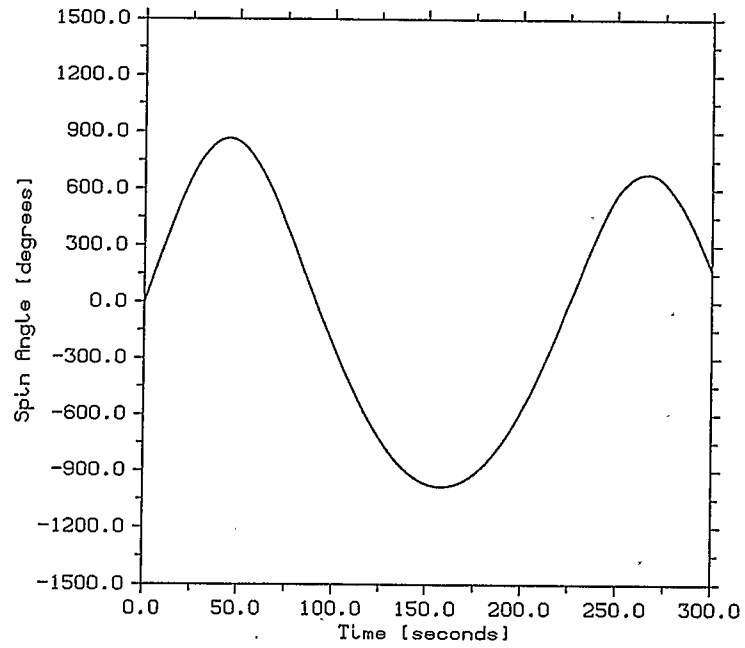


Figure 3.2: Type 0 Rattleback: Spin Angle vs. Time
 Parameters: $M = 1, h = 1, g = 1, I_1 = 4, I_2 = 1, I_3 = 3.5, \sigma_{11} = 0.25, \sigma_{12} = 0.05, \sigma_{22} = 0.25, t_{step} = 0.005$
 Initial conditions: $u_1 = 0.05, u_2 = 0, \omega_1 = 0, \omega_2 = 0, \omega_3 = 0.5$

Wobble angle as a Function of Time

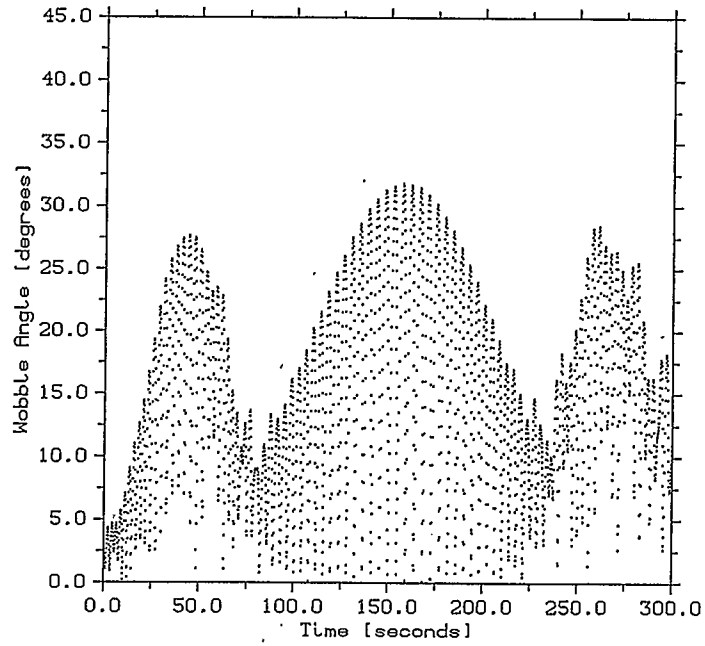


Figure 3.3: Type 0 Rattleback: Wobble Angle vs. Time

Parameters: $M = 1, h = 1, g = 1, I_1 = 4, I_2 = 1, I_3 = 3.5, \sigma_{11} = 0.25, \sigma_{12} = 0.05, \sigma_{22} = 0.25, t_{step} = 0.005$

Initial conditions: $u_1 = 0.05, u_2 = 0, \omega_1 = 0, \omega_2 = 0, \omega_3 = 0.5$

Note: There are two frequencies: a high frequency and a low beat frequency of the local maximums. A spin reversal occurs at time when there is a local maximum of the low beat frequency (see Figure 3.2).

3.3.2 Type 1 Rattleback

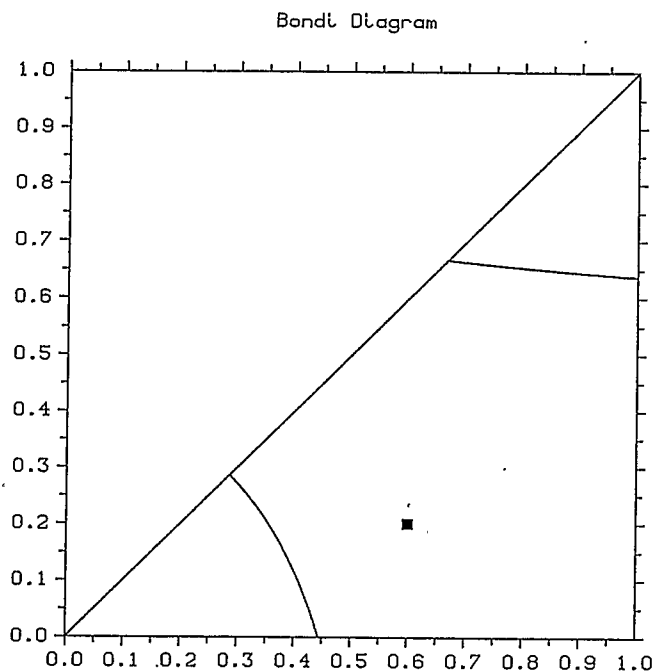


Figure 3.4: Type 1 Rattleback: Bondi Diagram

Parameters:

$$M = 1, h = 1, g = 1, I_1 = 4, I_2 = 1, I_3 = 3.5, \sigma_{11} = 0.24, \sigma_{12} = 0.12, \sigma_{22} = 0.56$$

Bondi Parameters:

$$\Theta = 0.6, \Phi = 0.2, \Psi = -0.8, \alpha = 5, \beta = 2, \gamma = 3.5, \kappa = 1.008, \mu = -0.633$$

1. $E = E_{min}$

The rattleback is not moving. There is only one equilibrium point:

$$[0, 0, 1, 0, 0, 0].$$

2. $E_{min} < E < E_H$

The rattleback has two equilibrium points: $[0, 0, 1, 0, 0, \pm\omega_3]$ These are the Walker equilibria. They are both unstable.

3. $E > E_H$

At a high enough energy, one of the two Walker equilibria becomes stable. Its eigenvalues cross the imaginary axis and a Hopf bifurcation occurs. There are still two Walker equilibria $[0, 0, 1, 0, 0, \pm\omega_3]$, but one of them is stable. The other Walker equilibrium is still unstable and will remain so. Now the rattleback exhibits a bias in one direction. If spun in the unstable direction, it will change direction on its own. Walker [26] described this behaviour in one of the earliest papers on the rattleback. He thus proved that stable motion is possible without friction or dissipation. Some sample parameter values that would yield a Type 1 rattleback are: $I_1 = 4, I_2 = 3, I_3 = 2, \sigma_{11} = 0.25, \sigma_{12} = 0.05, \sigma_{22} = 0.25$. Other parameter values: $I_1 = 4, I_2 = 1, I_3 = 3.5, \sigma_{11} = 0.24, \sigma_{12} = 0.12, \sigma_{22} = 0.56$. The following graph shows the relative positions of line $Q(w)$ and parabola $P(w)$ in this case:

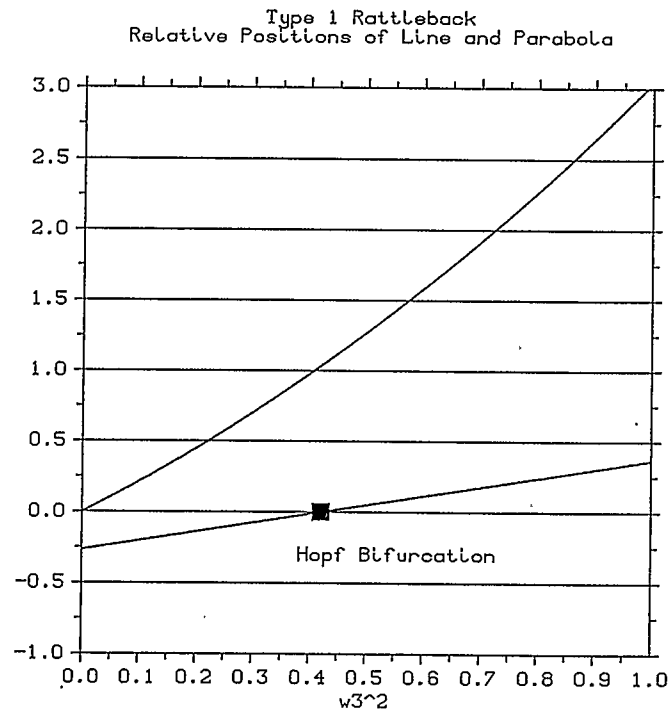


Figure 3.5: Type 1 Rattleback: Routh-Hurwitz Stability Criteria
Graphs of Parabola $P(w)$ and Line $Q(w)$

Parameters:

$$M = 1, h = 1, g = 1, I_1 = 4, I_2 = 1, I_3 = 3.5, \sigma_{11} = 0.24, \sigma_{12} = 0.12, \sigma_{22} = 0.56$$

$$\text{Hopf Bifurcation: } \omega_3 = -0.6488856842$$

It is evident from this figure that a change in stability occurs when $\omega_3 = -0.6488856842$.

The following graph shows how the eigenvalues of the characteristic equation change when ω_3 changes from -0.5 to -0.6488856842 to -1:

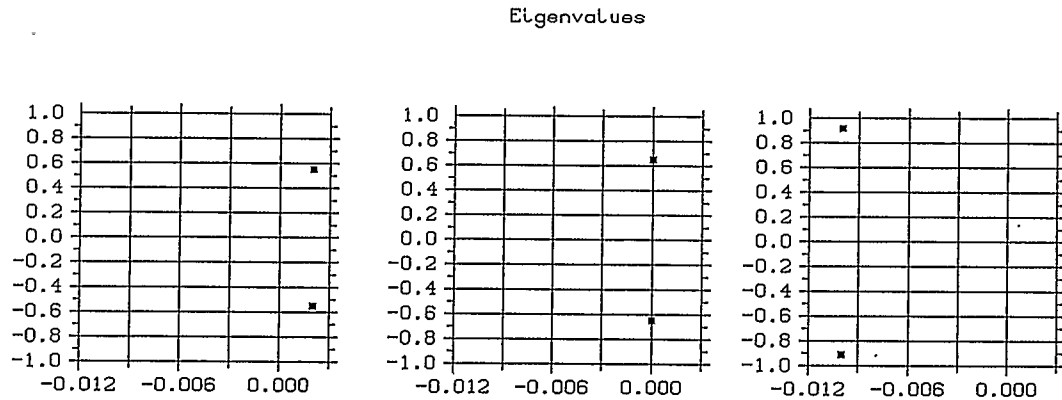


Figure 3.6: Type 1 Rattleback: Eigenvalues Crossing the Imaginary Axis

Parameters:

$$M = 1, h = 1, g = 1, I_1 = 4, I_2 = 1, I_3 = 3.5, \sigma_{11} = 0.24, \sigma_{12} = 0.12, \sigma_{22} = 0.56$$

$$\text{Hopf Bifurcation: } \omega_3 = -0.6488856842$$

Note: A pair of eigenvalues with negative real parts cannot be seen in each of the graphs due to the scale chosen.

Left Graph: $\omega_3 = -0.5$, eigenvalues: $-0.077 \pm 1.492i, +0.002 \pm 0.552i$

Middle Graph: $\omega_3 = -0.6488856842$, eigenvalues: $-0.097 \pm 1.565i, 0 \pm 0.649i$

Right Graph: $\omega_3 = -1$, eigenvalues: $-0.14 \pm 1.783i, -0.01 \pm 0.914i$

It is evident that depending on the initial spin, the Type 1 rattleback can exhibit two qualitatively different behaviours. For small spin, the Walker equilibria are unstable and the wobbling motion increases with time. Numerical simulations did detect an increase in the wobbling motion; however, even for large values of time elapsed at most one reversal was observed. Therefore, the numerical simulations

suggest that as $t \rightarrow \infty$ the rattleback spins in the stable direction while wobbling forever. Shown below are numerical simulations that demonstrate the instability of the Walker equilibria for small initial spin. For similar numerical experiments, see also [10].

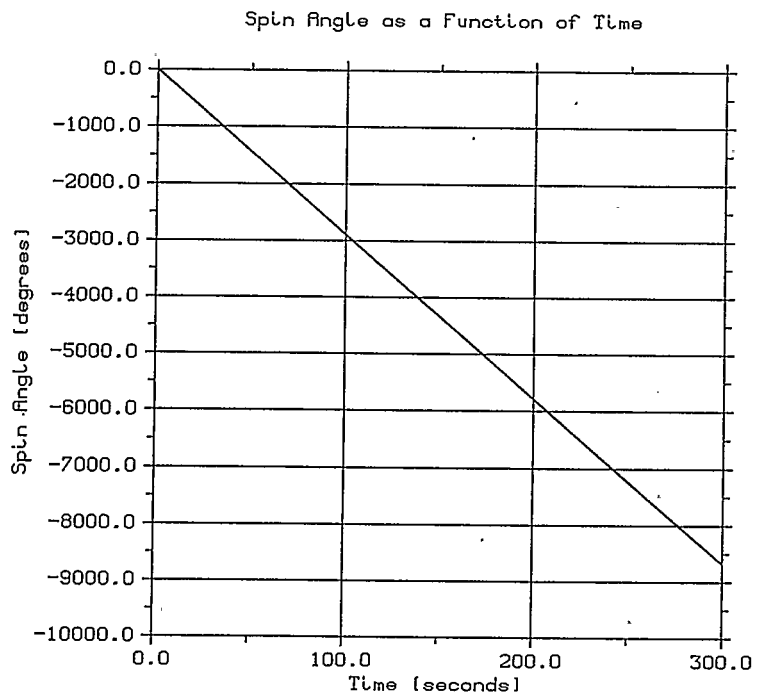


Figure 3.7: Type 1 Rattleback, $\omega_3 = -0.5$
 Parameters: $M=1, h=1, g=1, I_1 = 4, I_2 = 1, I_3 = 3.5, \sigma_{11} = 0.24, \sigma_{12} = 0.12, \sigma_{22} = 0.56, t_{step} = 0.001$
 Initial Conditions: $u_1 = 0.05, u_2 = 0, \omega_1 = 0, \omega_2 = 0, \omega_3 = -0.5$

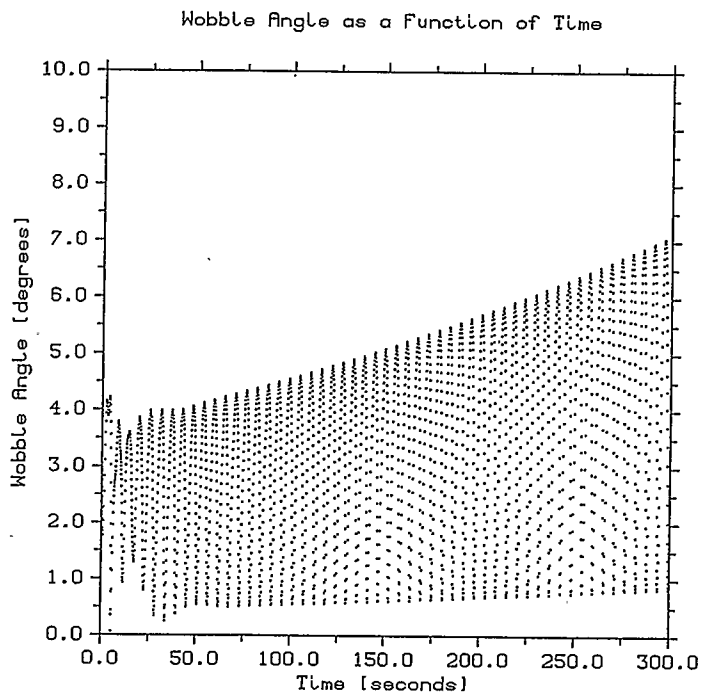


Figure 3.8: Type 1 Rattleback, $\omega_3 = -0.5$

Parameters: $M=1, h=1, g=1, I_1 = 4, I_2 = 1, I_3 = 3.5, \sigma_{11} = 0.24, \sigma_{12} = 0.12, \sigma_{22} = 0.56, t_{step} = 0.001$

Initial Conditions: $u_1 = 0.05, u_2 = 0, \omega_1 = 0, \omega_2 = 0, \omega_3 = -0.5$

Note: Even though the wobbling motion appears to be unstable, after a long numerical simulation it eventually leveled off while the spin angle did *not* reverse. This may indicate that while locally the equilibrium is unstable, globally the orbit does *not* end at the other equilibrium and the rattleback wobbles with a near-constant amplitude

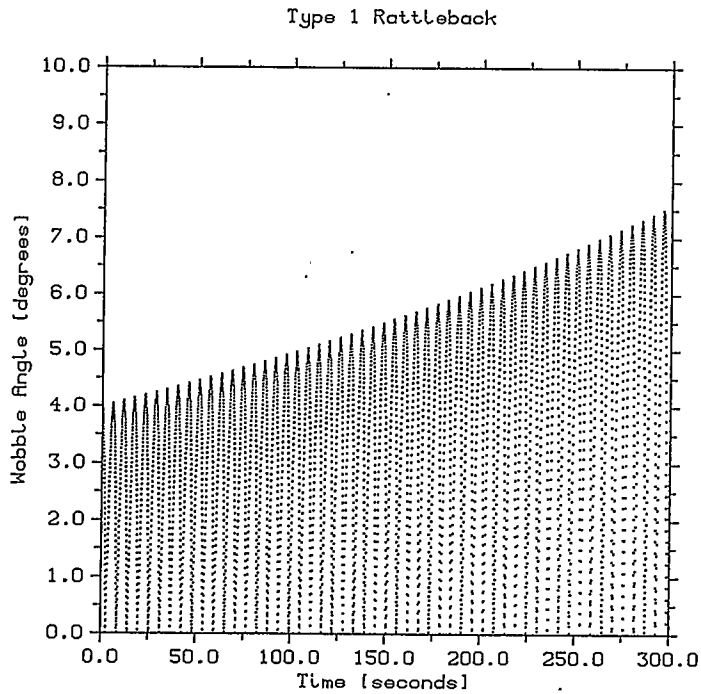


Figure 3.9: Type 1 Rattleback

Graph of solution of linearized equation: $y = 4|e^{0.002t} \cos .552t|$

Recall from Figure 3.6 that a $+0.002 \pm 0.552i$ is a pair of eigenvalues corresponding to the parameters given in Figure 3.8. Therefore, this figure is very similar to Figure 3.8

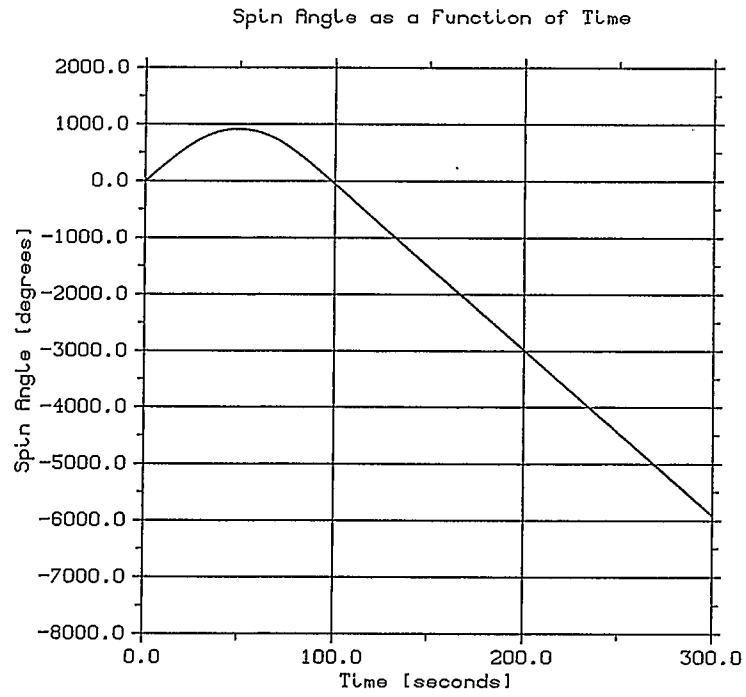


Figure 3.10: Type 1 Rattleback, $\omega_3 = 0.5$
 Parameters: $M=1, h=1, g=1, I_1 = 4, I_2 = 1, I_3 = 3.5, \sigma_{11} = 0.24, \sigma_{12} = 0.12, \sigma_{22} = 0.56, t_{step} = 0.001$
 Initial Conditions: $u_1 = 0.05, u_2 = 0; \omega_1 = 0, \omega_2 = 0, \omega_3 = 0.5$

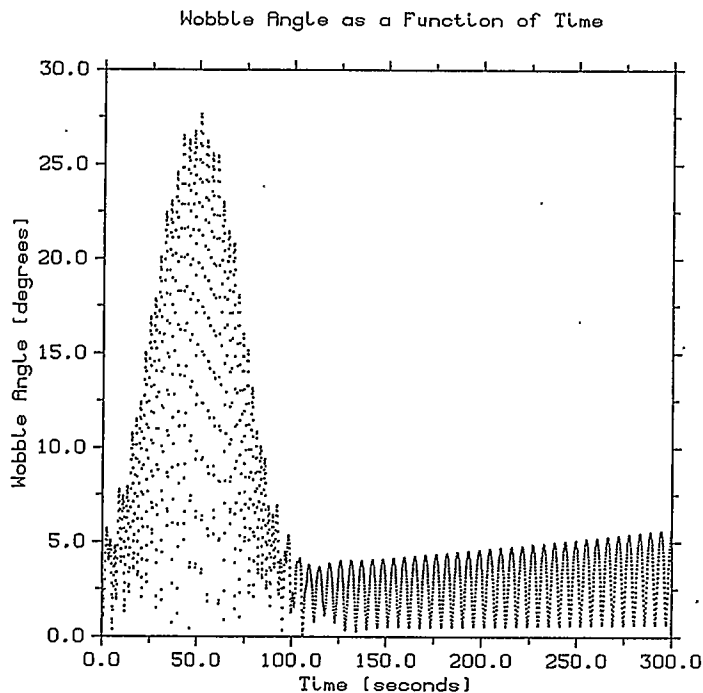


Figure 3.11: Type 1 Rattleback, $\omega_3 = 0.5$
 Parameters: $M=1, h=1, g=1, I_1 = 4, I_2 = 1, I_3 = 3.5, \sigma_{11} = 0.24, \sigma_{12} = 0.12, \sigma_{22} = 0.56, t_{step} = 0.001$
 Initial Conditions: $u_1 = 0.05, u_2 = 0, \omega_1 = 0, \omega_2 = 0, \omega_3 = 0.5$

However, for high initial spin a Hopf bifurcation occurs and one of the two Walker equilibria becomes stable. The rattleback exhibits a spin bias in one direction and when it starts moving in that direction, the wobbling decays:

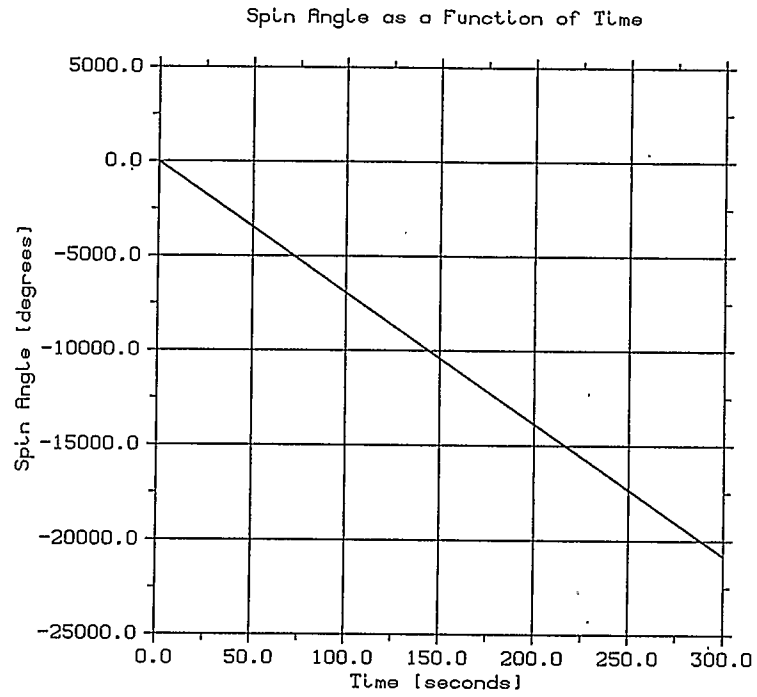


Figure 3.12: Type 1 Rattleback, $\omega_3 = -1.2$
 Parameters: $M=1, h=1, g=1, I_1 = 4, I_2 = 1, I_3 = 3.5, \sigma_{11} = 0.24, \sigma_{12} = 0.12, \sigma_{22} = 0.56, t_{step} = 0.001$
 Initial Conditions: $u_1 = 0.05, u_2 = 0, \omega_1 = 0, \omega_2 = 0, \omega_3 = -1.2$

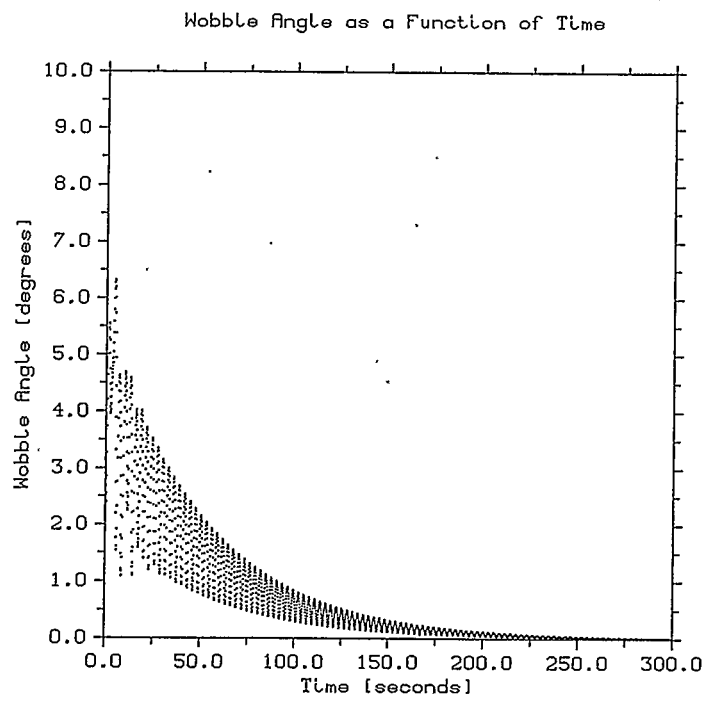


Figure 3.13: Type 1 Rattleback, $\omega_3 = -1.2$
 Parameters: $M=1, h=1, g=1, I_1 = 4, I_2 = 1, I_3 = 3.5, \sigma_{11} = 0.24, \sigma_{12} = 0.12, \sigma_{22} =$
 $0.56, t_{step} = 0.001$
 Initial Conditions: $u_1 = 0.05, u_2 = 0, \omega_1 = 0, \omega_2 = 0, \omega_3 = -1.2$

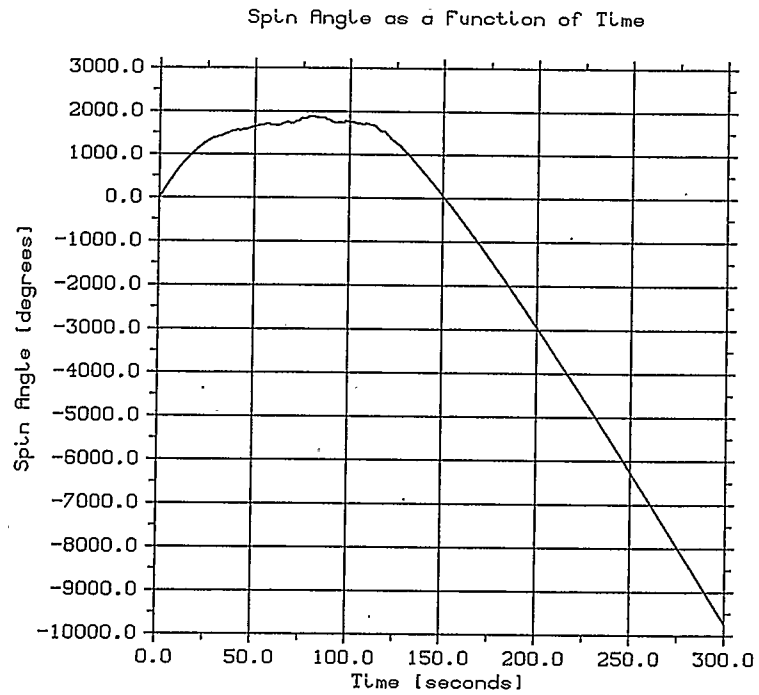


Figure 3.14: Type 1 Rattleback, $\omega_3 = 1.2$
 Parameters: $M=1, h=1, g=1, I_1 = 4, I_2 = 1, I_3 = 3.5, \sigma_{11} = 0.24, \sigma_{12} = 0.12, \sigma_{22} =$
 $0.56, t_{step} = 0.001$
 Initial Conditions: $u_1 = 0.05, u_2 = 0, \omega_1 = 0, \omega_2 = 0, \omega_3 = 1.2$

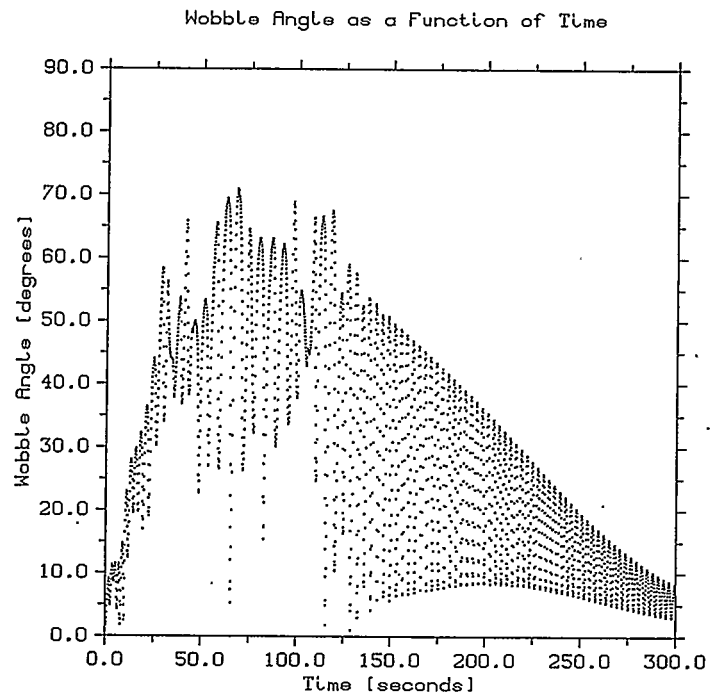


Figure 3.15: Type 1 Rattleback, $\omega_3 = 1.2$
 Parameters: $M=1, h=1, g=1, I_1 = 4, I_2 = 1, I_3 = 3.5, \sigma_{11} = 0.24, \sigma_{12} = 0.12, \sigma_{22} =$
 $0.56, t_{step} = 0.001$
 Initial Conditions: $u_1 = 0.05, u_2 = 0, \omega_1 = 0, \omega_2 = 0, \omega_3 = 1.2$

3.3.3 Type 2 Rattleback

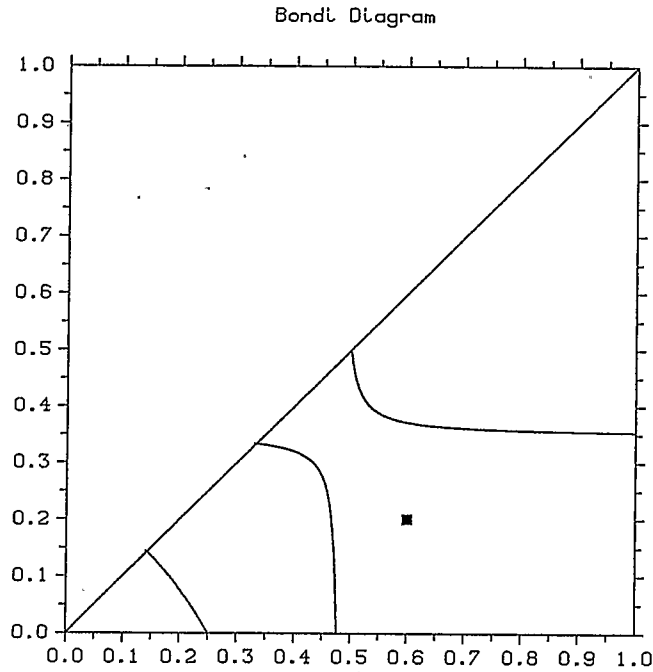


Figure 3.16: Type 2A Rattleback: Bondi Diagram

Parameters:

$$M = 1, h = 1, g = 1, I_1 = 4, I_2 = 3, I_3 = 2, \sigma_{11} = 0.24, \sigma_{12} = 0.12, \sigma_{22} = 0.56$$

Bondi Parameters:

$$\Theta = 0.6, \Phi = 0.2, \Psi = -0.8, \alpha = 5, \beta = 4, \gamma = 2, \kappa = -0.050, \mu = -1.133$$

1. $E = E_{min}$

The rattleback is not moving. There is only one equilibrium point:

$$[0, 0, 1, 0, 0, 0].$$

2. $E_{min} < E < E_H$

The rattleback has two equilibrium points: $[0, 0, 1, 0, 0, \pm\omega_3]$ These are the Walker equilibria. They are both unstable.

3. $E_H < E < E_{P_1}$

One of the two Walker equilibria becomes stable. Its eigenvalues cross the imaginary axis and a Hopf bifurcation occurs. There are still two Walker equilibria $[0, 0, 1, 0, 0, \pm\omega_3]$, but one of them is stable. The rattleback exhibits a bias in one direction, as is evident from the following numerical simulations.

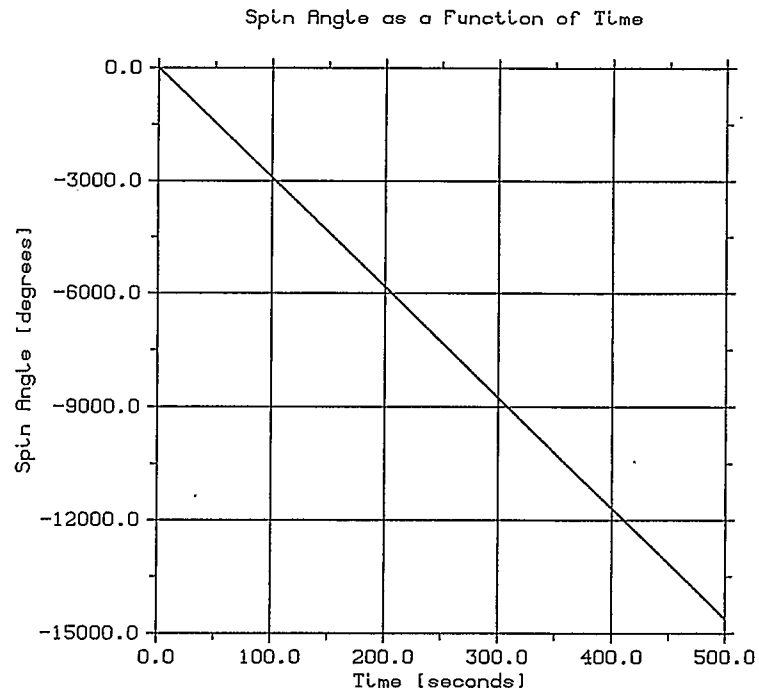


Figure 3.17: Type 2A Rattleback, $\omega_3 = -0.5$

Parameters:

$M=1, h=1, g=1, I_1 = 4, I_2 = 3, I_3 = 2, \sigma_{11} = 0.24, \sigma_{12} = 0.12, \sigma_{22} = 0.56, t_{step} = 0.001$

Initial Conditions: $u_1 = 0.05, u_2 = 0, \omega_1 = 0, \omega_2 = 0, \omega_3 = -0.5$

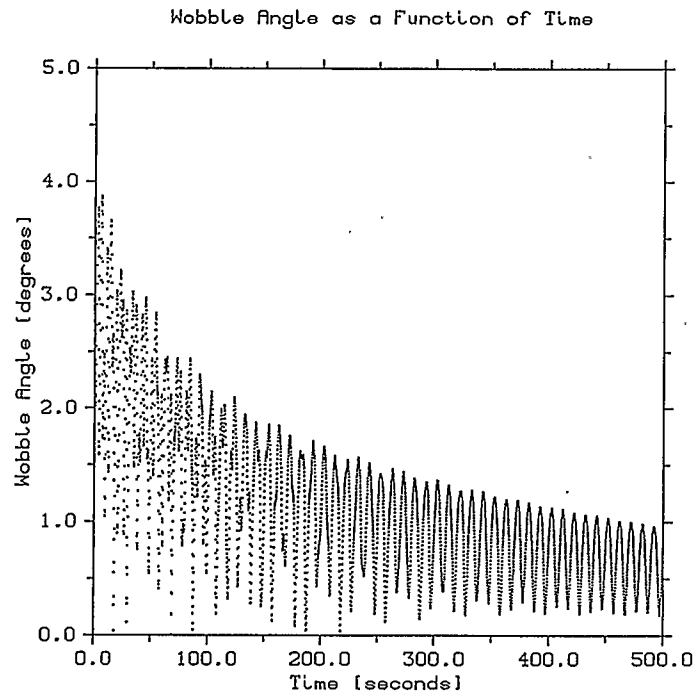


Figure 3.18: Type 2A Rattleback, $\omega_3 = -0.5$

Parameters:

$M=1, h=1, g=1, I_1 = 4, I_2 = 3, I_3 = 2, \sigma_{11} = 0.24, \sigma_{12} = 0.12, \sigma_{22} = 0.56, t_{step} = 0.001$

Initial Conditions: $u_1 = 0.05, u_2 = 0, \omega_1 = 0, \omega_2 = 0, \omega_3 = -0.5$

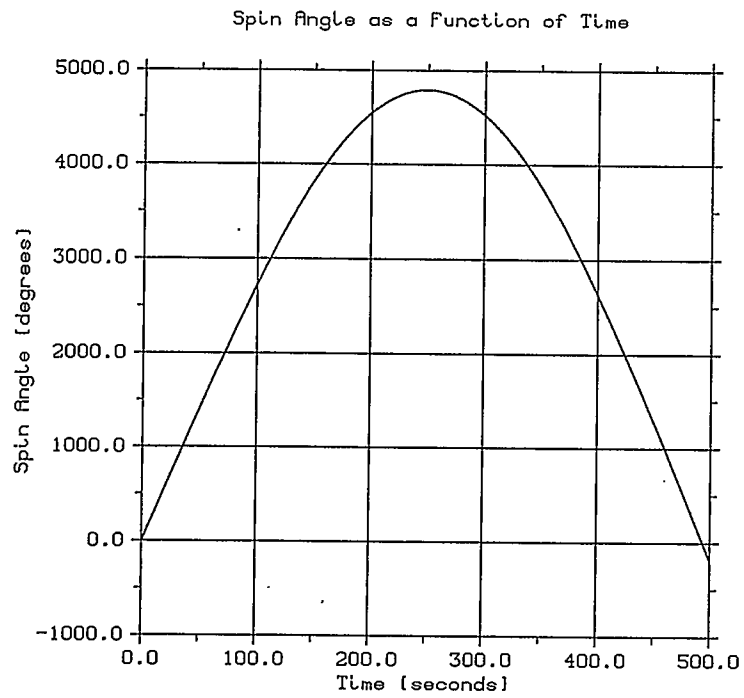


Figure 3.19: Type 2A Rattleback, $\omega_3 = 0.5$

Parameters:

$M=1, h=1, g=1, I_1 = 4, I_2 = 3, I_3 = 2, \sigma_{11} = 0.24, \sigma_{12} = 0.12, \sigma_{22} = 0.56, t_{step} = 0.001$

Initial Conditions: $u_1 = 0.05, u_2 = 0, \omega_1 = 0, \omega_2 = 0, \omega_3 = 0.5$

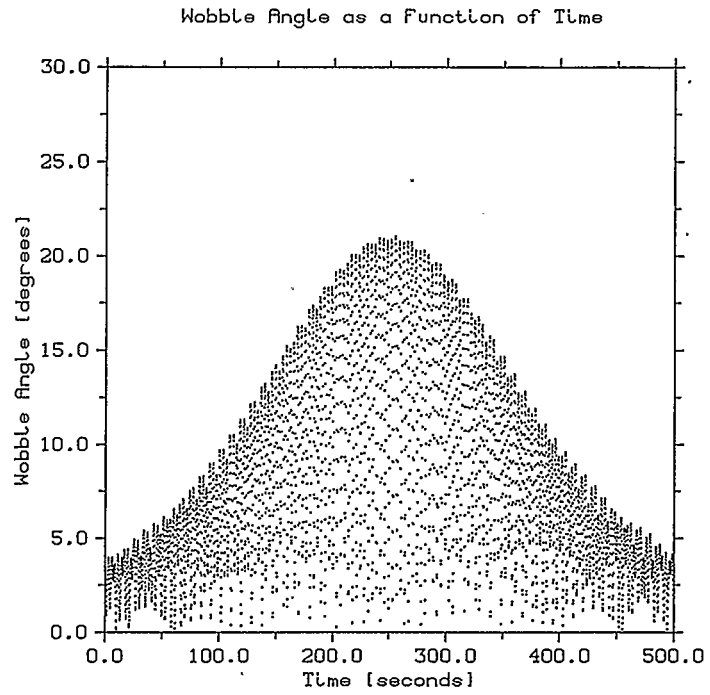


Figure 3.20: Type 2A Rattleback, $\omega_3 = 0.5$

Parameters:

$M=1, h=1, g=1, I_1 = 4, I_2 = 3, I_3 = 2, \sigma_{11} = 0.24, \sigma_{12} = 0.12, \sigma_{22} = 0.56, t_{step} = 0.001$

Initial Conditions: $u_1 = 0.05, u_2 = 0, \omega_1 = 0, \omega_2 = 0, \omega_3 = 0.5$

4. $E_{P_1} < E < E_{P_2}$

When the energy is above E_{P_1} , two eigenvalues of the one stable Walker equilibrium are both real and negative. One of these eigenvalues crosses the imaginary axis at the origin, and a pitchfork bifurcation occurs. Four new equilibria appear in addition to the two Walker equilibria. Both Walker equilibria are now unstable. Of the four new equilibria, two are stable and the other two are unstable. The rattleback exhibits bias in one direction and spins at an axis other than the vertical. For some rattlebacks, no further bifurcations of the Walker equilibrium occur. The following graph displays the relative positions of line $Q(w)$ and parabola $P(w)$ in this case:

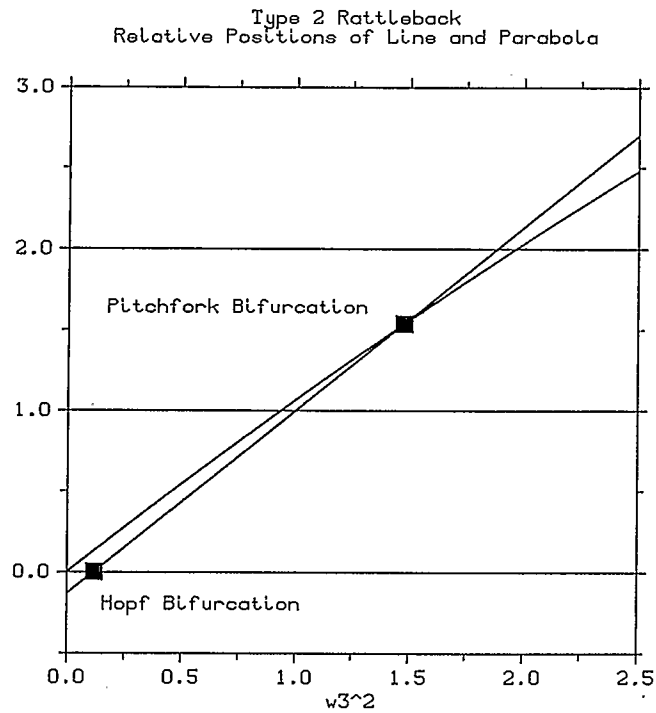


Figure 3.21: Type 2 Rattleback: Routh-Hurwitz Stability Criteria
 Graphs of Parabola $P(w)$ and Line $Q(w)$
 Parameters: $M=1, h=1, g=1, I_1 = 4, I_2 = 3, I_3 = 2, \sigma_{11} = 0.24, \sigma_{12} = 0.12, \sigma_{22} = 0.56$
 Hopf bifurcation: $\omega_3 = -0.3429971703$
 Pitchfork bifurcation: $\omega_3 = -1.214417405$

The following eigenvalue graphs demonstrate numerically that the pitchfork bifurcation at $\omega_3 = -1.214417405$:

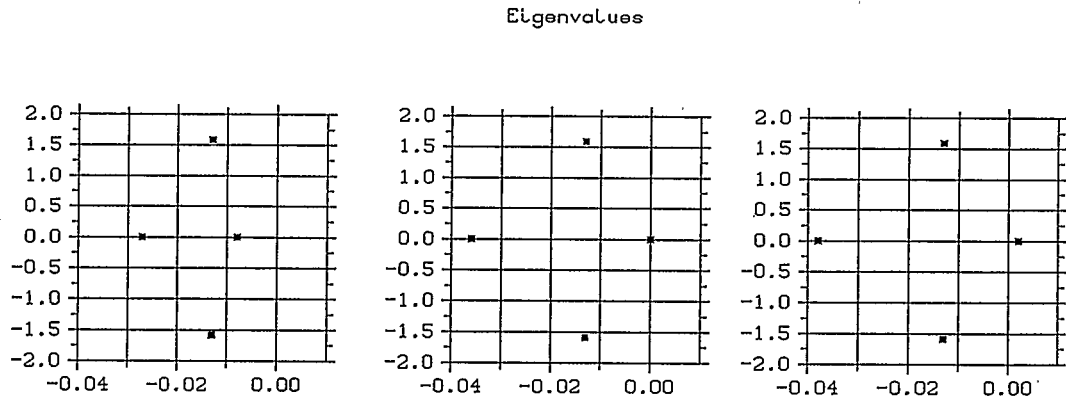


Figure 3.22: Type 2 Rattleback: Eigenvalues for 3 different ω_3

These three graphs from left to right demonstrate the following numerical values:

Leftmost graph: $\omega_3 = -1.213$, eigenvalues: $-0.008, -0.0273, -0.013 \pm 1.585i$

Middle graph: $\omega_3 = -1.214417405$, eigenvalues: $0, -0.036, -0.013 \pm 1.586i$

Rightmost graph: $\omega_3 = -1.215$, eigenvalues: $+0.002, -0.038, -0.013 \pm 1.583i$

The following numerical simulations show how the rattleback behaves for different initial spins.

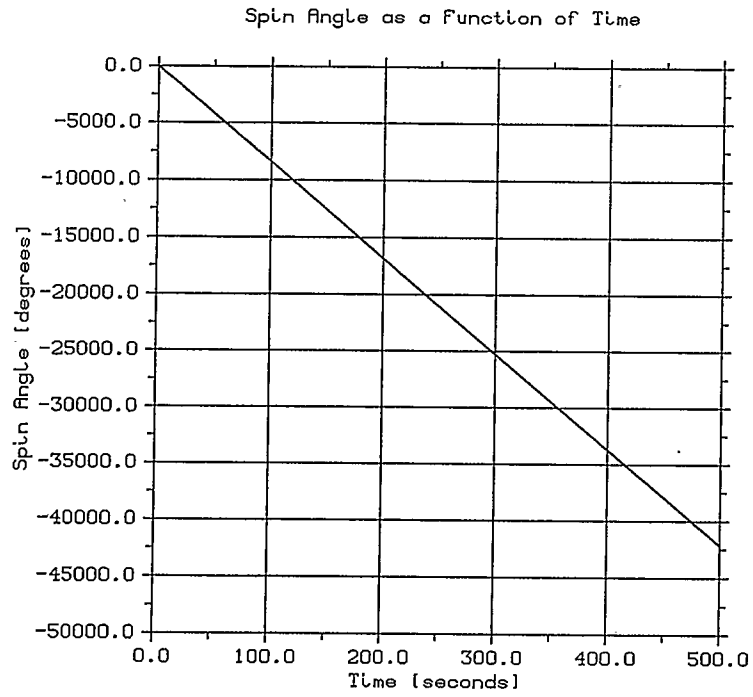


Figure 3.23: Type 2A Rattleback, $\omega_3 = -1.5$

Parameters:

$M=1, h=1, g=1, I_1 = 4, I_2 = 3, I_3 = 2, \sigma_{11} = 0.24, \sigma_{12} = 0.12, \sigma_{22} = 0.56, t_{step} = 0.001$

Initial Conditions: $u_1 = 0.05, u_2 = 0, \omega_1 = 0, \omega_2 = 0, \omega_3 = -1.5$

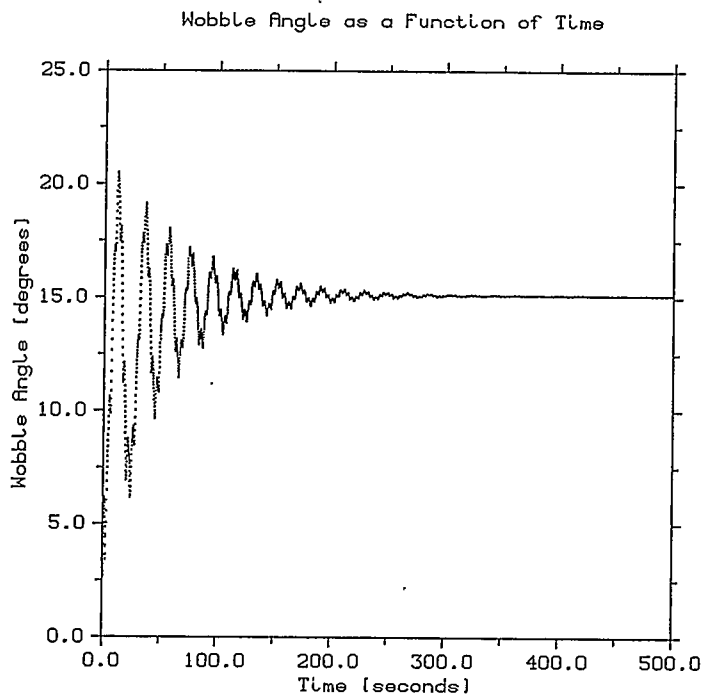


Figure 3.24: Type 2A Rattleback, $\omega_3 = -1.5$

Parameters:

$M=1, h=1, g=1, I_1 = 4, I_2 = 3, I_3 = 2, \sigma_{11} = 0.24, \sigma_{12} = 0.12, \sigma_{22} = 0.56, t_{step} = 0.001$

Initial Conditions: $u_1 = 0.05, u_2 = 0, \omega_1 = 0, \omega_2 = 0, \omega_3 = -1.5$

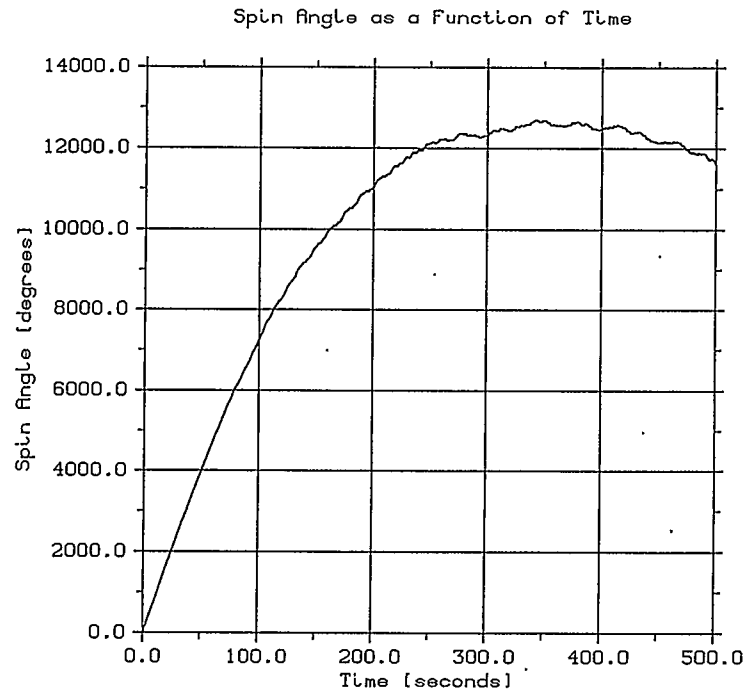


Figure 3.25: Type 2A Rattleback, $\omega_3 = 1.5$

Parameters:

$M=1, h=1, g=1, I_1 = 4, I_2 = 3, I_3 = 2, \sigma_{11} = 0.24, \sigma_{12} = 0.12, \sigma_{22} = 0.56, t_{step} = 0.001$

Initial Conditions: $u_1 = 0.05, u_2 = 0, \omega_1 = 0, \omega_2 = 0, \omega_3 = 1.5$

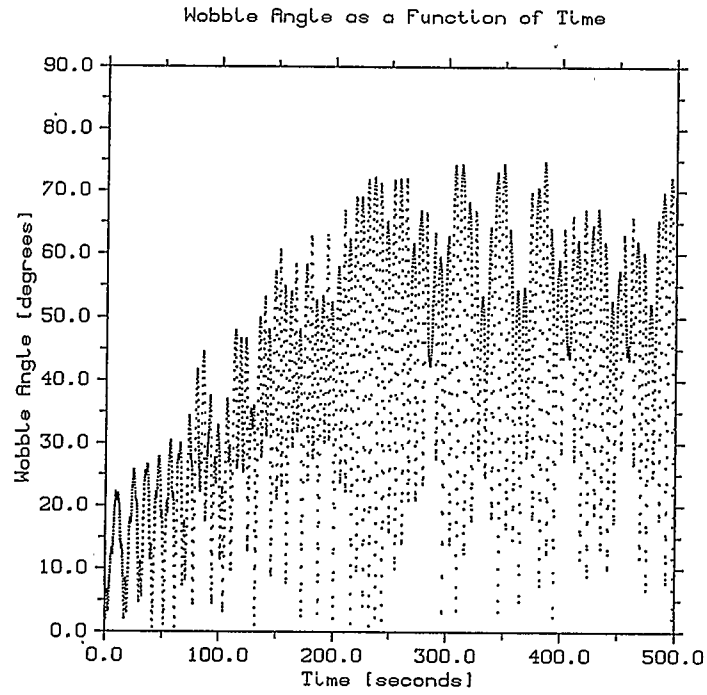


Figure 3.26: Type 2A Rattleback, $\omega_3 = 1.5$

Parameters:

$M=1, h=1, g=1, I_1 = 4, I_2 = 3, I_3 = 2, \sigma_{11} = 0.24, \sigma_{12} = 0.12, \sigma_{22} = 0.56, t_{step} = 0.001$

Initial Conditions: $u_1 = 0.05, u_2 = 0, \omega_1 = 0, \omega_2 = 0, \omega_3 = -1.5$

Other possible parameters for Type 2A rattleback are: $I_1 = 40, I_2 = 10, I_3 = 35, \sigma_{11} = 0.24, \sigma_{12} = 0.12, \sigma_{22} = 0.56$. Or: $I_1 = 40, I_2 = 10, I_3 = 35, \sigma_{11} = 0.25, \sigma_{12} = 0.05, \sigma_{22} = 0.25$.

5. $E > E_{P_2}$

At an even higher energy ($E > E_{P_2}$), a new pitchfork bifurcation occurs for some values of the parameters and now there are a total of ten equilibria. Example: $I_1 = 50, I_2 = 40, I_3 = 20, \sigma_{11} = 0.24, \sigma_{12} = 0.12, \sigma_{22} = 0.56, \kappa = 0.3, \mu = -0.001$. Note that in this last example, the rattleback would be in "Type 1" region of Bondi's diagram which is clearly not the case. The following graph displays the relative positions of line and parabola in this case:

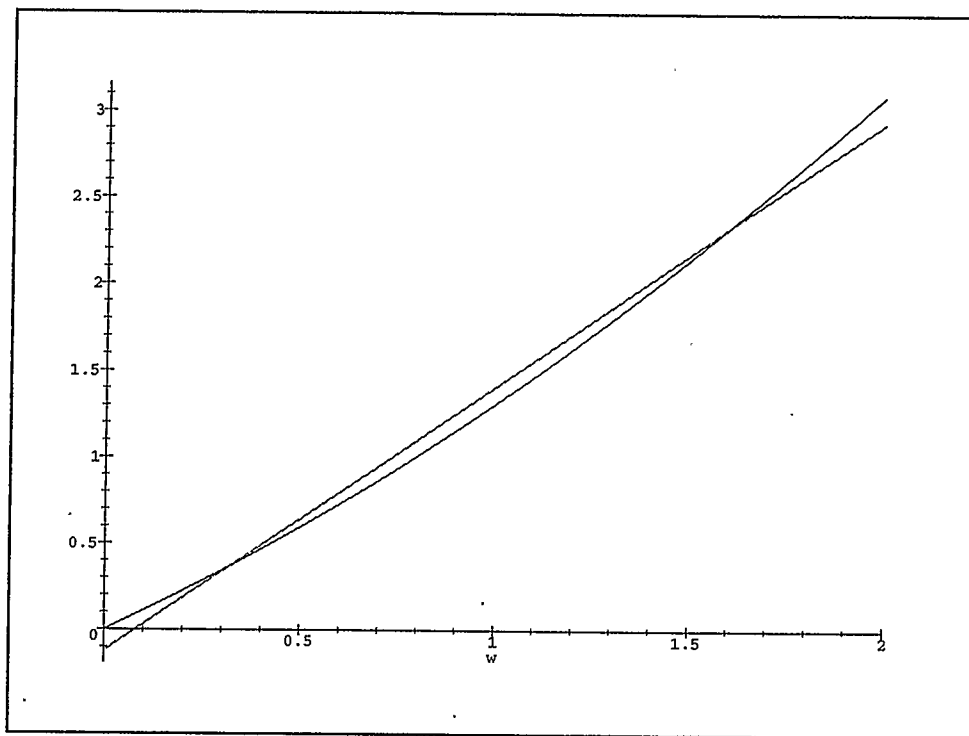


Figure 3.27: Type 2B Rattleback

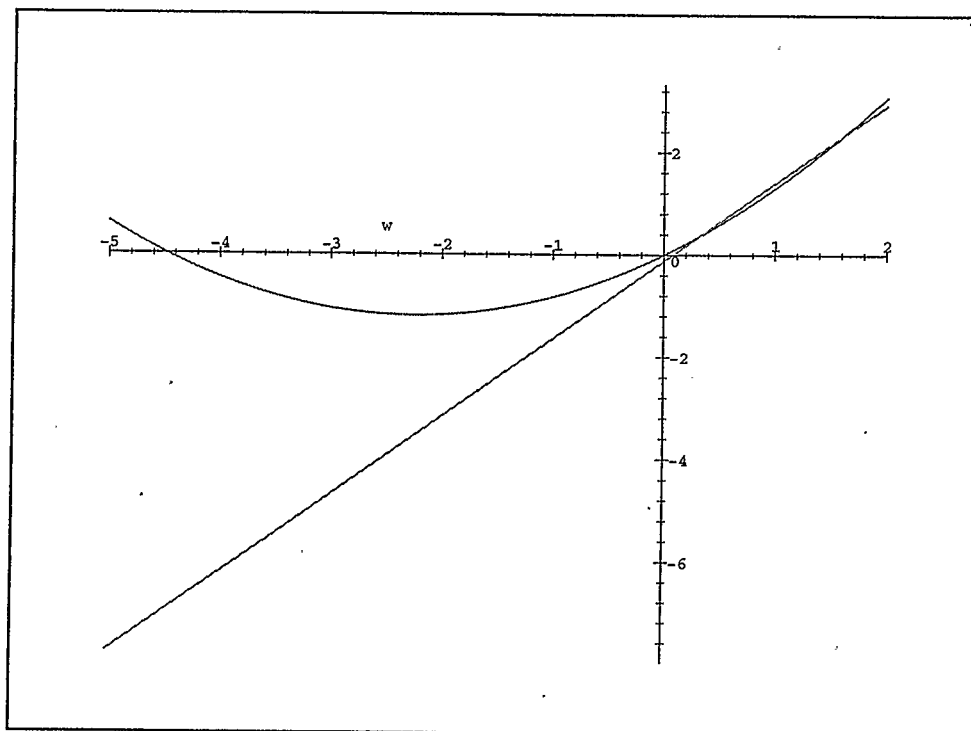


Figure 3.28: Type 2B Rattleback

3.4 Calculation of the Rotation Matrix $A(t)$ and Translation Vector $v(t)$ for the Rattleback

Solution of the differential equations for $[u_1, u_2, u_3]$ and $[\omega_1, \omega_2, \omega_3]$ would not be sufficient to find the exact motion of the rattleback. At any moment of time, the rattleback's position can be described by its orientation in space (given by a 3×3 orthogonal matrix $A(t)$) and a translation of its centre of mass (given by a 3-dimensional vector $v(t)$). The matrix $A(t)$ satisfies the following equation:

$$\dot{A} = A \begin{bmatrix} 0 & -\omega_3 & \omega_2 \\ \omega_3 & 0 & -\omega_1 \\ -\omega_2 & \omega_1 & 0 \end{bmatrix} \quad (3.22)$$

Let the components of $A(t)$ be:

$$A(t) = \begin{bmatrix} a_1 & b_1 & c_1 \\ a_2 & b_2 & c_2 \\ a_3 & b_3 & c_3 \end{bmatrix} \quad (3.23)$$

The components of $A(t)$ can be found as follows:

$$\begin{aligned}
\dot{a}_1 &= b_1\omega_3 - c_1\omega_2 \\
\dot{a}_2 &= b_2\omega_3 - c_2\omega_2 \\
\dot{a}_3 &= b_3\omega_3 - c_3\omega_2 \\
\dot{b}_1 &= c_1\omega_1 - a_1\omega_3 \\
\dot{b}_2 &= c_2\omega_1 - a_2\omega_3 \\
\dot{b}_3 &= c_3\omega_1 - a_3\omega_3 \\
\dot{c}_1 &= a_1\omega_2 - b_1\omega_1 \\
\dot{c}_2 &= a_2\omega_2 - b_2\omega_1 \\
\dot{c}_3 &= a_3\omega_2 - b_3\omega_1
\end{aligned} \tag{3.24}$$

Now let the translation vector be $[v_1, v_2, v_3]$. Its components can be found as follows:

$$\begin{aligned}
v_1 &= -a_1x - b_1y - c_1z \\
v_2 &= -a_2x - b_2y - c_2z \\
v_3 &= -a_3x - b_3y - c_3z
\end{aligned} \tag{3.25}$$

Here $[x, y, z]$ is the inverse of the Gauss map, depending on $[u_1, u_2, u_3]$. In conclusion a complete set of differential equations for the rattleback consists of 18 equations to be solved simultaneously: find $[u_1, u_2, u_3]$, $[\omega_1, \omega_2, \omega_3]$, $A(t)$ (9 equations) and $[v_1, v_2, v_3]$. Then if the rest position of a point on the rattleback is (q_1, q_2, q_3) , its position (p_1, p_2, p_3) after time t can be found using the equations:

$$\begin{aligned}
p_1 &= a_1q_1 + b_1q_2 + c_1q_3 + v_1 \\
p_2 &= a_2q_1 + b_2q_2 + c_2q_3 + v_2 \\
p_3 &= a_3q_1 + b_3q_2 + c_3q_3 + v_3
\end{aligned} \tag{3.26}$$

Chapter 4

Conclusion

4.1 New Results for the Euler Top

Somewhat surprisingly, this thesis has demonstrated that even for a centuries-old problem such as the Euler top there are new mathematical identities to be discovered. In collaboration with L. Bates and R. Cushman, the author of this thesis has found that the difference $(\xi(t_3) - \xi(t_1)) - (\vartheta(\tau) - \vartheta(0))$ can equal $0, 2\pi$ or -2π depending on the parameters chosen. An explanation for the phenomenon is provided in this thesis. The explanation is based on a subtle observation about how the motion takes place on a torus imbedded in $SO(3)$.

4.2 New Results for the Rattleback

Here is a summary of the new results for the rattleback that have been discovered in this thesis:

- There are more numerical simulations and graphs than in all previous rattleback papers combined.
- The numerical simulations indicate that for a Type 0 rattleback, spin reversal occurs at the time of the local maximum of the lower beat frequency of the wobble angle.
- For Type 1 rattleback, when the energy is low the numerical simulations show that

the rattleback does *not* reverse infinitely many times, as Bondi [6] or Garcia and Hubbart [10] imply. When the rattleback starts moving in the stable spin direction, the local maximums of the wobble angle asymptotically approach some constant angle. In practice, this means that for low energies a Type 1 rattleback spins in the stable direction while wobbling forever.

- Hermans [13] describes rattlebacks with two or ten equilibria, depending on the relative positions of the line and parabola that emerge from the Routh-Hurwitz stability criteria. In this thesis, a new configuration is found that yields *six* equilibria. A rattleback with six equilibria is called Type 2A rattleback, to distinguish it from a rattleback with ten equilibria - Type 2B rattleback.

Bibliography

- [1] V. Arnold. Sur la geometrie differentielle des groupes de lie de dimension infinie et ses applications a l'hydrodynamique des fluides parfaits. *Ann. Inst. Fourier, Grenoble*, 16,1:319-361, 1966.
- [2] V. I. Arnold. and A. Avez. *Ergodic Problems of Classical Mechanics*. W.A. Benjamin, New York, 1968.
- [3] V. I. Arnold. *Mathematical Methods of Classical Mechanics*. Springer-Verlag. New York, 1978.
- [4] I.S. Astapov. Rotational stability of a celtic stone. *Vestnik Moskovskogo Universiteta. Mekhanika*, 35(2):97–100, 1980. Pages may be different in English translation.
- [5] Allan J. Boardman. The Mysterious Celt. *Fine Woodworking*, pages 68-69, July/August 1985.
- [6] Sir Hermann Bondi. The rigid body dynamics of unidirectional spin. *Proc. R. Soc. London, A*, 405:265–274, 1986.
- [7] Richard H. Cushman and Larry M. Bates. *Global Aspects of Classical Integrable Systems*. Birkhauser Verlag, P.O. Box 133, CH-4010 Basel, Switzerland, 1997.
- [8] G. Darboux. Cours de mecanique, 1886.
- [9] L. Euler. Du mouvement de rotation des corps solides autour d'un axe variable. *Mem. Acad. Roy. Sci. et Belles-Lettres de Berlin*, 14(1765):154–193, 1758.

- [10] A. Garcia and M. Hubbard. Spin reversal of the rattleback: Theory and experiment. *Proc. R. Soc. London, A*, 418:165–197, 1988.
- [11] H.G.E. Graumann. Nonholonomic symmetry reduction of the rattleback and related planar rolling problems. Master's thesis, University of Calgary, 1994.
- [12] John Guckenheimer and Philip Holmes. Nonlinear Oscillations, Dynamical Systems, and Bifurcations of Vector Fields. Springer-Verlag, New York, 1983.
- [13] Joost Hermans. *Rolling Rigid Bodies with and without Symmetries*. PhD thesis, Universiteit Utrecht, 1995.
- [14] Thomas R. Kane and David A. Levinson. Realistic mathematical modeling of the rattleback. *International Journal of Non-Linear Mechanics*, 17(3):175–186, 1982.
- [15] A.V. Karapetyan. Hopf bifurcation in the problem of motion of a heavy rigid body over a rough plane. *Inv. AN SSSR. Mekhanika Tverdogo Tela*, 20(2):19–24, 1985. Pages may be different in English translation.
- [16] M. L. Lecomte. Sur l'herpolhode. *Bull. Soc. Math. France*, XXXIV:40–41, 1906.
- [17] Mark Levi. Geometric Phases in the Motion of Rigid Bodies. *Archive for Rational Mechanics and Analysis*, 122:213–219, 1993.
- [18] K. Magnus. *Kreisel: Theorie und Anwendungen*. Springer-Verlag, Berlin, 1971.
- [19] K. Magnus. Die stabilität der drehbewegungen eines unsymmetrischen korpers auf horizontaler unterlage. *Theorie und Praxis der Ingenieurwissenschaften*, S:19–23, 1971.

- [20] K. Magnus. Zur theorie der keltischen wackelsteine. *Zeitschrift fur angewandte mathematik und mechanik*, 54(4):54–55, 1974.
- [21] R. Montgomery. How much the rigid body rotate? A Berry's phase from the 18th century *American Journal of Physics*, 59 (5), 1991.
- [22] R. Montgomery J. Marsden and T. Ratiu. Reduction, symmetry and phases in mechanics. *Mem. Amer. Math. Soc.*, 88, 1990.
- [23] L. Poinsot. Theorie nouvelle de la rotation des corps. Paris, 1834.
- [24] E. J. Routh. *The Advanced Part of a Treatise on the Dynamics of a System of Rigid Bodies*. Macmillian and Co., London, 4 edition, 1884.
- [25] J. Walker. The Amateur Scientist - the Mysterious Rattleback: A Stone That Spins in One Direction and Then Reverses *Scientific American*, pages 172-184, October 1979.
- [26] G.T.Walker. On a dynamical top. *Quarterly Journal of Pure and Applied Mathematics*, 28:175–184, 1896.
- [27] E. T. Whittaker. *A Treatise on the Analytical Dynamics of Particles and Rigid Bodies*. Cambridge University Press, Cambridge, 1989.

Appendix A

Computer Program for the Euler Top

The computer program that ran the simulations was written in FORTRAN 90 and is supplied in this appendix. There are two files to be compiled and linked:

"euler.f90" (code lines from PROGRAM EULER to END PROGRAM EULER)

"subroutines.f90" (code lines from MODULE SUBROUTINES to END MODULE SUBROUTINES).

On most machines, compiling and linking can be accomplished with commands similar to the following:

```
f90 subroutines.f90 euler.f90
```

This compiles and links the files, then creates an executable file. On UNIX machines the name of the executable file is "a.out". The input variables and initial conditions are entered in a separate text file "data" in the following order: $I_1, I_2, I_3, L, \theta_i, \phi_i, \psi_i, dt, t_f$. Once the nine numbers for file "data" are entered with spaces between them, executing the file "a.out" produces two output files: "output1" and "output2". The file output1 has 12 columns: $t, \omega_1, \omega_2, \omega_3, \vartheta, \xi, r, x_h, y_h, x_r, y_r, z_r$. Here t is time, $[\omega_1, \omega_2, \omega_3]$ are the components of the instantaneous angular velocity in the rotating frame (the solutions of the Euler equations). ϑ is the projection angle. ξ is the angle swept by the herpolhode and r is its radius at a time t . $[x_h, y_h]$ are the coordinates of the herpolhode points, while $[x_r, y_r, z_r]$ are the 3-D coordinates of the rotation using the solid ball model. These quantities can then be plotted using a standard graphics package. For example, here are the commands used in MATLAB

to produce a herpolhode graph:

```
>> load('output1');  
>> x=output1(:,8);  
>> y=output1(:,9);  
>> plot(x,y)
```

The file output2 has the following entries: $t_1, \xi(t_1), \vartheta(t_1), t_3, \xi(t_3), \vartheta(t_3), \tau = t_3 - t_1, \xi(t_3) - \xi(t_1), \vartheta(t_3) - \vartheta(t_1), \vartheta(t_3) - \vartheta(t_1) - (\xi(t_3) - \xi(t_1)), L^2 - 2I_2E$. The numbers in this exact order can be seen to the right of each herpolhode graph in this thesis.

The lines on this page should be written in file "euler.f90".

```
PROGRAM EULER
USE SUBROUTINES
IMPLICIT NONE
OPEN(UNIT=100,FILE='data')
READ(100,*) A,B,C,L,THETA0,PHIO,PSIO,H,TF
CLOSE(UNIT=100)
CALL INITIAL
T=0.0D0
OPEN(UNIT=210,FILE='output1')
OPEN(UNIT=220,FILE='output2')
DO WHILE (T.LE.TF)
CALL RUNGE
CALL HERPOLHODE
CALL SO3
WRITE(210,310) T,W1,W2,W3,THETA1,THETA_HERPOLHODE,&
RADIUS, HERPOLHODE1D, HERPOLHODE2D, R1, R2, R3
ENDDO
WRITE(220,*) T1,H1,TH1,T3,H3,TH3,DT,DH,DTH,DIFF,L1
310 FORMAT(12(F6.3,2X))
END PROGRAM EULER.
```

All the lines from here on should be written in a file "subroutines.f90".

```

MODULE SUBROUTINES

IMPLICIT NONE

REAL(8),PUBLIC:: T,H,A,B,C,L,THETAO,PHIO,PSIO,A1,A2,A3,&
B1,B2,B3,C1,C2,C3,THETA1,W1,W2,W3,PI,HERPOLHODE1D,&
HERPOLHODE2D,THETA_HERPOLHODE,RADIUS,DELTA1,XPOINT1,&
YPOINT1,XPOINT2,YPOINT2,XPOINT3,YPOINT3,R1,R2,R3,&
THETA2,TF,E,T1,T3,H1,H3,TH1,TH3,DT,DH,DTH,DIFF,L1,&
RMAX,RMIN

REAL(4),PUBLIC:: VECTOR114,VECTOR124,VECTOR214,&
VECTOR224

LOGICAL,PUBLIC:: TIME_TO_EXIT=.FALSE.,SWITCH1=.TRUE.,&
SWITCH2=.FALSE.,DELTA1SWITCH=.FALSE.,&
DELTA01SWITCH=.FALSE.

REAL(8),PRIVATE:: W1DOT1,W1DOT2,W1DOT3,W1DOT4,W2DOT1,W2DOT2,W2DOT3,&
W2DOT4,W3DOT1,W3DOT2,W3DOT3,W3DOT4,&
THETA1DOT1,THETA1DOT2,THETA1DOT3,THETA1DOT4

CONTAINS

FUNCTION W1DOT(W1,W2,W3)
REAL(8) W1DOT,W1,W2,W3
W1DOT=(B-C)*W2*W3/A

```

```
END FUNCTION W1DOT
```

```
FUNCTION W2DOT(W1,W2,W3)
```

```
REAL(8) W2DOT,W1,W2,W3
```

```
W2DOT=(C-A)*W1*W3/B
```

```
END FUNCTION W2DOT
```

```
FUNCTION W3DOT(W1,W2,W3)
```

```
REAL(8) W3DOT,W1,W2,W3
```

```
W3DOT=(A-B)*W1*W2/C
```

```
END FUNCTION W3DOT
```

```
FUNCTION THETA1DOT(W1,W2,W3)
```

```
REAL(8) THETA1DOT,W1,W2,W3
```

```
IF((L**2-(A*W1)**2).NE.0) THEN
```

```
THETA1DOT=L*(B*W2**2+C*W3**2)/(L**2-(A*W1)**2)
```

```
ELSE
```

```
TIME_TO_EXIT=.TRUE.
```

```
ENDIF
```

```
END FUNCTION THETA1DOT
```

```
SUBROUTINE RUNGE
```

```
!*****
```

```

!
! Fourth order Runge-Kutta solver of the differential
! equations defined in MODULE FUNCTIONS.
!
! INPUT VARIABLES:
! REAL(8) H (STEP SIZE)
! INPUT/OUTPUT VARIABLES (UPDATED IN THE SUBROUTINE):
! REAL(8) T,W1,W2,W3,THETA1,A1,A2,A3,B1,B2,B3,C1,C2,C3
! All the above variables are defined as REAL(8),PUBLIC
! in MODULE VARIABLES1.
!*****

W1DOT1=H*W1DOT(W1,W2,W3)
W2DOT1=H*W2DOT(W1,W2,W3)
W3DOT1=H*W3DOT(W1,W2,W3)
THETA1DOT1=H*THETA1DOT(W1,W2,W3)
W1DOT2=H*W1DOT(W1+0.5D0*W1DOT1,W2+0.5D0*W2DOT1,&
W3+0.5D0*W3DOT1)
W2DOT2=H*W2DOT(W1+0.5D0*W1DOT1,W2+0.5D0*W2DOT1,&
W3+0.5D0*W3DOT1)
W3DOT2=H*W3DOT(W1+0.5D0*W1DOT1,W2+0.5D0*W2DOT1,&
W3+0.5D0*W3DOT1)
THETA1DOT2=H*THETA1DOT(W1+0.5D0*W1DOT1,W2+0.5D0*W2DOT1,&
W3+0.5D0*W3DOT1)

```

$$W1DOT3=H*W1DOT(W1+0.5D0*W1DOT2,W2+0.5D0*W2DOT2,& \\ W3+0.5D0*W3DOT2)$$

$$W2DOT3=H*W2DOT(W1+0.5D0*W1DOT2,W2+0.5D0*W2DOT2,& \\ W3+0.5D0*W3DOT2)$$

$$W3DOT3=H*W3DOT(W1+0.5D0*W1DOT2,W2+0.5D0*W2DOT2,& \\ W3+0.5D0*W3DOT2)$$

$$THETA1DOT3=H*THETA1DOT(W1+0.5D0*W1DOT2,W2+0.5D0*W2DOT2,& \\ W3+0.5D0*W3DOT2)$$

$$W1DOT4=H*W1DOT(W1+W1DOT3,W2+W2DOT3,W3+W3DOT3)$$

$$W2DOT4=H*W2DOT(W1+W1DOT3,W2+W2DOT3,W3+W3DOT3)$$

$$W3DOT4=H*W3DOT(W1+W1DOT3,W2+W2DOT3,W3+W3DOT3)$$

$$THETA1DOT4=H*THETA1DOT(W1+W1DOT3,W2+W2DOT3,W3+W3DOT3)$$

$$T=T+H$$

$$W1=W1+(W1DOT1+2.0D0*W1DOT2+2.0D0*W1DOT3+W1DOT4)/6.0D0$$

$$W2=W2+(W2DOT1+2.0D0*W2DOT2+2.0D0*W2DOT3+W2DOT4)/6.0D0$$

$$W3=W3+(W3DOT1+2.0D0*W3DOT2+2.0D0*W3DOT3+W3DOT4)/6.0D0$$

$$THETA1=THETA1+(THETA1DOT1+2.0D0*THETA1DOT2+2.0D0* &$$

$$THETA1DOT3+THETA1DOT4)/6.0D0$$

$$A3=A*W1/L$$

$$B3=B*W2/L$$

$$C3=C*W3/L$$

$$A1=(DSQRT(1-A3**2))*DCOS(THETA1)$$

```

A2=(DSQRT(1-A3**2))*DSIN(THETA1)
B1=-(A3*B3*DCOS(THETA1)+C3*DSIN(THETA1))/DSQRT(1-A3**2)
B2=(C3*DCOS(THETA1)-A3*B3*DSIN(THETA1))/DSQRT(1-A3**2)
C1=-(A3*C3*DCOS(THETA1)-B3*DSIN(THETA1))/DSQRT(1-A3**2)
C2=-(B3*DCOS(THETA1)+A3*C3*DSIN(THETA1))/DSQRT(1-A3**2)

```

```

END SUBROUTINE RUNGE

```

```

SUBROUTINE HERPOLHODE

```

```

!*****

```

```

!
```

```

! Using the output from SUBROUTINE RUNGE and SUBROUTINE ROTATE,
! SUBROUTINE HERPOLHODE does the following:

```

```

!
```

```

! 1. Computes the new 2-D point of the herpolhode curve

```

```

! x-coordinate = HERPOLHODE1D = HERPOLHODE1

```

```

! y-coordinate = HERPOLHODE2D = HERPOLHODE2

```

```

!
```

```

! 2. Updates the angle of the new vector relative to the
! starting vector (this angle is equal to THETA_HERPOLHODE)

```

```

!
```

```

! 3. Finds the 2 points when the radius of the herpolhode
! is a maximum (with 1 maximum between the 2 points skipped)

```

```

! First point: (VECTOR114,VECTOR124)
! Second point: (VECTOR214,VECTOR224)
!
! 4. Finds the angle (DELTA1) between the 2 points
!
!*****
REAL(8) RPOINT1,RPOINT2,RPOINT3

!FINDING THE HERPOLHODE COORDINATES FROM ROTATION MATRIX
HERPOLHODE1D=A1*W1+B1*W2+C1*W3
HERPOLHODE2D=A2*W1+B2*W2+C2*W3
!END FINDING THE HERPOLHODE COORDINATES FROM ROTATION MATRIX
RADIUS=SQRT(HERPOLHODE1D**2+HERPOLHODE2D**2)
XPOINT3=XPOINT2
YPOINT3=YPOINT2
XPOINT2=XPOINT1
YPOINT2=YPOINT1
XPOINT1=HERPOLHODE1D
YPOINT1=HERPOLHODE2D
IF(((XPOINT1**2+YPOINT1**2)*(XPOINT2**2+YPOINT2**2)).NE.0)&
THETA_HERPOLHODE=THETA_HERPOLHODE+DACOS((XPOINT1*&
XPOINT2+YPOINT1*YPOINT2)/DSQRT((XPOINT1**2+YPOINT1**2)*&
(XPOINT2**2+YPOINT2**2)))

```

```
IF (SWITCH1.OR.SWITCH2) THEN
RPOINT1=XPOINT1**2+YPOINT1**2
RPOINT2=XPOINT2**2+YPOINT2**2
RPOINT3=XPOINT3**2+YPOINT3**2
IF ((RPOINT2.GT.RPOINT1).AND.(RPOINT2.GT.RPOINT3)) THEN
IF(SWITCH1.AND.(.NOT.SWITCH2)) THEN
VECTOR114=XPOINT2
VECTOR124=YPOINT2

T1=T
H1=THETA_HERPOLHODE
TH1=THETA1

DELTA01SWITCH=.TRUE.
ENDIF
IF (SWITCH1.AND.SWITCH2) THEN
SWITCH1=.FALSE.
SWITCH2=.FALSE.
VECTOR214=XPOINT2
VECTOR224=YPOINT2
DELTA1=ACOS((VECTOR114*VECTOR214+VECTOR124*VECTOR224)/&
Sqrt((VECTOR114**2+VECTOR124**2)*(VECTOR214**2+VECTOR224**2)))

T3=T
```

```
H3=THETA_HERPOLHODE
TH3=THETA1
DT=T3-T1
DH=H3-H1
DTH=TH3-TH1
DIFF=DTH-DH
DELTA1SWITCH=.TRUE.
ENDIF
IF ((.NOT.SWITCH1).AND.SWITCH2) THEN
SWITCH1=.TRUE.
SWITCH2=.TRUE.
ENDIF
IF (SWITCH1.AND.(.NOT.SWITCH2)) THEN
SWITCH1=.FALSE.
SWITCH2=.TRUE.
ENDIF
ENDIF
ENDIF
END SUBROUTINE HERPOLHODE
```

```
SUBROUTINE S03
```

```
!*****
```

```
!
```

```

! Using the output of SUBROUTINE ROTATE, SUBROUTINE S03
! calculates the point (R1,R2,R3) and angle (THETA2) that
! is equivalent to the matrix of rotation, according to
! the solid ball model.

```

```
!
```

```
!*****
```

```
REAL(8) TRACE
```

```
TRACE=A1+B2+C3
```

```
THETA2=DACOS(0.5D0*(TRACE-1.0D0))
```

```
R1=THETA2*(B3-C2)/(2.0D0*DSIN(THETA2))
```

```
R2=THETA2*(C1-A3)/(2.0D0*DSIN(THETA2))
```

```
R3=THETA2*(A2-B1)/(2.0D0*DSIN(THETA2))
```

```
END SUBROUTINE S03
```

```
SUBROUTINE INITIAL
```

```
!INPUT: A,B,C,L,THETA0,PHIO,PSIO,
```

```
!OUTPUT: A1,A2,A3,B1,B2,B3,C1,C2,C3,W1,W2,W3,THETA1 AT T=0
```

```
!OUTPUT: E,L1,RMIN,RMAX
```

```
PI=4.0D0*DATAN(1.0D0)
```

```
THETA0=(PI/180.0D0)*THETA0
```

```
PHIO=(PI/180.0D0)*PHIO
```

```
PSIO=(PI/180.0D0)*PSIO
```

```

A1=DCOS(THETAO)*DCOS(PHIO)*DCOS(PSIO)-DSIN(PHIO)*DSIN(PSIO)
A2=DCOS(THETAO)*DSIN(PHIO)*DCOS(PSIO)+DCOS(PHIO)*DSIN(PSIO)
A3=-DSIN(THETAO)*DCOS(PSIO)

B1=-DCOS(THETAO)*DCOS(PHIO)*DSIN(PSIO)-DSIN(PHIO)*DCOS(PSIO)
B2=-DCOS(THETAO)*DSIN(PHIO)*DSIN(PSIO)+DCOS(PHIO)*DCOS(PSIO)
B3=DSIN(THETAO)*DSIN(PSIO)

C1=DSIN(THETAO)*DCOS(PHIO)
C2=DSIN(THETAO)*DSIN(PHIO)
C3=DCOS(THETAO)

W1=A3*L/A
W2=B3*L/B
W3=C3*L/C

THETA1=DATAN(A2/A1)

E=0.5DO*(A*W1**2+B*W2**2+C*W3**2)

L1=L**2-2*B*E

TIME_TO_EXIT=.FALSE.

IF((A.GE.B).AND.(B.GE.C)) THEN
RMAX=(2.ODO/L)*DSQRT((L**2/(2.ODO*C)-E)*(E-L**2/(2.ODO*A)))
IF(L1.LT.0) THEN
RMIN=(2.ODO/L)*DSQRT((L**2/(2.ODO*C)-E)*(E-L**2/(2.ODO*B)))
ELSE
RMIN=(2.ODO/L)*DSQRT((L**2/(2.ODO*B)-E)*(E-L**2/(2.ODO*A)))
ENDIF
ENDIF

```

```
IF((A.LT.B).AND.(B.LT.C)) THEN
RMAX=(2.0D0/L)*DSQRT((L**2/(2.0D0*A)-E)*(E-L**2/(2.0D0*C)))
IF(L1.GE.0) THEN
RMIN=(2.0D0/L)*DSQRT((L**2/(2.0D0*B)-E)*(E-L**2/(2.0D0*C)))
ELSE
RMIN=(2.0D0/L)*DSQRT((L**2/(2.0D0*A)-E)*(E-L**2/(2.0D0*B)))
ENDIF
ENDIF

SWITCH1=.TRUE.
SWITCH2=.FALSE.
HERPOLHODE1D=A1*W1+B1*W2+C1*W3
HERPOLHODE2D=A2*W1+B2*W2+C2*W3
XPOINT1=HERPOLHODE1D
YPOINT1=HERPOLHODE2D
XPOINT2=XPOINT1
YPOINT2=YPOINT1
XPOINT3=XPOINT1
YPOINT3=YPOINT1
THETA_HERPOLHODE=0.0D0
DELTA01SWITCH=.FALSE.
DELTA1SWITCH=.FALSE.
END SUBROUTINE INITIAL

END MODULE SUBROUTINES
```

Appendix B

Computer Program for the Rattleback

The computer program that ran the simulations was written in FORTRAN 90 and is supplied in this appendix. There are two files to be compiled and linked:

"rattleback.f90" (code lines from PROGRAM RATTLEBACK to END PROGRAM RATTLEBACK)

"sub.f90" (code lines from MODULE SUBROUTINES to END MODULE SUBROUTINES).

On most machines, compiling and linking can be accomplished with commands similar to the following:

```
f90 sub.f90 rattleback.f90
```

This compiles and links the files, then creates an executable file. On UNIX machines the name of the executable file is "a.out". The input variables and initial conditions are entered in a separate text file "data" in the following order: $M, h, g, I_1, I_2, I_3, \sigma_{11}, \sigma_{12}, \sigma_{22}, dt, t_f, u_1, u_2, \omega_1, \omega_2, \omega_3$. Once the sixteen numbers for file "data" are entered with spaces between them, executing the file "a.out" produces the file "output". The file output has three columns: t, Γ, η . Here t is time, Γ is the spin angle and η is the wobble angle. These quantities can then be plotted using a standard graphics package. For example, here are the commands used in MATLAB to produce a graph of spin angle as a function of time:

```
>> load('output1');  
>> x=output1(:,1);  
>> y=output1(:,2);  
>> plot(x,y)
```

```
PROGRAM RATTLEBACK
USE SUBROUTINES
IMPLICIT NONE
OPEN(UNIT=100,FILE='data')
READ(100,*) M,H,G,I1,I2,I3,SIGMA11,SIGMA12,SIGMA22,S,TF,U1,U2,&
OMEGA1,OMEGA2,OMEGA3
CLOSE(UNIT=100)
OPEN(UNIT=200,FILE='output')
T=0.0D0
U3=DSQRT(1.0D0-U1**2-U2**2)
DO WHILE (T.LE.TF)
CALL COMPUTE
CALL RUNGE
WRITE(200,*) T,GAMMA,ETA
ENDDO
CLOSE(UNIT=200)
END PROGRAM RATTLEBACK
```

```

MODULE SUBROUTINES

IMPLICIT NONE

!*****

!VARIABLES:

!M=MASS

!G=ACCELERATION DUE TO GRAVITY

!H=DISTANCE FROM CENTRE OF MASS TO LOWEST POINT

! [U1,U2,U3]=VECTOR U

! [OMEGA1,OMEGA2,OMEGA3]=ANGULAR VELOCITY VECTOR

!SIGMA11,SIGMA12,SIGMA22=DETERMINE SHAPE OF RATTLEBACK

! I1,I2,I3=PRINCIPAL MOMENTS OF INERTIA

! [X,Y,Z]=INVERSE GAUSS MAP, FUNCTION OF [U1,U2,U3]

! [XDOT,YDOT,ZDOT]=TIME DERIVATIVE OF [X,Y,Z]

!S=STEP SIZE

!T=TIME

!TF=FINAL TIME

!GAMMA=SPIN ANGLE

!ETA=WOBBLE ANGLE

!*****

REAL(8),PUBLIC:: U1,U2,U3,OMEGA1,OMEGA2,OMEGA3,DELTA,ETA,&
X,Y,Z,SIGMA11,SIGMA12,SIGMA22,I1,I2,I3,XDOT,YDOT,ZDOT,&
S,T,TF,GAMMA,PI=3.14159265359D0,M,G,H

REAL(8),PRIVATE:: XYZ,XY,XZ,YZ,D,T11,T12,T13,T22,T23,T33,&
S1,S2,S3

```

```

REAL(8),PRIVATE:: U1DOT1,U1DOT2,U1DOT3,U1DOT4,&
U2DOT1,U2DOT2,U2DOT3,U2DOT4,U3DOT1,U3DOT2,U3DOT3,U3DOT4
REAL(8),PUBLIC:: OMEGA1DOT1,OMEGA1DOT2,OMEGA1DOT3,OMEGA1DOT4,&
OMEGA2DOT1,OMEGA2DOT2,OMEGA2DOT3,OMEGA2DOT4,&
OMEGA3DOT1,OMEGA3DOT2,OMEGA3DOT3,OMEGA3DOT4,&
GAMMADOT1,GAMMADOT2,GAMMADOT3,GAMMADOT4

```

CONTAINS

SUBROUTINE COMPUTE

```

DELTA=SIGMA11*SIGMA22-SIGMA12**2
X=(-SIGMA22*U1+SIGMA12*U2)/(DELTA*U3)
Y=(SIGMA12*U1-SIGMA11*U2)/(DELTA*U3)
Z=0.5D0*SIGMA11*X**2+SIGMA12*X*Y+0.5D0*SIGMA22*Y**2-H
XDOT=(-SIGMA22*(U2*OMEGA3-U3*OMEGA2)+SIGMA12*(U3*OMEGA1- &
U1*OMEGA3))/(DELTA*U3)+(SIGMA22*U1-SIGMA12*U2)*&
(U1*OMEGA2-U2*OMEGA1)/(DELTA*U3**2)
YDOT=(SIGMA12*(U2*OMEGA3-U3*OMEGA2)-SIGMA11*(U3*OMEGA1- &
U1*OMEGA3))/(DELTA*U3)+(SIGMA11*U2-SIGMA12*U1)*&
(U1*OMEGA2-U2*OMEGA1)/(DELTA*U3**2)
ZDOT=(-U1*XDOT-U2*YDOT)/U3
XYZ=X**2+Y**2+Z**2
XY=X**2+Y**2
XZ=X**2+Z**2
YZ=Y**2+Z**2

```

```

D=I1*I2*I3+M**2*XYZ*(I1*X**2+I2*Y**2+I3*Z**2)+&
M*(I1*I2*XY+I1*I3*XZ+I2*I3*YZ)
T11=(I2*I3+M**2*X**2*XYZ+M*(I2*XY+I3*XZ))/D
T22=(I1*I3+M**2*Y**2*XYZ+M*(I1*XY+I3*YZ))/D
T33=(I1*I2+M**2*Z**2*XYZ+M*(I1*XZ+I2*YZ))/D
T12=M*X*Y*(I3+M*XYZ)/D
T13=M*X*Z*(I2+M*XYZ)/D
T23=M*Y*Z*(I1+M*XYZ)/D
S1=M*(Y*Z*OMEGA2**2-Y**2*OMEGA2*OMEGA3-X*Y*OMEGA1*OMEGA3+&
X*Z*OMEGA1*OMEGA2+Z**2*OMEGA2*OMEGA3-Y*Z*OMEGA3**2+&
G*Y*U3-G*Z*U2)+(I2-I3)*OMEGA2*OMEGA3+&
M*(Y*(XDOT*OMEGA2-YDOT*OMEGA1)-Z*(ZDOT*OMEGA1-XDOT*OMEGA3))
S2=M*(X*Z*OMEGA3**2-Z**2*OMEGA1*OMEGA3-Z*Y*OMEGA1*OMEGA2+&
X*Y*OMEGA3*OMEGA2+X**2*OMEGA1*OMEGA3-X*Z*OMEGA1**2+&
G*Z*U1-G*X*U3)+(I3-I1)*OMEGA1*OMEGA3+&
M*(Z*(YDOT*OMEGA3-ZDOT*OMEGA2)-X*(XDOT*OMEGA2-YDOT*OMEGA1))
S3=M*(Y*X*OMEGA1**2-X**2*OMEGA2*OMEGA1-X*Z*OMEGA2*OMEGA3+&
Y*Z*OMEGA1*OMEGA3+Y**2*OMEGA2*OMEGA1-Y*X*OMEGA2**2+&
G*X*U2-G*Y*U1)+(I1-I2)*OMEGA1*OMEGA2+&
M*(X*(ZDOT*OMEGA1-XDOT*OMEGA3)-Y*(YDOT*OMEGA3-ZDOT*OMEGA2))
END SUBROUTINE COMPUTE

FUNCTION U1DOT(U1,U2,U3,OMEGA1,OMEGA2,OMEGA3)
REAL(8) U1DOT,U1,U2,U3,OMEGA1,OMEGA2,OMEGA3

```

```
U1DOT=U2*OMEGA3-U3*OMEGA2
```

```
END FUNCTION U1DOT
```

```
FUNCTION U2DOT(U1,U2,U3,OMEGA1,OMEGA2,OMEGA3)
```

```
REAL(8) U2DOT,U1,U2,U3,OMEGA1,OMEGA2,OMEGA3
```

```
U2DOT=U3*OMEGA1-U1*OMEGA3
```

```
END FUNCTION U2DOT
```

```
FUNCTION U3DOT(U1,U2,U3,OMEGA1,OMEGA2,OMEGA3)
```

```
REAL(8) U3DOT,U1,U2,U3,OMEGA1,OMEGA2,OMEGA3
```

```
U3DOT=U1*OMEGA2-U2*OMEGA1
```

```
END FUNCTION U3DOT
```

```
FUNCTION OMEGA1DOT(U1,U2,U3,OMEGA1,OMEGA2,OMEGA3)
```

```
REAL(8) OMEGA1DOT,U1,U2,U3,OMEGA1,OMEGA2,OMEGA3
```

```
OMEGA1DOT=T11*S1+T12*S2+T13*S3
```

```
END FUNCTION OMEGA1DOT
```

```
FUNCTION OMEGA2DOT(U1,U2,U3,OMEGA1,OMEGA2,OMEGA3)
```

```
REAL(8) OMEGA2DOT,U1,U2,U3,OMEGA1,OMEGA2,OMEGA3
```

```
OMEGA2DOT=T12*S1+T22*S2+T23*S3
```

```
END FUNCTION OMEGA2DOT
```

```
FUNCTION OMEGA3DOT(U1,U2,U3,OMEGA1,OMEGA2,OMEGA3)
```

```

REAL(8) OMEGA3DOT,U1,U2,U3,OMEGA1,OMEGA2,OMEGA3
OMEGA3DOT=T13*S1+T23*S2+T33*S3
.END FUNCTION OMEGA3DOT

```

```

FUNCTION GAMMADOT(U1,U2,U3,OMEGA1,OMEGA2,OMEGA3)
REAL(8) GAMMADOT,U1,U2,U3,OMEGA1,OMEGA2,OMEGA3
GAMMADOT=(U1*OMEGA1+U3*OMEGA3)/(1-U2**2)
END FUNCTION GAMMADOT

```

```

SUBROUTINE RUNGE

```

```

!CALL COMPUTE

```

```

U1DOT1=S*U1DOT(U1,U2,U3,OMEGA1,OMEGA2,OMEGA3)
U2DOT1=S*U2DOT(U1,U2,U3,OMEGA1,OMEGA2,OMEGA3)
U3DOT1=S*U3DOT(U1,U2,U3,OMEGA1,OMEGA2,OMEGA3)
OMEGA1DOT1=S*OMEGA1DOT(U1,U2,U3,OMEGA1,OMEGA2,OMEGA3)
OMEGA2DOT1=S*OMEGA2DOT(U1,U2,U3,OMEGA1,OMEGA2,OMEGA3)
OMEGA3DOT1=S*OMEGA3DOT(U1,U2,U3,OMEGA1,OMEGA2,OMEGA3)
GAMMADOT1=S*GAMMADOT(U1,U2,U3,OMEGA1,OMEGA2,OMEGA3)

```

```

U1DOT2=S*U1DOT(U1+0.5D0*U1DOT1,U2+0.5D0*U2DOT1,&
U3+0.5D0*U3DOT1,OMEGA1+0.5D0*OMEGA1DOT1,&
OMEGA2+0.5D0*OMEGA2DOT1,OMEGA3+0.5D0*OMEGA3DOT1)
U2DOT2=S*U2DOT(U1+0.5D0*U1DOT1,U2+0.5D0*U2DOT1,&
U3+0.5D0*U3DOT1,OMEGA1+0.5D0*OMEGA1DOT1,&

```

$\text{OMEGA2}+0.5\text{D0*OMEGA2DOT1}, \text{OMEGA3}+0.5\text{D0*OMEGA3DOT1})$
 $\text{U3DOT2}=\text{S*U3DOT}(\text{U1}+0.5\text{D0*U1DOT1}, \text{U2}+0.5\text{D0*U2DOT1}, \&$
 $\text{U3}+0.5\text{D0*U3DOT1}, \text{OMEGA1}+0.5\text{D0*OMEGA1DOT1}, \&$
 $\text{OMEGA2}+0.5\text{D0*OMEGA2DOT1}, \text{OMEGA3}+0.5\text{D0*OMEGA3DOT1})$
 $\text{OMEGA1DOT2}=\text{S*OMEGA1DOT}(\text{U1}+0.5\text{D0*U1DOT1}, \text{U2}+0.5\text{D0*U2DOT1}, \&$
 $\text{U3}+0.5\text{D0*U3DOT1}, \text{OMEGA1}+0.5\text{D0*OMEGA1DOT1}, \&$
 $\text{OMEGA2}+0.5\text{D0*OMEGA2DOT1}, \text{OMEGA3}+0.5\text{D0*OMEGA3DOT1})$
 $\text{OMEGA2DOT2}=\text{S*OMEGA2DOT}(\text{U1}+0.5\text{D0*U1DOT1}, \text{U2}+0.5\text{D0*U2DOT1}, \&$
 $\text{U3}+0.5\text{D0*U3DOT1}, \text{OMEGA1}+0.5\text{D0*OMEGA1DOT1}, \&$
 $\text{OMEGA2}+0.5\text{D0*OMEGA2DOT1}, \text{OMEGA3}+0.5\text{D0*OMEGA3DOT1})$
 $\text{OMEGA3DOT2}=\text{S*OMEGA3DOT}(\text{U1}+0.5\text{D0*U1DOT1}, \text{U2}+0.5\text{D0*U2DOT1}, \&$
 $\text{U3}+0.5\text{D0*U3DOT1}, \text{OMEGA1}+0.5\text{D0*OMEGA1DOT1}, \&$
 $\text{OMEGA2}+0.5\text{D0*OMEGA2DOT1}, \text{OMEGA3}+0.5\text{D0*OMEGA3DOT1})$
 $\text{GAMMADOT2}=\text{S*GAMMADOT}(\text{U1}+0.5\text{D0*U1DOT1}, \text{U2}+0.5\text{D0*U2DOT1}, \&$
 $\text{U3}+0.5\text{D0*U3DOT1}, \text{OMEGA1}+0.5\text{D0*OMEGA1DOT1}, \&$
 $\text{OMEGA2}+0.5\text{D0*OMEGA2DOT1}, \text{OMEGA3}+0.5\text{D0*OMEGA3DOT1})$

 $\text{U1DOT3}=\text{S*U1DOT}(\text{U1}+0.5\text{D0*U1DOT2}, \text{U2}+0.5\text{D0*U2DOT2}, \&$
 $\text{U3}+0.5\text{D0*U3DOT2}, \text{OMEGA1}+0.5\text{D0*OMEGA1DOT2}, \&$
 $\text{OMEGA2}+0.5\text{D0*OMEGA2DOT2}, \text{OMEGA3}+0.5\text{D0*OMEGA3DOT2})$
 $\text{U2DOT3}=\text{S*U2DOT}(\text{U1}+0.5\text{D0*U1DOT2}, \text{U2}+0.5\text{D0*U2DOT2}, \&$
 $\text{U3}+0.5\text{D0*U3DOT2}, \text{OMEGA1}+0.5\text{D0*OMEGA1DOT2}, \&$
 $\text{OMEGA2}+0.5\text{D0*OMEGA2DOT2}, \text{OMEGA3}+0.5\text{D0*OMEGA3DOT2})$
 $\text{U3DOT3}=\text{S*U3DOT}(\text{U1}+0.5\text{D0*U1DOT2}, \text{U2}+0.5\text{D0*U2DOT2}, \&$

$U3+0.5D0*U3DOT2, OMEGA1+0.5D0*OMEGA1DOT2, \&$
 $OMEGA2+0.5D0*OMEGA2DOT2, OMEGA3+0.5D0*OMEGA3DOT2)$
 $OMEGA1DOT3=S*OMEGA1DOT(U1+0.5D0*U1DOT2, U2+0.5D0*U2DOT2, \&$
 $U3+0.5D0*U3DOT2, OMEGA1+0.5D0*OMEGA1DOT2, \&$
 $OMEGA2+0.5D0*OMEGA2DOT2, OMEGA3+0.5D0*OMEGA3DOT2)$
 $OMEGA2DOT3=S*OMEGA2DOT(U1+0.5D0*U1DOT2, U2+0.5D0*U2DOT2, \&$
 $U3+0.5D0*U3DOT2, OMEGA1+0.5D0*OMEGA1DOT2, \&$
 $OMEGA2+0.5D0*OMEGA2DOT2, OMEGA3+0.5D0*OMEGA3DOT2)$
 $OMEGA3DOT3=S*OMEGA3DOT(U1+0.5D0*U1DOT2, U2+0.5D0*U2DOT2, \&$
 $U3+0.5D0*U3DOT2, OMEGA1+0.5D0*OMEGA1DOT2, \&$
 $OMEGA2+0.5D0*OMEGA2DOT2, OMEGA3+0.5D0*OMEGA3DOT2)$
 $GAMMADOT3=S*GAMMADOT(U1+0.5D0*U1DOT2, U2+0.5D0*U2DOT2, \&$
 $U3+0.5D0*U3DOT2, OMEGA1+0.5D0*OMEGA1DOT2, \&$
 $OMEGA2+0.5D0*OMEGA2DOT2, OMEGA3+0.5D0*OMEGA3DOT2)$

$U1DOT4=S*U1DOT(U1+U1DOT3, U2+U2DOT3, U3+U3DOT3, \&$
 $OMEGA1+OMEGA1DOT3, OMEGA2+OMEGA2DOT3, OMEGA3+OMEGA3DOT3)$
 $U2DOT4=S*U2DOT(U1+U1DOT3, U2+U2DOT3, U3+U3DOT3, \&$
 $OMEGA1+OMEGA1DOT3, OMEGA2+OMEGA2DOT3, OMEGA3+OMEGA3DOT3)$
 $U3DOT4=S*U3DOT(U1+U1DOT3, U2+U2DOT3, U3+U3DOT3, \&$
 $OMEGA1+OMEGA1DOT3, OMEGA2+OMEGA2DOT3, OMEGA3+OMEGA3DOT3)$
 $OMEGA1DOT4=S*OMEGA1DOT(U1+U1DOT3, U2+U2DOT3, U3+U3DOT3, \&$
 $OMEGA1+OMEGA1DOT3, OMEGA2+OMEGA2DOT3, OMEGA3+OMEGA3DOT3)$
 $OMEGA2DOT4=S*OMEGA2DOT(U1+U1DOT3, U2+U2DOT3, U3+U3DOT3, \&$

```

OMEGA1+OMEGA1DOT3, OMEGA2+OMEGA2DOT3, OMEGA3+OMEGA3DOT3)
OMEGA3DOT4=S*OMEGA3DOT(U1+U1DOT3, U2+U2DOT3, U3+U3DOT3, &
OMEGA1+OMEGA1DOT3, OMEGA2+OMEGA2DOT3, OMEGA3+OMEGA3DOT3)
GAMMADOT4=S*GAMMADOT(U1+U1DOT3, U2+U2DOT3, U3+U3DOT3, &
OMEGA1+OMEGA1DOT3, OMEGA2+OMEGA2DOT3, OMEGA3+OMEGA3DOT3)

```

```
T=T+S
```

```
U1=U1+(U1DOT1+2.0DO*U1DOT2+2.0DO*U1DOT3+U1DOT4)/6.0DO
```

```
U2=U2+(U2DOT1+2.0DO*U2DOT2+2.0DO*U2DOT3+U2DOT4)/6.0DO
```

```
U3=U3+(U3DOT1+2.0DO*U3DOT2+2.0DO*U3DOT3+U3DOT4)/6.0DO
```

```
OMEGA1=OMEGA1+(OMEGA1DOT1+2.0DO*OMEGA1DOT2+&
```

```
2.0DO*OMEGA1DOT3+OMEGA1DOT4)/6.0DO
```

```
OMEGA2=OMEGA2+(OMEGA2DOT1+2.0DO*OMEGA2DOT2+&
```

```
2.0DO*OMEGA2DOT3+OMEGA2DOT4)/6.0DO
```

```
OMEGA3=OMEGA3+(OMEGA3DOT1+2.0DO*OMEGA3DOT2+&
```

```
2.0DO*OMEGA3DOT3+OMEGA3DOT4)/6.0DO
```

```
GAMMA=GAMMA+(GAMMADOT1+2.0DO*GAMMADOT2+&
```

```
2.0DO*GAMMADOT3+GAMMADOT4)/6.0DO
```

```
ETA=DACOS(U3)
```

```
END SUBROUTINE RUNGE
```

```
END MODULE SUBROUTINES
```

Appendix C

Tables of Elliptic Functions

C.1 Complete Elliptic Integral $K(k)$

k	K(k)	k	K(k)
0.00	1.570796	0.50	1.685760
0.01	1.570836	0.51	1.691263
0.02	1.570953	0.52	1.696972
0.03	1.571150	0.53	1.702885
0.04	1.571425	0.54	1.709009
0.05	1.571779	0.55	1.715354
0.06	1.572213	0.56	1.721930
0.07	1.572726	0.57	1.728747
0.08	1.573319	0.58	1.735815
0.09	1.573992	0.59	1.743146
0.10	1.574746	0.60	1.750754
0.11	1.575581	0.61	1.758651
0.12	1.576497	0.62	1.766853
0.13	1.577497	0.63	1.775376
0.14	1.578579	0.64	1.784236
0.15	1.579746	0.65	1.793454
0.16	1.580997	0.66	1.803050
0.17	1.582334	0.67	1.813045
0.18	1.583757	0.68	1.823466
0.19	1.585268	0.69	1.834339
0.20	1.586868	0.70	1.845694
0.21	1.588558	0.71	1.857564
0.22	1.590338	0.72	1.869985
0.23	1.592212	0.73	1.882999
0.24	1.594179	0.74	1.896650
0.25	1.596242	0.75	1.910990
0.26	1.598402	0.76	1.926075
0.27	1.600661	0.77	1.941970
0.28	1.603020	0.78	1.958748
0.29	1.605482	0.79	1.976494
0.30	1.608049	0.80	1.995303
0.31	1.610722	0.81	2.015287
0.32	1.613504	0.82	2.036575
0.33	1.616397	0.83	2.059319
0.34	1.619404	0.84	2.083701
0.35	1.622528	0.85	2.109935
0.36	1.625771	0.86	2.138283
0.37	1.629137	0.87	2.169065
0.38	1.632628	0.88	2.202677
0.39	1.636248	0.89	2.239622
0.40	1.640000	0.90	2.280549
0.41	1.643888	0.91	2.326312
0.42	1.647917	0.92	2.378071
0.43	1.652090	0.93	2.437458
0.44	1.656411	0.94	2.506865
0.45	1.660888	0.95	2.590011
0.46	1.665520	0.96	2.693143
0.47	1.670317	0.97	2.827995
0.48	1.675284	0.98	3.020980
0.49	1.680426	0.99	3.356601

C.2 $f(t) = \text{sn}(t | m = k^2)$

$t \backslash m$	0.000	0.100	0.200	0.300	0.400	0.500	0.600	0.700	0.800	0.900	1.000
0.0	0.000	0.000	0.000	0.000	0.000	0.000	0.000	0.000	0.000	0.000	0.000
0.1	0.100	0.100	0.100	0.100	0.100	0.100	0.100	0.100	0.100	0.100	0.100
0.2	0.199	0.199	0.198	0.198	0.198	0.198	0.198	0.198	0.198	0.198	0.197
0.3	0.296	0.295	0.295	0.294	0.294	0.294	0.293	0.293	0.293	0.292	0.291
0.4	0.389	0.388	0.388	0.387	0.386	0.385	0.384	0.383	0.382	0.381	0.380
0.5	0.479	0.478	0.476	0.474	0.472	0.471	0.469	0.467	0.466	0.464	0.462
0.6	0.565	0.562	0.559	0.556	0.554	0.551	0.548	0.545	0.543	0.540	0.537
0.7	0.644	0.640	0.636	0.632	0.628	0.624	0.620	0.616	0.612	0.608	0.604
0.8	0.717	0.712	0.707	0.702	0.696	0.691	0.686	0.680	0.675	0.669	0.664
0.9	0.783	0.777	0.770	0.764	0.757	0.750	0.744	0.737	0.730	0.723	0.716
1.0	0.841	0.834	0.826	0.819	0.811	0.803	0.795	0.787	0.778	0.770	0.762
1.1	0.891	0.883	0.875	0.866	0.858	0.849	0.839	0.830	0.820	0.811	0.800
1.2	0.932	0.924	0.916	0.907	0.897	0.888	0.878	0.867	0.856	0.845	0.834
1.3	0.964	0.956	0.948	0.940	0.930	0.920	0.910	0.899	0.887	0.875	0.862
1.4	0.985	0.980	0.973	0.965	0.957	0.947	0.937	0.925	0.913	0.899	0.885
1.5	0.997	0.994	0.990	0.984	0.977	0.968	0.958	0.947	0.934	0.920	0.905
1.6	1.000	1.000	0.999	0.995	0.991	0.984	0.975	0.965	0.952	0.938	0.922
1.7	0.992	0.997	0.999	1.000	0.998	0.994	0.987	0.978	0.967	0.952	0.935
1.8	0.974	0.984	0.992	0.997	1.000	0.999	0.996	0.988	0.978	0.964	0.947
1.9	0.946	0.963	0.977	0.988	0.995	0.999	1.000	0.995	0.987	0.974	0.956
2.0	0.909	0.933	0.954	0.971	0.985	0.995	0.999	0.999	0.993	0.982	0.964
2.1	0.863	0.894	0.922	0.948	0.969	0.985	0.995	1.000	0.998	0.988	0.970
2.2	0.808	0.847	0.883	0.917	0.946	0.970	0.987	0.998	1.000	0.993	0.976
2.3	0.746	0.792	0.836	0.878	0.916	0.949	0.975	0.992	1.000	0.996	0.980
2.4	0.675	0.729	0.782	0.833	0.880	0.923	0.958	0.984	0.998	0.998	0.984
2.5	0.598	0.659	0.720	0.780	0.838	0.891	0.936	0.972	0.994	1.000	0.987
2.6	0.516	0.582	0.650	0.720	0.788	0.852	0.910	0.956	0.988	1.000	0.989
2.7	0.427	0.499	0.574	0.652	0.731	0.807	0.877	0.937	0.979	0.999	0.991
2.8	0.335	0.411	0.492	0.578	0.667	0.755	0.839	0.913	0.968	0.998	0.993
2.9	0.239	0.319	0.405	0.498	0.596	0.696	0.795	0.884	0.954	0.995	0.994
3.0	0.141	0.223	0.313	0.411	0.518	0.630	0.743	0.850	0.937	0.991	0.995
3.1	0.042	0.125	0.217	0.320	0.434	0.557	0.685	0.809	0.916	0.985	0.996
3.2	-0.058	0.025	0.119	0.225	0.345	0.478	0.620	0.763	0.891	0.978	0.997
3.3	-0.158	-0.075	0.019	0.127	0.251	0.392	0.547	0.710	0.861	0.970	0.997
3.4	-0.256	-0.174	-0.081	0.028	0.154	0.301	0.468	0.650	0.826	0.959	0.998
3.5	-0.351	-0.271	-0.180	-0.072	0.055	0.206	0.383	0.582	0.785	0.946	0.998
3.6	-0.443	-0.366	-0.276	-0.171	-0.045	0.108	0.292	0.508	0.737	0.931	0.999
3.7	-0.530	-0.456	-0.370	-0.268	-0.144	0.008	0.197	0.426	0.683	0.912	0.999
3.8	-0.612	-0.541	-0.459	-0.361	-0.242	-0.092	0.099	0.339	0.622	0.889	0.999
3.9	-0.688	-0.621	-0.544	-0.450	-0.336	-0.190	-0.001	0.246	0.553	0.862	0.999
4.0	-0.757	-0.695	-0.622	-0.534	-0.425	-0.286	-0.101	0.150	0.477	0.831	0.999
4.1	-0.818	-0.761	-0.694	-0.612	-0.510	-0.377	-0.199	0.051	0.394	0.794	0.999
4.2	-0.872	-0.821	-0.759	-0.683	-0.588	-0.464	-0.294	-0.049	0.305	0.750	1.000
4.3	-0.916	-0.872	-0.816	-0.747	-0.660	-0.545	-0.384	-0.148	0.212	0.701	1.000
4.4	-0.952	-0.915	-0.866	-0.804	-0.725	-0.619	-0.470	-0.245	0.114	0.644	1.000
4.5	-0.978	-0.949	-0.908	-0.854	-0.782	-0.686	-0.549	-0.338	0.014	0.579	1.000
4.6	-0.994	-0.975	-0.943	-0.896	-0.833	-0.746	-0.621	-0.425	-0.085	0.507	1.000
4.7	-1.000	-0.992	-0.969	-0.931	-0.876	-0.799	-0.686	-0.507	-0.184	0.428	1.000
4.8	-0.996	-0.999	-0.987	-0.959	-0.913	-0.845	-0.744	-0.581	-0.279	0.343	1.000
4.9	-0.982	-0.998	-0.998	-0.980	-0.943	-0.885	-0.795	-0.649	-0.369	0.251	1.000
5.0	-0.959	-0.988	-1.000	-0.993	-0.967	-0.918	-0.840	-0.709	-0.454	0.155	1.000

\ m	0.000	0.100	0.200	0.300	0.400	0.500	0.600	0.700	0.800	0.900	1.000
t \											
5.1	-0.926	-0.969	-0.994	-0.999	-0.984	-0.945	-0.878	-0.762	-0.532	0.056	1.000
5.2	-0.883	-0.941	-0.980	-0.999	-0.995	-0.967	-0.910	-0.809	-0.603	-0.044	1.000
5.3	-0.832	-0.905	-0.959	-0.991	-1.000	-0.983	-0.937	-0.849	-0.666	-0.143	1.000
5.4	-0.773	-0.860	-0.929	-0.977	-0.999	-0.993	-0.958	-0.883	-0.723	-0.239	1.000
5.5	-0.706	-0.806	-0.891	-0.955	-0.992	-0.999	-0.975	-0.912	-0.772	-0.331	1.000
5.6	-0.631	-0.745	-0.846	-0.926	-0.978	-1.000	-0.988	-0.936	-0.815	-0.418	1.000
5.7	-0.551	-0.677	-0.793	-0.890	-0.959	-0.995	-0.996	-0.956	-0.852	-0.498	1.000
5.8	-0.465	-0.602	-0.732	-0.846	-0.933	-0.986	-1.000	-0.972	-0.883	-0.571	1.000
5.9	-0.374	-0.520	-0.664	-0.795	-0.901	-0.971	-0.999	-0.984	-0.909	-0.636	1.000
6.0	-0.279	-0.433	-0.590	-0.737	-0.862	-0.951	-0.995	-0.992	-0.931	-0.694	1.000
6.1	-0.182	-0.342	-0.509	-0.672	-0.816	-0.925	-0.987	-0.998	-0.950	-0.745	1.000
6.2	-0.083	-0.247	-0.422	-0.599	-0.763	-0.893	-0.975	-1.000	-0.965	-0.789	1.000
6.3	0.017	-0.149	-0.331	-0.521	-0.703	-0.855	-0.958	-0.999	-0.977	-0.826	1.000
6.4	0.117	-0.050	-0.236	-0.436	-0.635	-0.811	-0.936	-0.995	-0.986	-0.859	1.000
6.5	0.215	0.050	-0.138	-0.346	-0.561	-0.760	-0.909	-0.989	-0.992	-0.886	1.000
6.6	0.312	0.150	-0.038	-0.252	-0.481	-0.701	-0.877	-0.978	-0.997	-0.909	1.000
6.7	0.405	0.247	0.061	-0.155	-0.395	-0.636	-0.839	-0.965	-0.999	-0.928	1.000
6.8	0.494	0.342	0.161	-0.056	-0.303	-0.563	-0.794	-0.947	-1.000	-0.944	1.000
6.9	0.578	0.434	0.258	0.044	-0.208	-0.484	-0.743	-0.926	-0.998	-0.958	1.000
7.0	0.657	0.521	0.352	0.144	-0.110	-0.399	-0.685	-0.899	-0.995	-0.969	1.000
7.1	0.729	0.602	0.442	0.241	-0.010	-0.309	-0.619	-0.868	-0.989	-0.977	1.000
7.2	0.794	0.677	0.528	0.336	0.090	-0.214	-0.547	-0.831	-0.981	-0.985	1.000
7.3	0.850	0.746	0.607	0.426	0.188	-0.116	-0.468	-0.787	-0.970	-0.990	1.000
7.4	0.899	0.807	0.680	0.511	0.284	-0.016	-0.382	-0.738	-0.957	-0.994	1.000
7.5	0.938	0.860	0.747	0.591	0.377	0.084	-0.291	-0.681	-0.940	-0.997	1.000
7.6	0.968	0.905	0.806	0.664	0.464	0.182	-0.196	-0.617	-0.919	-0.999	1.000
7.7	0.988	0.941	0.857	0.730	0.546	0.278	-0.098	-0.546	-0.895	-1.000	1.000
7.8	0.999	0.969	0.901	0.789	0.621	0.370	0.002	-0.468	-0.866	-1.000	1.000
7.9	0.999	0.988	0.937	0.841	0.690	0.457	0.101	-0.384	-0.831	-0.999	1.000
8.0	0.989	0.998	0.964	0.885	0.751	0.538	0.200	-0.294	-0.791	-0.996	1.000
8.1	0.970	0.999	0.984	0.922	0.806	0.613	0.295	-0.199	-0.745	-0.993	1.000
8.2	0.941	0.991	0.996	0.952	0.853	0.681	0.385	-0.101	-0.692	-0.988	1.000
8.3	0.902	0.975	1.000	0.975	0.894	0.741	0.470	-0.001	-0.631	-0.982	1.000
8.4	0.855	0.949	0.996	0.990	0.927	0.795	0.549	0.098	-0.563	-0.975	1.000
8.5	0.798	0.914	0.984	0.998	0.954	0.842	0.622	0.196	-0.488	-0.965	1.000
8.6	0.734	0.872	0.964	1.000	0.975	0.882	0.687	0.291	-0.407	-0.954	1.000
8.7	0.663	0.820	0.935	0.994	0.989	0.916	0.745	0.382	-0.319	-0.940	1.000
8.8	0.585	0.761	0.899	0.981	0.998	0.943	0.796	0.466	-0.225	-0.923	1.000
8.9	0.501	0.695	0.855	0.962	1.000	0.965	0.840	0.544	-0.128	-0.902	1.000
9.0	0.412	0.621	0.804	0.935	0.996	0.982	0.878	0.615	-0.029	-0.878	1.000
9.1	0.319	0.541	0.744	0.900	0.986	0.993	0.910	0.679	0.071	-0.849	1.000
9.2	0.223	0.456	0.678	0.859	0.970	0.999	0.937	0.736	0.170	-0.815	1.000
9.3	0.124	0.365	0.604	0.810	0.948	1.000	0.959	0.786	0.265	-0.775	1.000
9.4	0.025	0.271	0.525	0.754	0.920	0.996	0.975	0.829	0.357	-0.729	1.000
9.5	-0.075	0.174	0.439	0.691	0.884	0.987	0.988	0.867	0.442	-0.676	1.000
9.6	-0.174	0.075	0.349	0.620	0.842	0.972	0.996	0.898	0.521	-0.616	1.000
9.7	-0.272	-0.025	0.254	0.543	0.793	0.953	1.000	0.925	0.593	-0.549	1.000
9.8	-0.366	-0.125	0.157	0.460	0.737	0.928	0.999	0.947	0.658	-0.474	1.000
9.9	-0.458	-0.223	0.058	0.371	0.673	0.896	0.995	0.964	0.715	-0.392	1.000
10.0	-0.544	-0.319	-0.042	0.278	0.603	0.859	0.987	0.978	0.765	-0.303	1.000

C.3 $f(t) = \text{cn}(t \mid m = k^2)$

$t \backslash m$	0.000	0.100	0.200	0.300	0.400	0.500	0.600	0.700	0.800	0.900	1.000
0.0	1.000	1.000	1.000	1.000	1.000	1.000	1.000	1.000	1.000	1.000	1.000
0.1	0.995	0.995	0.995	0.995	0.995	0.995	0.995	0.995	0.995	0.995	0.995
0.2	0.980	0.980	0.980	0.980	0.980	0.980	0.980	0.980	0.980	0.980	0.980
0.3	0.955	0.955	0.956	0.956	0.956	0.956	0.956	0.956	0.956	0.957	0.957
0.4	0.921	0.921	0.922	0.922	0.923	0.923	0.923	0.924	0.924	0.925	0.925
0.5	0.878	0.879	0.879	0.880	0.881	0.882	0.883	0.884	0.885	0.886	0.887
0.6	0.825	0.827	0.829	0.831	0.833	0.835	0.836	0.838	0.840	0.842	0.844
0.7	0.765	0.768	0.771	0.775	0.778	0.781	0.784	0.787	0.791	0.794	0.797
0.8	0.697	0.702	0.707	0.713	0.718	0.723	0.728	0.733	0.738	0.743	0.748
0.9	0.622	0.630	0.638	0.645	0.653	0.661	0.668	0.676	0.683	0.691	0.698
1.0	0.540	0.552	0.563	0.574	0.585	0.596	0.607	0.617	0.628	0.638	0.648
1.1	0.454	0.469	0.484	0.499	0.514	0.529	0.543	0.558	0.572	0.586	0.599
1.2	0.362	0.382	0.402	0.422	0.441	0.460	0.479	0.498	0.516	0.534	0.552
1.3	0.267	0.293	0.317	0.342	0.367	0.391	0.415	0.439	0.462	0.485	0.507
1.4	0.170	0.200	0.231	0.261	0.291	0.321	0.350	0.380	0.408	0.437	0.465
1.5	0.071	0.106	0.142	0.178	0.214	0.250	0.286	0.321	0.356	0.391	0.425
1.6	-0.029	0.012	0.053	0.095	0.137	0.180	0.222	0.264	0.306	0.347	0.388
1.7	-0.129	-0.083	-0.036	0.012	0.060	0.109	0.158	0.207	0.257	0.305	0.354
1.8	-0.227	-0.177	-0.125	-0.072	-0.017	0.038	0.095	0.152	0.209	0.265	0.322
1.9	-0.323	-0.270	-0.214	-0.155	-0.095	-0.032	0.031	0.096	0.162	0.227	0.293
2.0	-0.416	-0.360	-0.301	-0.238	-0.172	-0.103	-0.032	0.041	0.116	0.191	0.266
2.1	-0.505	-0.448	-0.386	-0.320	-0.249	-0.174	-0.095	-0.013	0.070	0.156	0.241
2.2	-0.589	-0.532	-0.469	-0.400	-0.325	-0.245	-0.159	-0.068	0.026	0.122	0.219
2.3	-0.666	-0.611	-0.548	-0.478	-0.400	-0.315	-0.222	-0.123	-0.019	0.089	0.199
2.4	-0.737	-0.685	-0.624	-0.554	-0.474	-0.385	-0.287	-0.179	-0.064	0.057	0.180
2.5	-0.801	-0.752	-0.694	-0.626	-0.546	-0.455	-0.351	-0.235	-0.109	0.025	0.163
2.6	-0.857	-0.813	-0.760	-0.694	-0.616	-0.523	-0.415	-0.292	-0.155	-0.007	0.148
2.7	-0.904	-0.867	-0.819	-0.758	-0.683	-0.591	-0.480	-0.350	-0.202	-0.039	0.134
2.8	-0.942	-0.912	-0.870	-0.816	-0.745	-0.656	-0.544	-0.409	-0.250	-0.071	0.121
2.9	-0.971	-0.948	-0.914	-0.867	-0.803	-0.718	-0.607	-0.468	-0.299	-0.103	0.110
3.0	-0.990	-0.975	-0.950	-0.911	-0.855	-0.777	-0.669	-0.527	-0.349	-0.137	0.099
3.1	-0.999	-0.992	-0.976	-0.947	-0.901	-0.830	-0.728	-0.587	-0.401	-0.171	0.090
3.2	-0.998	-1.000	-0.993	-0.974	-0.939	-0.879	-0.785	-0.646	-0.454	-0.207	0.081
3.3	-0.987	-0.997	-1.000	-0.992	-0.968	-0.920	-0.837	-0.704	-0.508	-0.244	0.074
3.4	-0.967	-0.985	-0.997	-1.000	-0.988	-0.954	-0.884	-0.760	-0.564	-0.283	0.067
3.5	-0.936	-0.962	-0.984	-0.997	-0.998	-0.979	-0.924	-0.813	-0.620	-0.323	0.060
3.6	-0.897	-0.931	-0.961	-0.985	-0.999	-0.994	-0.956	-0.862	-0.675	-0.366	0.055
3.7	-0.848	-0.890	-0.929	-0.963	-0.990	-1.000	-0.980	-0.905	-0.730	-0.411	0.049
3.8	-0.791	-0.841	-0.888	-0.932	-0.970	-0.996	-0.995	-0.941	-0.783	-0.458	0.045
3.9	-0.726	-0.784	-0.839	-0.893	-0.942	-0.982	-1.000	-0.969	-0.833	-0.506	0.040
4.0	-0.654	-0.719	-0.783	-0.845	-0.905	-0.958	-0.995	-0.989	-0.879	-0.557	0.037
4.1	-0.575	-0.648	-0.720	-0.791	-0.860	-0.926	-0.980	-0.999	-0.919	-0.608	0.033
4.2	-0.490	-0.572	-0.651	-0.730	-0.809	-0.886	-0.956	-0.999	-0.952	-0.661	0.030
4.3	-0.401	-0.490	-0.578	-0.665	-0.752	-0.839	-0.923	-0.989	-0.977	-0.714	0.027
4.4	-0.307	-0.404	-0.500	-0.594	-0.689	-0.786	-0.883	-0.970	-0.993	-0.765	0.025
4.5	-0.211	-0.315	-0.418	-0.520	-0.623	-0.728	-0.836	-0.941	-1.000	-0.815	0.022
4.6	-0.112	-0.223	-0.334	-0.444	-0.554	-0.666	-0.784	-0.905	-0.996	-0.862	0.020
4.7	-0.012	-0.130	-0.247	-0.364	-0.482	-0.601	-0.727	-0.862	-0.983	-0.904	0.018
4.8	0.087	-0.035	-0.159	-0.284	-0.408	-0.534	-0.668	-0.814	-0.960	-0.940	0.016
4.9	0.187	0.059	-0.071	-0.201	-0.333	-0.466	-0.606	-0.761	-0.929	-0.968	0.015
5.0	0.284	0.154	0.019	-0.118	-0.257	-0.397	-0.543	-0.705	-0.891	-0.988	0.013

\ m	0.000	0.100	0.200	0.300	0.400	0.500	0.600	0.700	0.800	0.900	1.000
t \											
5.1	0.378	0.247	0.108	-0.035	-0.180	-0.326	-0.479	-0.647	-0.847	-0.998	0.012
5.2	0.469	0.338	0.197	0.049	-0.103	-0.256	-0.414	-0.588	-0.798	-0.999	0.011
5.3	0.554	0.426	0.284	0.132	-0.025	-0.185	-0.350	-0.528	-0.746	-0.990	0.010
5.4	0.635	0.511	0.370	0.215	0.052	-0.115	-0.285	-0.469	-0.691	-0.971	0.009
5.5	0.709	0.592	0.453	0.297	0.130	-0.044	-0.221	-0.409	-0.636	-0.943	0.008
5.6	0.776	0.667	0.533	0.378	0.207	0.027	-0.158	-0.351	-0.580	-0.908	0.007
5.7	0.835	0.736	0.609	0.457	0.283	0.097	-0.094	-0.293	-0.524	-0.867	0.007
5.8	0.886	0.799	0.681	0.533	0.359	0.168	-0.031	-0.236	-0.470	-0.821	0.006
5.9	0.927	0.854	0.748	0.606	0.434	0.239	0.032	-0.180	-0.416	-0.772	0.005
6.0	0.960	0.901	0.808	0.676	0.507	0.309	0.096	-0.124	-0.364	-0.720	0.005
6.1	0.983	0.940	0.861	0.741	0.578	0.379	0.159	-0.069	-0.313	-0.668	0.004
6.2	0.997	0.969	0.907	0.800	0.647	0.449	0.223	-0.014	-0.264	-0.615	0.004
6.3	1.000	0.989	0.944	0.854	0.711	0.518	0.287	0.040	-0.215	-0.563	0.004
6.4	0.993	0.999	0.972	0.900	0.772	0.585	0.351	0.095	-0.168	-0.513	0.003
6.5	0.977	0.999	0.990	0.938	0.828	0.650	0.416	0.151	-0.122	-0.464	0.003
6.6	0.950	0.989	0.999	0.968	0.877	0.713	0.480	0.207	-0.077	-0.417	0.003
6.7	0.914	0.969	0.998	0.988	0.919	0.772	0.545	0.263	-0.032	-0.372	0.002
6.8	0.869	0.940	0.987	0.998	0.953	0.826	0.608	0.321	0.013	-0.329	0.002
6.9	0.816	0.901	0.966	0.999	0.978	0.875	0.670	0.379	0.058	-0.288	0.002
7.0	0.754	0.854	0.936	0.990	0.994	0.917	0.729	0.438	0.103	-0.249	0.002
7.1	0.685	0.798	0.897	0.970	1.000	0.951	0.785	0.497	0.148	-0.211	0.002
7.2	0.608	0.736	0.849	0.942	0.996	0.977	0.837	0.557	0.195	-0.175	0.001
7.3	0.526	0.666	0.794	0.905	0.982	0.993	0.884	0.616	0.243	-0.141	0.001
7.4	0.439	0.591	0.733	0.859	0.959	1.000	0.924	0.675	0.292	-0.107	0.001
7.5	0.347	0.511	0.665	0.807	0.926	0.997	0.957	0.732	0.342	-0.075	0.001
7.6	0.251	0.426	0.592	0.748	0.886	0.983	0.981	0.787	0.393	-0.043	0.001
7.7	0.153	0.338	0.515	0.683	0.838	0.961	0.995	0.838	0.446	-0.011	0.001
7.8	0.054	0.246	0.434	0.614	0.784	0.929	1.000	0.883	0.501	0.021	0.001
7.9	-0.046	0.153	0.350	0.541	0.724	0.889	0.995	0.923	0.556	0.053	0.001
8.0	-0.146	0.059	0.264	0.465	0.660	0.843	0.980	0.956	0.612	0.085	0.001
8.1	-0.244	-0.036	0.177	0.387	0.592	0.790	0.956	0.980	0.667	0.118	0.001
8.2	-0.339	-0.130	0.088	0.306	0.521	0.733	0.923	0.995	0.722	0.152	0.001
8.3	-0.431	-0.224	-0.002	0.224	0.449	0.671	0.882	1.000	0.776	0.186	0.000
8.4	-0.519	-0.316	-0.091	0.141	0.374	0.607	0.836	0.995	0.826	0.223	0.000
8.5	-0.602	-0.405	-0.180	0.058	0.299	0.540	0.783	0.981	0.873	0.261	0.000
8.6	-0.679	-0.490	-0.268	-0.026	0.222	0.472	0.727	0.957	0.914	0.300	0.000
8.7	-0.749	-0.572	-0.354	-0.109	0.145	0.402	0.667	0.924	0.948	0.342	0.000
8.8	-0.811	-0.649	-0.437	-0.192	0.068	0.332	0.606	0.885	0.974	0.386	0.000
8.9	-0.865	-0.719	-0.518	-0.274	-0.010	0.262	0.542	0.839	0.992	0.431	0.000
9.0	-0.911	-0.784	-0.595	-0.356	-0.087	0.191	0.478	0.788	1.000	0.479	0.000
9.1	-0.948	-0.841	-0.668	-0.435	-0.164	0.120	0.414	0.734	0.997	0.528	0.000
9.2	-0.975	-0.890	-0.735	-0.512	-0.241	0.050	0.349	0.677	0.985	0.579	0.000
9.3	-0.992	-0.931	-0.797	-0.586	-0.317	-0.021	0.285	0.618	0.964	0.631	0.000
9.4	-1.000	-0.963	-0.851	-0.657	-0.393	-0.092	0.221	0.559	0.934	0.684	0.000
9.5	-0.997	-0.985	-0.898	-0.723	-0.467	-0.162	0.157	0.499	0.897	0.736	0.000
9.6	-0.985	-0.997	-0.937	-0.785	-0.539	-0.233	0.094	0.439	0.854	0.787	0.000
9.7	-0.962	-1.000	-0.967	-0.840	-0.609	-0.304	0.030	0.380	0.805	0.836	0.000
9.8	-0.930	-0.992	-0.988	-0.888	-0.676	-0.374	-0.033	0.322	0.753	0.881	0.000
9.9	-0.889	-0.975	-0.998	-0.928	-0.739	-0.443	-0.096	0.265	0.699	0.920	0.000
10.0	-0.839	-0.948	-0.999	-0.960	-0.798	-0.512	-0.160	0.208	0.644	0.953	0.000

C.4 $f(t) = \text{dn}(t | m = k^2)$

$\backslash m$ \backslash $t \backslash$	0.000	0.100	0.200	0.300	0.400	0.500	0.600	0.700	0.800	0.900	1.000
0.0	1.000	1.000	1.000	1.000	1.000	1.000	1.000	1.000	1.000	1.000	1.000
0.1	1.000	1.000	0.999	0.999	0.998	0.998	0.997	0.997	0.996	0.996	0.995
0.2	1.000	0.998	0.996	0.994	0.992	0.990	0.988	0.986	0.984	0.982	0.980
0.3	1.000	0.996	0.991	0.987	0.983	0.978	0.974	0.970	0.965	0.961	0.957
0.4	1.000	0.992	0.985	0.977	0.970	0.962	0.955	0.947	0.940	0.932	0.925
0.5	1.000	0.989	0.977	0.966	0.954	0.943	0.932	0.920	0.909	0.898	0.887
0.6	1.000	0.984	0.968	0.952	0.937	0.921	0.905	0.890	0.874	0.859	0.844
0.7	1.000	0.979	0.959	0.938	0.918	0.897	0.877	0.857	0.837	0.817	0.797
0.8	1.000	0.974	0.949	0.923	0.898	0.873	0.847	0.822	0.797	0.772	0.748
0.9	1.000	0.969	0.939	0.908	0.878	0.848	0.817	0.787	0.757	0.727	0.698
1.0	1.000	0.965	0.929	0.894	0.858	0.823	0.788	0.753	0.718	0.683	0.648
1.1	1.000	0.960	0.920	0.880	0.840	0.800	0.760	0.720	0.679	0.639	0.599
1.2	1.000	0.956	0.912	0.868	0.823	0.778	0.733	0.688	0.643	0.598	0.552
1.3	1.000	0.953	0.906	0.857	0.809	0.759	0.709	0.659	0.609	0.558	0.507
1.4	1.000	0.951	0.900	0.849	0.796	0.743	0.688	0.633	0.577	0.521	0.465
1.5	1.000	0.949	0.897	0.842	0.786	0.729	0.670	0.610	0.549	0.487	0.425
1.6	1.000	0.949	0.895	0.838	0.779	0.718	0.655	0.591	0.524	0.457	0.388
1.7	1.000	0.949	0.895	0.837	0.776	0.711	0.644	0.575	0.503	0.429	0.354
1.8	1.000	0.950	0.896	0.838	0.775	0.708	0.637	0.562	0.485	0.404	0.322
1.9	1.000	0.953	0.900	0.841	0.777	0.707	0.633	0.554	0.470	0.383	0.293
2.0	1.000	0.955	0.904	0.847	0.782	0.711	0.633	0.549	0.459	0.364	0.266
2.1	1.000	0.959	0.911	0.855	0.790	0.718	0.637	0.548	0.452	0.349	0.241
2.2	1.000	0.963	0.919	0.865	0.801	0.728	0.644	0.551	0.448	0.337	0.219
2.3	1.000	0.968	0.927	0.877	0.815	0.741	0.656	0.557	0.448	0.327	0.199
2.4	1.000	0.973	0.937	0.890	0.831	0.758	0.670	0.568	0.451	0.321	0.180
2.5	1.000	0.978	0.947	0.904	0.848	0.777	0.688	0.582	0.458	0.317	0.163
2.6	1.000	0.983	0.957	0.919	0.867	0.798	0.710	0.600	0.468	0.316	0.148
2.7	1.000	0.987	0.966	0.934	0.887	0.821	0.734	0.621	0.482	0.318	0.134
2.8	1.000	0.992	0.975	0.949	0.907	0.846	0.760	0.646	0.500	0.323	0.121
2.9	1.000	0.995	0.983	0.962	0.926	0.870	0.788	0.673	0.521	0.331	0.110
3.0	1.000	0.998	0.990	0.974	0.945	0.895	0.818	0.703	0.545	0.342	0.099
3.1	1.000	0.999	0.995	0.984	0.962	0.919	0.848	0.736	0.573	0.355	0.090
3.2	1.000	1.000	0.999	0.992	0.976	0.941	0.877	0.770	0.604	0.372	0.081
3.3	1.000	1.000	1.000	0.998	0.987	0.961	0.906	0.805	0.638	0.392	0.074
3.4	1.000	0.998	0.999	1.000	0.995	0.977	0.932	0.839	0.674	0.415	0.067
3.5	1.000	0.996	0.997	0.999	0.999	0.989	0.955	0.873	0.712	0.441	0.060
3.6	1.000	0.993	0.992	0.996	1.000	0.997	0.974	0.905	0.752	0.470	0.055
3.7	1.000	0.990	0.986	0.989	0.996	1.000	0.988	0.934	0.792	0.502	0.049
3.8	1.000	0.985	0.979	0.980	0.988	0.998	0.997	0.959	0.831	0.537	0.045
3.9	1.000	0.981	0.970	0.969	0.977	0.991	1.000	0.979	0.869	0.575	0.040
4.0	1.000	0.976	0.961	0.956	0.963	0.979	0.997	0.992	0.904	0.616	0.037
4.1	1.000	0.971	0.951	0.942	0.947	0.964	0.988	0.999	0.936	0.658	0.033
4.2	1.000	0.966	0.941	0.927	0.928	0.945	0.974	0.999	0.962	0.702	0.030
4.3	1.000	0.961	0.931	0.912	0.909	0.923	0.955	0.992	0.982	0.747	0.027
4.4	1.000	0.957	0.922	0.898	0.889	0.899	0.931	0.979	0.995	0.792	0.025
4.5	1.000	0.954	0.914	0.884	0.869	0.875	0.905	0.959	1.000	0.835	0.022
4.6	1.000	0.951	0.907	0.871	0.850	0.850	0.877	0.935	0.997	0.877	0.020
4.7	1.000	0.950	0.901	0.860	0.832	0.825	0.847	0.906	0.986	0.914	0.018
4.8	1.000	0.949	0.897	0.851	0.816	0.802	0.817	0.874	0.968	0.946	0.016
4.9	1.000	0.949	0.895	0.844	0.803	0.780	0.788	0.840	0.944	0.971	0.015
5.0	1.000	0.950	0.894	0.839	0.791	0.761	0.759	0.805	0.914	0.989	0.013

\ m	0.000	0.100	0.200	0.300	0.400	0.500	0.600	0.700	0.800	0.900	1.000
t \											
5.1	1.000	0.952	0.896	0.837	0.783	0.744	0.733	0.770	0.880	0.999	0.012
5.2	1.000	0.955	0.899	0.837	0.777	0.730	0.709	0.736	0.842	0.999	0.011
5.3	1.000	0.958	0.903	0.840	0.775	0.719	0.688	0.704	0.803	0.991	0.010
5.4	1.000	0.962	0.910	0.845	0.775	0.712	0.670	0.674	0.763	0.974	0.009
5.5	1.000	0.967	0.917	0.852	0.779	0.708	0.655	0.646	0.723	0.949	0.008
5.6	1.000	0.972	0.926	0.862	0.786	0.707	0.644	0.621	0.685	0.918	0.007
5.7	1.000	0.977	0.935	0.873	0.795	0.710	0.637	0.600	0.648	0.881	0.007
5.8	1.000	0.982	0.945	0.886	0.807	0.717	0.633	0.582	0.614	0.841	0.006
5.9	1.000	0.986	0.955	0.900	0.822	0.727	0.633	0.568	0.582	0.797	0.005
6.0	1.000	0.991	0.965	0.915	0.838	0.740	0.637	0.558	0.553	0.753	0.005
6.1	1.000	0.994	0.974	0.930	0.857	0.756	0.644	0.551	0.528	0.708	0.004
6.2	1.000	0.997	0.982	0.945	0.876	0.775	0.656	0.548	0.506	0.664	0.004
6.3	1.000	0.999	0.989	0.958	0.896	0.796	0.670	0.549	0.487	0.621	0.004
6.4	1.000	1.000	0.994	0.971	0.916	0.819	0.689	0.554	0.472	0.580	0.003
6.5	1.000	1.000	0.998	0.982	0.935	0.844	0.710	0.562	0.460	0.542	0.003
6.6	1.000	0.999	1.000	0.990	0.953	0.868	0.734	0.574	0.452	0.506	0.003
6.7	1.000	0.997	1.000	0.996	0.968	0.893	0.760	0.590	0.448	0.474	0.002
6.8	1.000	0.994	0.997	1.000	0.981	0.917	0.788	0.610	0.447	0.444	0.002
6.9	1.000	0.991	0.993	1.000	0.991	0.940	0.818	0.633	0.450	0.418	0.002
7.0	1.000	0.986	0.988	0.997	0.998	0.959	0.848	0.659	0.457	0.394	0.002
7.1	1.000	0.982	0.980	0.991	1.000	0.976	0.877	0.688	0.467	0.374	0.002
7.2	1.000	0.977	0.972	0.983	0.998	0.989	0.906	0.719	0.480	0.357	0.001
7.3	1.000	0.972	0.962	0.972	0.993	0.997	0.932	0.752	0.497	0.343	0.001
7.4	1.000	0.967	0.953	0.960	0.984	1.000	0.955	0.787	0.518	0.332	0.001
7.5	1.000	0.962	0.943	0.946	0.971	0.998	0.974	0.822	0.542	0.324	0.001
7.6	1.000	0.958	0.933	0.932	0.956	0.992	0.988	0.856	0.569	0.319	0.001
7.7	1.000	0.955	0.924	0.917	0.939	0.980	0.997	0.889	0.599	0.316	0.001
7.8	1.000	0.952	0.915	0.902	0.920	0.965	1.000	0.920	0.633	0.317	0.001
7.9	1.000	0.950	0.908	0.888	0.900	0.946	0.997	0.947	0.669	0.320	0.001
8.0	1.000	0.949	0.902	0.875	0.880	0.925	0.988	0.969	0.707	0.326	0.001
8.1	1.000	0.949	0.898	0.863	0.860	0.901	0.974	0.986	0.746	0.335	0.001
8.2	1.000	0.950	0.895	0.853	0.842	0.877	0.954	0.996	0.786	0.347	0.001
8.3	1.000	0.951	0.894	0.846	0.825	0.852	0.931	1.000	0.825	0.362	0.000
8.4	1.000	0.954	0.895	0.840	0.810	0.827	0.905	0.997	0.864	0.380	0.000
8.5	1.000	0.957	0.898	0.837	0.797	0.804	0.876	0.986	0.900	0.401	0.000
8.6	1.000	0.961	0.902	0.837	0.787	0.782	0.847	0.970	0.932	0.426	0.000
8.7	1.000	0.966	0.908	0.839	0.780	0.762	0.817	0.948	0.959	0.453	0.000
8.8	1.000	0.971	0.916	0.843	0.776	0.745	0.787	0.921	0.979	0.483	0.000
8.9	1.000	0.976	0.924	0.850	0.775	0.731	0.759	0.890	0.993	0.517	0.000
9.0	1.000	0.981	0.933	0.859	0.777	0.720	0.733	0.857	1.000	0.553	0.000
9.1	1.000	0.985	0.943	0.870	0.782	0.712	0.709	0.823	0.998	0.593	0.000
9.2	1.000	0.990	0.953	0.882	0.789	0.708	0.688	0.788	0.988	0.634	0.000
9.3	1.000	0.993	0.963	0.896	0.800	0.707	0.670	0.753	0.971	0.677	0.000
9.4	1.000	0.996	0.972	0.911	0.813	0.710	0.655	0.720	0.948	0.722	0.000
9.5	1.000	0.998	0.981	0.926	0.829	0.716	0.644	0.689	0.918	0.767	0.000
9.6	1.000	1.000	0.988	0.941	0.846	0.726	0.637	0.660	0.885	0.811	0.000
9.7	1.000	1.000	0.994	0.955	0.865	0.739	0.633	0.633	0.848	0.854	0.000
9.8	1.000	0.999	0.998	0.968	0.885	0.755	0.633	0.610	0.809	0.893	0.000
9.9	1.000	0.998	1.000	0.979	0.905	0.774	0.637	0.591	0.769	0.928	0.000
10.0	1.000	0.995	1.000	0.988	0.924	0.794	0.644	0.575	0.729	0.958	0.000